Volume 3. Issue 6 - December 2015

Transactions on Networks and Communications

ISSN: 2054-7420

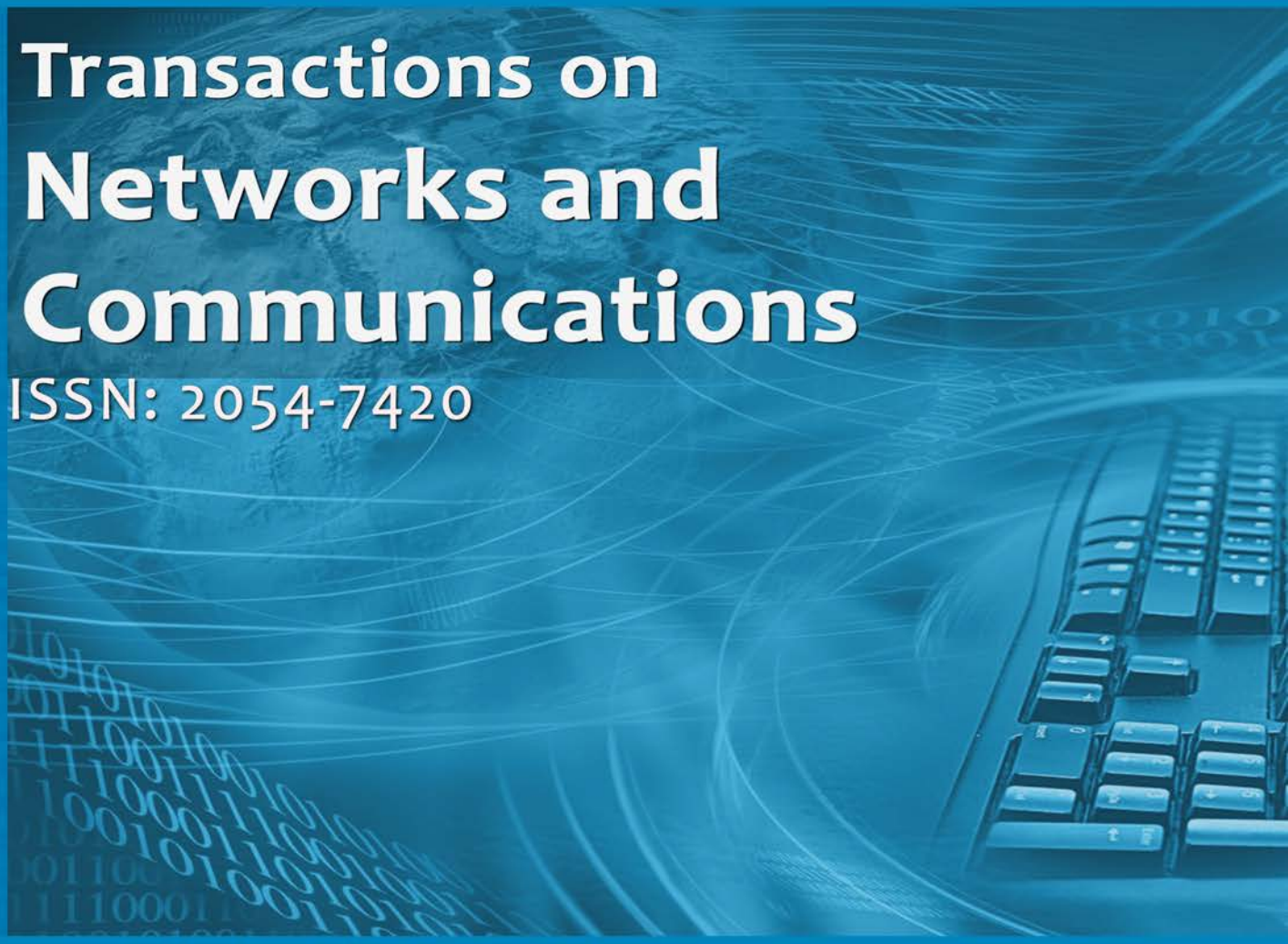

Society for Sciences and Education - United Kingdom

TABLE OF CONTENTS

EDITORIAL ADVISORY BOARD

DISCLAIMER

All the contributions are published in good faith and intentions to promote and encourage research activities around the globe. The contributions are property of their respective authors/owners and the journal is not responsible for any content that hurts someone's views or feelings etc.

SOCIETY FOR SCIENCE AND EDUCATION
UNITED KINGDOM

TNC TRANSACTIONS ON NETWORKS AND COMMUNICATIONS

VOLUME 3, ISSUE 6
ISSN: 2054 -7420

Development of a Web-Based Musculoskeletal Pain Management Information System

[1]Oluwole B. Olajide, [2]Ikechukwu Nwosu and [3]Samson Oluyemi Sogunro
[1]College of Physical & Applied Sciences, McPherson University, Ajebo, Ogun State, Nigeria;
[2]Faculty of Arts, Computing, Engineering and Social Sciences, Sheffield Hallam University; Sheffield, UK;
ob.olajide@gmail.com; ronsynwosu@gmail.com; samson.sogunro@gmail.com

ABSTRACT

Musculoskeletal symptoms among adolescents are related to the time spent using a computer, but little is known about the seriousness of the symptoms or how much they affect everyday life. The purpose of the present study was to examine the intensity of musculoskeletal pain and level of inconvenience to everyday life, in relation to time spent using a computer. This paper developed a system that determines the likelihood of musculoskeletal pain and uses the data stored from the likelihood in developing a predictive model to re-evaluate future data; achieved by – identifying the risk factors and their relationship with the likelihood of musculoskeletal pain, design the system which will be used in the development and implement the design using java programming language.

The methodology of the system involved the identification of the requirements and their relationship with the determination of musculoskeletal pain likelihood; the model involved the allocation of points to each label of the risk factors. Ranges of the sum of points are then used to determine the musculoskeletal pain of each user. The input risk factors' data were collected from a number of participants as patients which were processed in determining their respective status (unlikely, likely, benign and malignant)-the data was later converted into an .arff file format. For the implementation, the software used in performing the detection was implemented in java using the Netbeans IDE 7.1 while the predictive models were implemented using the java API,– a java oriented; data mining tool used for performing classification and forecasting. At baseline a self-administered questionnaire was distributed to 853 participants from 46 different work sites (382 men and 471 women) who, at baseline, had been free from neck and upper extremity symptoms during the preceding month. Work-related exposures, individual factors, and symptoms from the neck and upper extremities were assessed.

Observations of working technique were performed by ergonomists using an ergonomic checklist. Incidence data were collected asking for information on the occurrence of neck, shoulder and arm/hand symptoms. Perceived exertion was rated on a modified scale ranging from 0 (very, very light) to 14 (very, very strenuous). Perceived comfort was rated on a 9-point scale ranging from -4 (very, very poor) to +4 (very, very good) in relation to the chair, computer screen, keyboard, and computer mouse. It was also observed that correct alignment with the computer reduces all the musculoskeletal pain and thus corrects the computer users about the use of ergonomic sitting posture when using the computer. There was a strong association between high perceived exertion and the development of neck, shoulder, and

DOI: 10.14738/tnc.36.1569
Publication Date: 10th November 2015
URL: http://dx.doi.org/10.14738/tnc.36.1569

arm/hand symptoms. Moreover, there was an association between poor perceived comfort and neck pain. Surveillance of computer users may include perceived exertion and comfort to target individuals at risk for neck and upper extremity symptoms.

Keywords: Musculoskeletal Pain; Management Information System; Web Based Development.

1 Introduction

As a body of knowledge, human-factors engineering is a collection of data and principles about human characteristics, capabilities, and limitations in relation to machines, jobs, and environments [1]. As a process, it refers to the design of machines, machine systems, work methods, and environments to take into account the safety, comfort, and productiveness of human users and operators [15]. As a profession, human-factors engineering includes a range of scientists and engineers from several disciplines that are concerned with individuals and small groups at work [5].

The terms human-factors engineering and human engineering are used interchangeably on the North American continent. In Europe, Japan, and most of the rest of the world the prevalent term is ergonomics, a word made up of the Greek words, ergon, meaning “work,” and nomos, meaning “law” [42]. Despite minor differences in emphasis, the terms human-factors engineering and ergonomics may be considered synonymous.

Human factors and human engineering were used in the 1920s and '30s to refer to problems of human relations in industry, an older connotation that has gradually dropped out of use [4]. Some small specialized groups prefer such labels as bioastronautics, biodynamic, bioengineering, and manned-systems technology; these represent special emphases whose differences are much smaller than the similarities in their aims and goals.

The data and principles of human-factors engineering are concerned with human performance, behavior, and training in man-machine systems; the design and development of man-machine systems; and systems-related biological or medical research. Because of its broad scope, human-factors engineering draws upon parts of such social or physiological sciences as anatomy, anthropometry, applied physiology, environmental medicine, psychology, sociology, and toxicology, as well as parts of engineering, industrial design, and operations research [16].

Musculoskeletal pains and aches are prevalent in the general population in many countries. Within the European Union (EU) a 12 month prevalence of 23% has been reported for work related musculoskeletal disorders [15]. In Sweden the prevalence of these disorders has decreased slightly during recent years but it still constitutes one of the major risk factors leading to long term sick leave.

Apart from individual suffering and a decrease in the quality of life, these disorders place a heavy economic burden on society due to costs connected to long term sick leave, poorer work performance and reduced productivity [27]. The causes of work related neck and upper extremity symptoms continue to be insufficiently understood. Both cross sectional and longitudinal studies have suggested, however, that factors related to the individual (e.g. age and gender), working technique, working postures, muscular rest and perceived muscle tension as well as factors related to the work place or work organization, such as workplace layout, repetitive and constrained work and psychosocial working conditions, may be potential risk factors [13].

Similar risk factors have been found for computer work. For instance, poor working technique or work style, as described by [13] has been shown to be associated with an increased risk of developing symptoms indicative of neck and upper extremity disorders. Over the years, several models have been developed in an attempt to identify and explain possible links between different exposures, early signs of incipient musculoskeletal pain conditions and more manifest musculoskeletal outcome.

One of these models is the ecological model of musculoskeletal disorders in office work, presented by [29]. A modified version of this model, specifically targeting computer work has been proposed by Rempel in 2006.

Musculoskeletal discomforts are common occupational problems in healthcare workers whose job tasks involve repetitive motion and assumption of awkward positions. They are major causes of disability worldwide often resulting in job modification and outright resignation by many healthcare practitioners [32]. This work aimed to assess the prevalence and risk factors for musculoskeletal discomfort/pain prevalence of Work Related Musculoskeletal Discomforts (WRMD), risk factors to WRMD amongst computer users. Results revealed that the mean age of the respondents was 38.36±7.96 years.

Results showed that 90.6% of computer users suffered symptoms of work related musculoskeletal complaints. Weight of the computer users and the duration of work session were reported as the possible risk factors for the development of musculoskeletal discomforts/pain [10]. This paper presents a web based musculoskeletal monitoring system with in-built predictive model for musculoskeletal pain among computer users.

2 Literature Review

2.1 Musculoskeletal Pain in Nigeria

[17] reported that in indigenous Africans, 650,000 people of estimated 965 million have computer use related problems. The burden of musculoskeletal pain in Nigeria is due to neglected working condition factors; mainly because of lack of orientation or under-reporting [2]. This is not peculiar to Nigeria but most parts of Africa.

In a study of musculoskeletal registry literature update from all over the world, only 1% of the literature emanated from Africa compared to 34% and 42% from Europe and Asia respectively. This is partly due to inaccurate population statistics which makes age specific incidence rates impossible or if available inaccurate. Other reasons are inadequate diagnostic facilities, limited access to care etc.

Inadequate technical manpower and infrastructure as well as quality of ergonomics data systems all contribute to inaccurate data on ergonomic burden. Annually, there are about 100,000 new musculoskeletal pain cases in Nigeria, this is estimated to increase to 500,000 in 2010 [2]. [41] estimates that incidence of musculoskeletal pain in Nigerian men and women by 2020 will be 807/1000 and 709/1000. This is as a result of increase in the use of computers.

2.2 Ergonomic Problem and Technology

Human factors and ergonomics are concerned with the "fit" between the user, equipment and their environments. It takes account of the user's capabilities and limitations in seeking to ensure that tasks, functions, information and the environment suit each user. To assess the fit between a person and the used technology, human factors specialists or ergonomists consider the job (activity) being done and the

demands on the user; the equipment used (its size, shape, and how appropriate it is for the task), and the information used (how it is presented, accessed, and changed). Ergonomics draws on many disciplines in its study of humans and their environments, including anthropometry, biomechanics and basically the engineering field.

One of the most prevalent types of work-related injuries is musculoskeletal disorders. Work-related musculoskeletal disorders (WRMDs) result in persistent pain, loss of functional capacity and work disability, but their initial diagnosis is difficult because they are mainly based on complaints of pain and other symptoms. Every year 1.8 million U.S. workers experience WRMDs and nearly 600,000 of the injuries are serious enough to cause workers to miss work.

Certain jobs or work conditions cause a higher rate worker complaints of undue strain, localized fatigue, discomfort, or pain that does not go away after overnight rest. These types of jobs are often those involving activities such as repetitive and forceful exertions; frequent, heavy, or overhead lifts; awkward work positions; or use of vibrating equipment.

The Occupational Safety and Health Administration (OSHA) have found substantial evidence that ergonomics programs can cut workers' compensation costs, increase productivity and decrease employee turnover. Therefore, it is important to gather data to identify jobs or work conditions that are most problematic, using sources such as injury and illness logs, medical records, and job analyses.

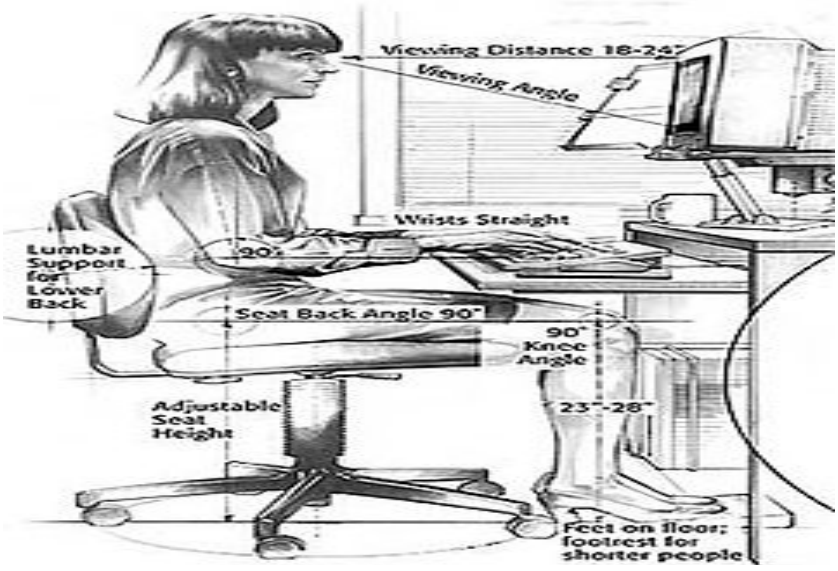

Figure 1: A Schematic View of Ergonomic use of a Computer

2.3 Prediction of Musculoskeletal Pain

The area of musculoskeletal pain prediction has been an area of study by many public health officials. It has become a way of easily mitigating the likelihood of the existence of the disease by determining the disease in its earlier stages [4].

Although the accurate prediction of musculoskeletal pain is not clear, oncologists have tried determining musculoskeletal pain likelihood via a number of data mining tools and bringing into view the risk factors that are responsible for the disease [31].

According to [16] prediction of musculoskeletal pain has provided estimates for future trends, useful to service planners, and highlights for tobacco control, to reduce numbers of musculoskeletal pain in Northern Ireland. The use of regression models proved to be the most practical means by which relatively short-term future patterns of musculoskeletal pain mortality can be estimated.

[22] stated also that genetic algorithm is a useful search procedure that searches from one population of points to another; thus directing the search to the beast solution so far rendering it as a global solution to non-linear functions.

According to [17] the genetic algorithm was used by Dr. Wolberg of the University of Wisconsin, Madison in correctly diagnosing pain as being either benign or malignant based on data from automated microscopic examination of cells collected by needle aspiration.

Musculoskeletal pain can affect the body's muscles, joints, tendons, ligaments and nerves. Most work-related musculoskeletal pain develops over time and is caused either by the work itself or by the employees' working environment. MSD's can also occur in the patient’s life outside work either through sport - tennis (elbow); music - guitar playing or a hobby - on-line tracing of a family tree.

These external work events can be exacerbated by their daily profession. They can also result from fractures sustained in an accident. Typically, musculoskeletal pains affect the back, neck, shoulders and upper limbs; less often they affect the lower limbs.

Health problems range from discomfort, minor aches and pains, to more serious medical conditions requiring time of musculoskeletal pain are a priority for the EU in its Community strategy. Reducing the musculoskeletal load of work is part of the 'Lisbon objective', which aims to create 'quality jobs' by:

- Enabling workers to stay in employment; and
- Ensuring that work and workplaces are suitable for a diverse population.

In an attempt to overcome limitations inherent in conventional computer-aided diagnosis, investigators have created programs that simulate expert human reasoning [35]. Hopes that such a strategy would lead to clinically useful programs have not been fulfilled, but many of the problems impeding creation of effective artificial intelligence programs have been solved.

Strategies have been developed to limit the number of hypotheses that a program must consider and to incorporate pathophysiologic reasoning. The latter innovation permits a program to analyse cases in which one disorder influences the presentation of another.

Prototypes embodying such reasoning can explain their conclusions in medical terms that can be reviewed by the user. Despite these advances, further major research and developmental efforts will be necessary before expert performance by the computer becomes a reality [3]. The steady expansion of medical knowledge has made it more difficult for the physician to remain a part of medicine outside a narrow field.

Consultation with a specialist is a solution when the clinical problem lies beyond the physician's competence, but frequently expert opinion is either unavailable or not available in a timely fashion. Attempts have been made to develop computer programs that can serve as consultants.

By the early 1970s it became clear that conventional tools such as flow charts, pattern matching and Bayes' theorem were unable to deal with most complex clinical problems. Investigators then began to study the expert physician to obtain detailed insights into the basic nature of clinical problem solving.

The results derived from such studies have subsequently formed the basis for computational models of the cognitive phenomena, and these models have further been converted into so-called artificial intelligence programs [42].

Many of the early efforts to apply artificial intelligence methods to real problems, including medical reasoning; have primarily used rule-based systems. Such programs are typically easy to create, because their knowledge is catalogued in the form of "if ... then..." rules used in chains of deduction to reach a conclusion. In many relatively well-constrained domains rule-based programs have begun to show skilled behaviour [31].

This is true in several narrow domains of medicine as well, but most serious clinical problems are so broad and complex that straightforward attempts to chain together larger sets of rules encounter major difficulties. Problems arise principally from the fact that rule-based programs do not embody a model of disease or clinical reasoning. In the absence of such models, the addition of new rules leads to unanticipated interactions between rules and thus to serious degradation of program performance.

Given the difficulties encountered with rule-based systems, more recent efforts to use artificial intelligence in medicine have focused on programs organized around models of disease. Efforts to develop such programs have led to substantial progress in our understanding of clinical expertise, in the translation of such expertise into cognitive models, and in the conversion of various models into promising experimental programs.

Of equal importance, these programs have been steadily improved through the correction of flaws shown by confronting them with various clinical problems. We will focus on how improved representation of clinical knowledge and sophisticated problem-solving strategies has advanced the field of artificial intelligence in medicine.

Our purpose is to provide an overview of artificial intelligence in medicine to the physician who has had little contact with computer science. We will not concentrate on individual programs; rather, we will draw on the key insights of such programs to create a coherent picture of artificial intelligence in medicine and the promising directions in which the field is moving.

We will therefore describe the behaviour not of a single existing program but the approach taken by one or another of the many programs to which we refer. It remains an important challenge to combine successfully the best characteristics of these programs to build effective computer-based medical expert systems. Several collections of papers provide detailed descriptions of the programs on which our analysis is based. Any program designed to serve as a consultant to the physician must contain certain basic features. It must have a store of medical knowledge expressed as descriptions of possible diseases. Depending on the breadth of the clinical domain, the number of hypotheses in the database can range from a few to many thousands.

In the simplest conceivable representation of such knowledge, each disease hypothesis identifies all of the features that can occur in the particular disorder. In addition, the program must be able to match

what is known about the patient with its store of information. Even the most sophisticated programs typically depend on this basic strategy [42].

The simplest version of such programs operates in the following fashion when presented with the chief complaint and when later given additional facts.

- For each possible disease (diagnosis) determine whether the given findings are to be expected.
- Score each disease (diagnosis) by counting the number of given findings that would have been expected.
- Rank-order the possible diseases (diagnoses) according to their scores.
- The power of such a simple program can be greatly enhanced through the use of a mechanism that poses questions designed to elicit useful information. Take, for example, an expansion of the basic program by the following strategy:
- Select the highest-ranking hypothesis and ask whether one of the features of that disease, not yet considered, is present or absent.
- If inquiry has been made about all possible features of the highest-ranked hypothesis, ask about the features of the next best hypothesis.
- If a new finding is offered, begin again with step; otherwise, print out the rank-ordered diagnoses and their respective supportive findings and stop.

Steps 1 through 3 contain a primitive evaluation of the available information, and steps 4 through 6 contain an equally simple information-gathering strategy that determines what information to seek next. But such a program fails to capture many of the techniques responsible for expert performance. For example, the ranking process does not take into account how frequently particular features occur in a given disease.

The program, furthermore, has no knowledge of pathophysiology and is not able to take stock of the severity of an illness. The most serious problem is that each new finding sets into motion a search process tantamount to considering all disease states appearing in a textbook of medicine. Even for a high-speed computer this is not a practical diagnostic strategy and for this reason research has turned to the study of how experts perform.

The physician's ability to sharply limit the number of hypotheses under active consideration at any one time is a key element in expert performance [28]. Computer programs that use the strategies of experts can accomplish this same goal and devote the bulk of their computational resources to the sophisticated evaluation of a small number of hypotheses.

Controlling the proliferation of hypotheses is only the first step in creating effective artificial intelligence programs [26]. To deal with the circumstance in which one disease influences the clinical presentation of another, the program must also have the capacity to reason from cause to effect. Moreover, the required pathophysiologic knowledge must be organized in a hierarchical fashion so that the information becomes more detailed as one progress to deeper levels of the knowledge base.

Quantitative information, or rough qualitative estimates, must also be added to the causal links if the program is to separate the contribution of each of several disorders to a complex clinical picture [42].

The cognitive models that embody these principles provide the basis for computer programs that use the chief complaint and other available information to reduce the range of diagnostic possibilities. The narrowing process can be viewed as passive in that the program makes all possible progress without requesting further facts.

The passive phase completed, the program moves to an active mode of posing questions to the physician. This process is interactive with each new fact stimulating additional analysis that further reduces the number of diagnostic possibilities. In the following discussion, attention will be directed primarily to the passive narrowing process because this strategy plays a central role in clinical problem solving and because more is known about this process than about the active collection of new information [27].

2.4 Related Work

Various numbers of researches exists concerning musculoskeletal pain prediction although with varying factors and data mining methodology applied. According to [37], in the development of a musculoskeletal pain prediction model incorporating familial and personal risk factors he was able to determine the risk of the likelihood of the disease; although using only a limited number of risk factors while excluding occupational, environmental, social and dietary factors.

[7] performed a network-based survival analysis on two musculoskeletal pain datasets with the intention of determining how long a after an operation may the disease recur. [8] also performed a research on the determination of the positive association between the waist-hip ratio and the likelihood of musculoskeletal pain risk in urbanized Nigerian, although limited only to waist-hip ratio as a risk factor.

3 Methods

3.1 Use Case Diagrams

Use Cases are a requirements discovery technique first introduced in the object method. In its simplest form, a use case identifies the actors (in this case; the end-users and the administrators) involved in an interaction and the names and the types of the interaction. The use case diagram in Figure 2 describes all the actors and the interactions, which are possible by either users of the system.

The function of each use cases are described as follows:

i. **Enter Personal Data**: Each patient is prompted to register and login into the system to provide their personal data which consists of Name, Sex, age, ethnicity, occupation and city of residence;
ii. **Enter Medical Data**: Each patient is prompted after filing in their personal data to add their medical data which consists of information about the modifiable and non-modifiable risk factors;
iii. **Determine Musculoskeletal Pain Status**: Each patient is then prompted to submit the information which is used by the system in determining the status of the patient which can either be none, likely, benign or malignant;
iv. **Perform Prediction Analysis**: the doctor can perform the required predictive analysis by using the information available in the database – provided by the patients; and
v. **Generate Report**: after performing the required prediction analysis, the doctor can view the results via a report generated after analysis.

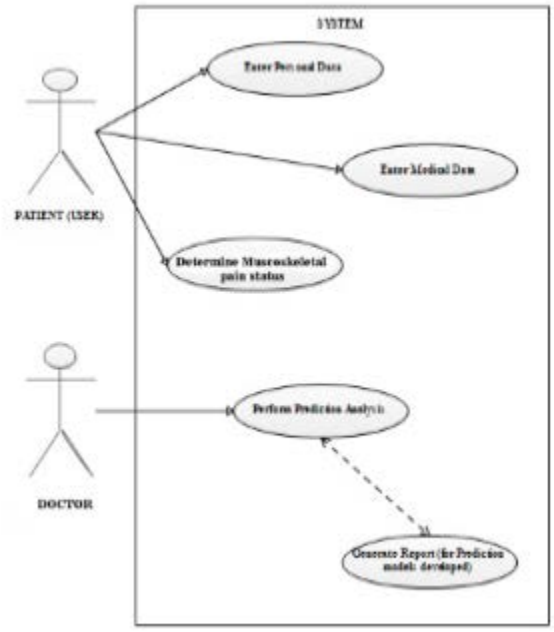

Figure 2: Use-Case diagram of user interaction with the system

3.2 System Architecture

This is the assessment, description or explanation of a system based on careful consideration or investigation of its operation. It is also described as the detailed explanation of a system to understand it better and draw conclusions from it. This is done by considering input, manipulating it and getting the desired output. Inputs for the software are the information (personal and medical information) that will be entered by the user of the software system.

The patient enters the personal data which includes the name, age, location, sex and previous medical records and automatically becomes a user. This goes into the system and is stored in the database of the musculoskeletal pain management system.

The system can be assessed by the patient and the doctor while the data given by the user is processed by the predictive system. Both the personal data and the medical data are stored in the musculoskeletal pain management systems' storage device which is also the database. After the prediction is done, the result is given as output.

The software was not meant to replace the specialist or doctor, yet it was developed to assist general practitioner and specialist in diagnosing and predicting patient's condition from certain rules or "experience". Patient with high-risk factors or symptoms or predicted to be highly effected with certain diseases or illness, could be short listed to see the specialist for further treatment. Employing the technology especially Artificial Intelligence (AI) techniques in medical applications could reduce the cost, time, human expertise and medical error.

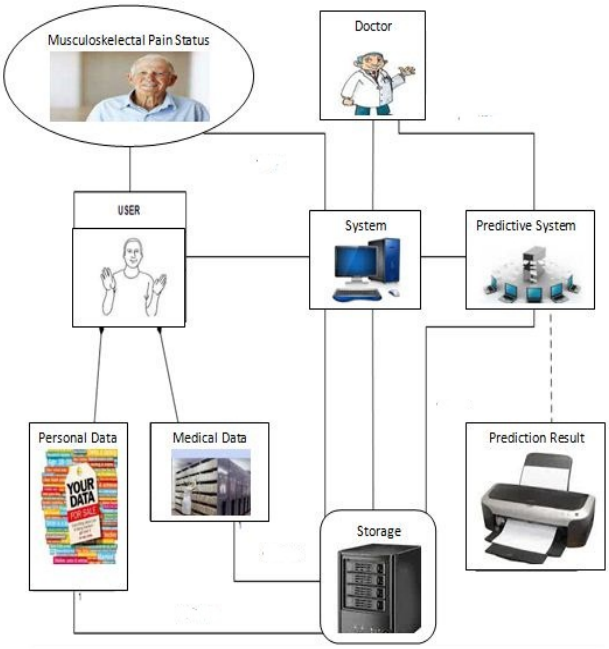

Figure 3: System Architecture of Musculoskeletal Pain Management Information System

4 The Prototype

4.1 Implementation

During implementation, the user interface of the software was implemented using the Netbeans 7.1 IDE (Integrated Development Environment), the predictive models are applied via the weka.jar file which is stored as a library whose methods are called and manipulated by the GUI. The data which is used in storing data and manipulating the predictive models was stored in .arff file format.

They are developed to facilitate the users computing environment. These interfaces were mainly implemented using Java programming language.

This user interface acts as the access point into the system for patients, doctors and administrators. Users are required to select their respective identification; patients are to select user while the doctor selects the administrator button.

4.1.1 Welcoming the User

The moment the application is being run; the system prompts the user to log in either as a patient (Figure 4), or as a doctor. For a patient user who wants to use the system, he may log in by selecting patient from the radio button as shown in the figure above. After log in, the user is prompted to fill in his/her personal and medical information.

4.1.2 Patient Medical Information

After every user is granted access to the system, the user is prompted to provide their personal information (Figure 4) and their medical information which consists of the modifiable and non-modifiable risk factors (Figure 5). The information provided by the user is populated into the database of the system;

and is also retrieved by the system in determine the musculoskeletal pain status of the user and in performing predictive analysis by the doctor.

4.1.3 Musculoskeletal Pain Status Report

After the user provides his/her personal and medical information, the system then performs the required analysis needed in order to determine the musculoskeletal pain status of the patient by printing the results (see Figure 6) and also by providing recommendations to the patient as advice towards mitigating likelihood. But, the recommendations are made only to the non-modifiable risk factors.

4.1.4 Doctor's Activity

After a number of determinations were made by the detection system, the stored data was prepared for predictive analysis. After the doctor logs into the system, the data provided by the user can further perform either of two (3) predictive models on the patient data: Bayes' naïve, J48-trees multi-layer perception classifications (see Figure 5). The results of the three predictive models were compared and decisions made depending on the doctor's discretion.

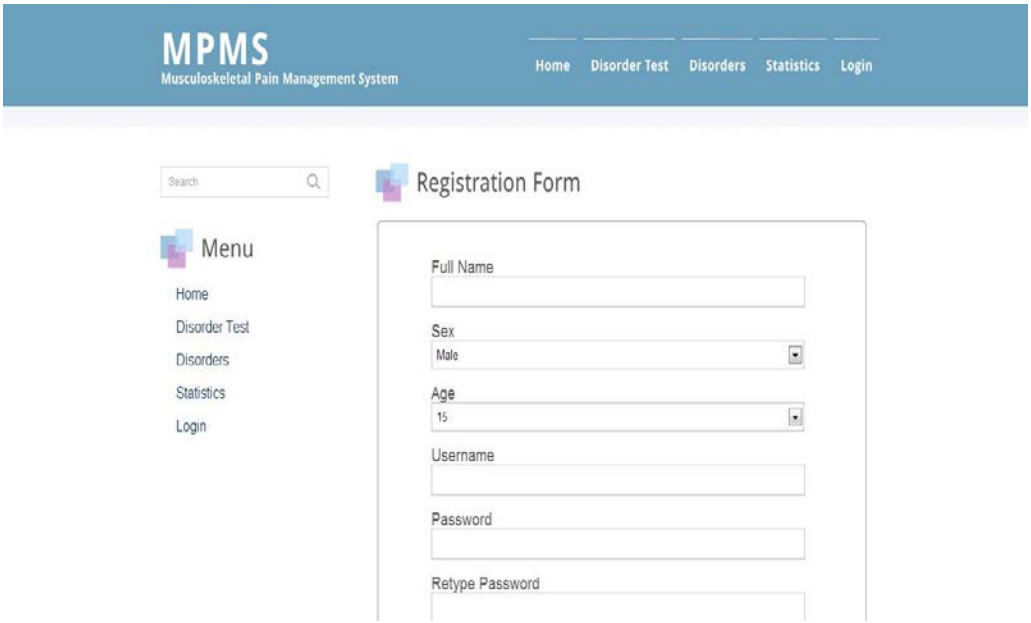

Figure 4: User Personal Information Window

4.2 Welcome Page

The moment the application is being run; the system prompts the user to log in either as a patient (Figure 4), or as a doctor. For a patient user who wants to use the system, he may log in by selecting patient from the radio button as shown in the figure above. After log in, the user is prompted to fill in his/her personal and medical information. This includes the full name, the sex, age, previous medical record, and the user registering the password twice for confirmation.

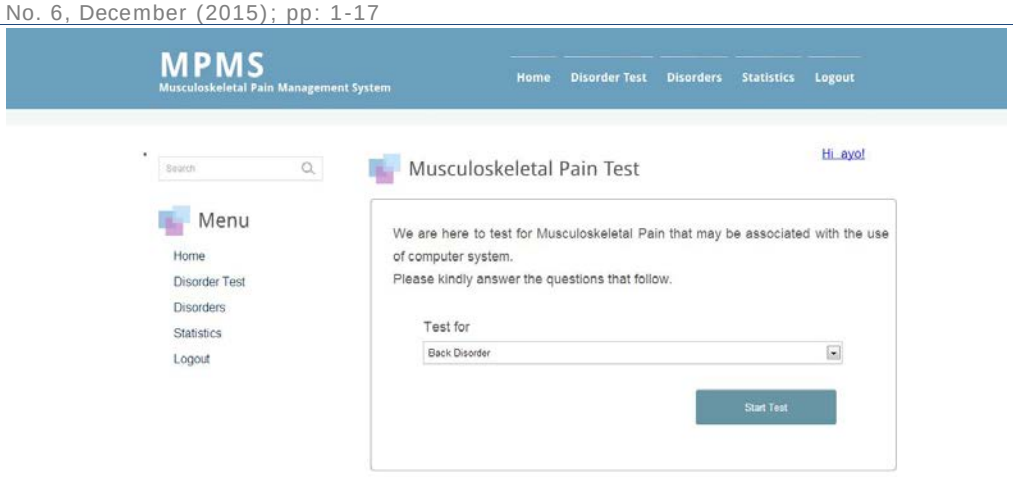

Figure 5: Medical Information Window

After every user is granted access to the system, the user is prompted to provide their personal information (Figure 4) and their medical information which consists of the modifiable and non-modifiable risk factors (Figure 5). The information provided by the user is populated into the database of the system; and is also retrieved by the system in determine the musculoskeletal pain status of the user and in performing predictive analysis by the doctor.

The user then answers a series of questions relating to the musculoskeletal disorder and awaits the result.

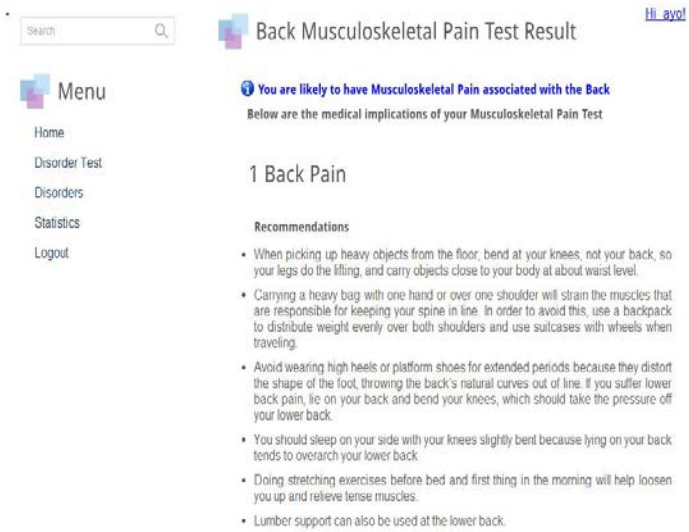

Figure 6: The Musculoskeletal Pain Status Report Window

After the user provides his/her personal and medical information, the system then performs the required analysis needed in order to determine the musculoskeletal pain status of the patient by printing the results (see Figure 6) and also by providing recommendations to the patient as advice towards mitigating likelihood. But, the recommendations are made only to the non-modifiable risk factors. Recommendations are also given to the user about musculoskeletal pain treatment and best practices.

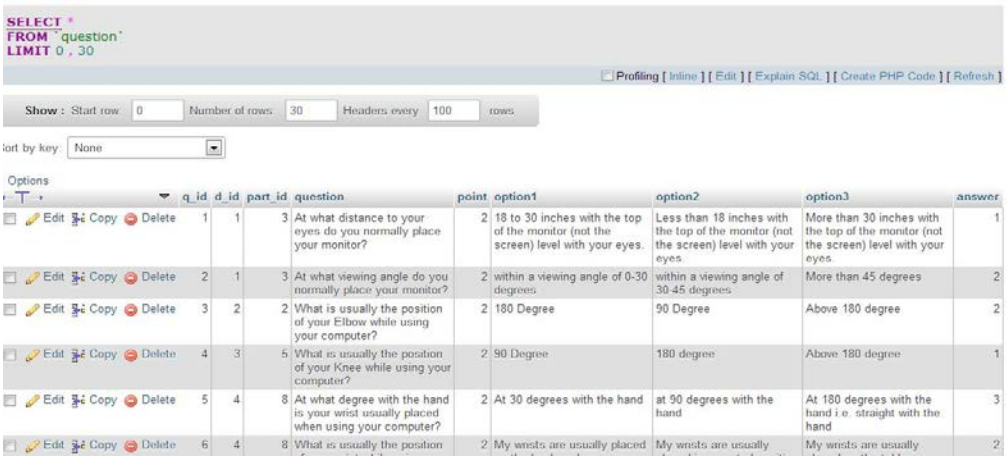

```
SELECT *
FROM `question`
LIMIT 0 , 30
```

Profiling [Inline] [Edit] [Explain SQL] [Create PHP Code] [Refresh]

Show : Start row: 0 Number of rows: 30 Headers every: 100 rows

Sort by key: None

Options

	q_id	d_id	part_id	question	point	option1	option2	option3	answer
Edit Copy Delete	1	1	3	At what distance to your eyes do you normally place your monitor?	2	18 to 30 inches with the top of the monitor (not the screen) level with your eyes.	Less than 18 inches with the top of the monitor (not the screen) level with your eyes.	More than 30 inches with the top of the monitor (not the screen) level with your eyes.	1
Edit Copy Delete	2	1	3	At what viewing angle do you normally place your monitor?	2	within a viewing angle of 0-30 degrees	within a viewing angle of 30-45 degrees	More than 45 degrees	2
Edit Copy Delete	3	2	2	What is usually the position of your Elbow while using your computer?	2	180 Degree	90 Degree	Above 180 degree	2
Edit Copy Delete	4	3	5	What is usually the position of your Knee while using your computer?	2	90 Degree	180 degree	Above 180 degree	1
Edit Copy Delete	5	4	8	At what degree with the hand is your wrist usually placed when using your computer?	2	At 30 degrees with the hand	at 90 degrees with the hand	At 180 degrees with the hand i.e. straight with the hand	3
Edit Copy Delete	6	4	8	What is usually the position	2	My wrists are usually placed	My wrists are usually	My wrists are usually	2

Figure 7: Questionnaire Data

5 Conclusion

The musculoskeletal pain detection and prediction software system was discovered to be of good use to the public health sector; especially with the interactive user-interface it has and with its ability to provide effective detection of the disease just by identifying the risk factors associated with the disease. It is also very effective at predicting the likelihood of the disease in the lives of individuals by simply analyzing available and known cases using effective predictive models.

Musculoskeletal pain is indeed a major threat to the general populace of our nation, Nigeria; and it is imperative that means via which the progress and distribution of musculoskeletal pain must be developed and identified.

There is need for the Nigerian Public Health sector to look into ways via which this killer disease can be mitigated if not cured before it becomes a living menace in the lives of our mothers. Women are the procreators of life and the determining factor of human existence, if there is increasing growth in the number of deaths due to this disease then there is no hope for the future of the Nigerian child and the nation at large.

REFERENCES

[1] Andersen JH, Haahr JP, Frost P: Risk factors for more severe regional musculoskeletal symptoms: a two-year prospective study of a general working population. Arthritis Rheum 2007, 56(4):1355-1364. [http://www.av.se/dokument/statistik/officiell_stat/ARBORS2010.pdf].

[2] Arvidsson I, Axmon A, Skerfving S: Follow-up study of musculoskeletal disorders 20 months after the introduction of a mouse-based computer system. Scand J Work Environ Health 2008, 34(5): p. 374-380.

[3] Balogh I, Orbaek P, Ohlsson K, Nordander C, Unge J, Winkel J, Hansson GA: Self-assessed and directly measured occupational physical activitiesinfluenceof musculoskeletal complaints, age and gender. Appl Ergon 2004, 35(1): p. 49-56.

[4] Bongers PM, Ijmker S, van den Heuvel S, Blatter BM: Epidemiology of work related neck and upper limb problems: psychosocial and personal risk factors (part I) and effective interventions from a bio behavioural perspective (part II). J Occup Rehabil 2006, 16(3): p. 279-302.

[5] Bostrom M, Dellve L, Thomee S, Hagberg M: Risk factors for generally reduced productivity-a prospective cohort study of young adults with neck or upper-extremity musculoskeletal symptoms. Scand J Work Environ Health 2008, 34(2): p. 120-132

[6] Borg G: Psychophysical scaling with applications in physical work and the perception of exertion. Scand J Work Environ Health 1990, 16(Suppl 1): p. 55-58.

[7] Chih-lin A, Gustafsson M, Hansson GA: Effects of prismatic glasses including optometric correction on head and neck kinematics, perceived exertion and comfort during dental work in the oral cavity-a randomised controlled intervention. Appl Ergon 2012, 43(1): p. 246-253.

[8] Clement M: Risk of musculoskeletal disorders among females and males in repetitive/constrained work. Ergonomics 2009, 52(10): p. 1226-1239.

[9] Deitel M, Deitel C (1999a). Data Mining for Medical Database. Proceedings of the First National Conference on Artificial Intelligence Application in Industry. Kuala Lumpur, pp. 72-79.

[10] European Foundation for the improvment of living and working conditions. [http://www.eurofound.europa.eu/pubdocs/2006/98/en/2/ ef0698en.pdf].

[11] Ergonomic checklist for computer work. 1997 [http://www.sahlgrenska.se/upload/SU/omrade_6/Arbets-%20och%20Miljömedicin/AMM/fhvmetodik/checklista.pdf].

[12] Feuerstein M: Functional assessment for persons with musculoskeletal pain and impairment. J Occup Rehabil 2004, 14(3): p. 163-164.

[13] Feuerstein M, Nicholas RA: Development of a short form of the Workstyle measure. Occup Med 2006, 56(2): p. 94-99.

[14] Hajek k.l, Zelic, I., Lavrac, N., Najdenov, P., Rener-Primec, Z. (1999). Impact of machine Learning of the Diagnosis and Prognosis of First Cerebral Paroxysm. Machine Learning and Applications: Machine Learning in Medical Applications. Chania, Greece, p. 24-26.

[15] Hagberg M, Vilhemsson R, Tornqvist EW, Toomingas A: Incidence of selfreported reduced productivity owing to musculoskeletal symptoms: association with workplace and individual factors among computer users. Ergonomics 2007, 50(11): p. 1820-1834.

[16] Hanvold TN, Veiersted KB, Waersted M: A prospective study of neck, shoulder, and upper back pain among technical school students entering working life. J Adolesc Health 2010, 46(5): p. 488-494.

[17] Hansson GA, Balogh I, Bystrom JU, Ohlsson K, Nordander C, Asterland P, Sjolander S, Rylander L, Winkel J, Skerfving S: Questionnaire versus direct technical measurements in assessing postures and movements of the head, upper back, arms and hands. Scand J Work Environ Health 2001, 27(1): p. 30-40.

[18] Harrington CB, Siddiqui A, Feuerstein M: Workstyle as a predictor of pain and restricted work associated with upper extremity disorders: a prospective study. J Hand Surg Am 2009, 34(4)

[19] Juul-Kristensen B, Sogaard K, Stroyer J, Jensen C: Computer users' risk factors for developing shoulder, elbow and back symptoms. Scand J Work Environ Health 2004, 30(5): p. 390-398.

[20] Juul-Kristensen B, Jensen C: Self-reported workplace related ergonomic conditions as prognostic factors for musculoskeletal symptoms: the "BIT"follow up study on office workers. Occup Environ Med 2005, 62(3): p. 188-194.

[21] Karlqvist LK, Bernmark E, Ekenvall L, Hagberg M, Isaksson A, Rostö T: Computer mouse position as a determinant of posture, muscular load and perceived exertion. Scand J Work Environ Health 1998, 24(1): p. 62-73.

[22] Lindegård A, Wahlström J, Hagberg M, Hansson G-Å, Jonsson P, Wigaeus Tornqvist E: The impact of working technique on physical loads – an exposure profile among newspaper editors. Ergonomics 2003, 46(6): p. 598-615.

[23] Lindegård Andersson A: Working technique during computer work. Arbeteoch Hälsa 2007, 41:1

[24] Lindegård et al. BMC Musculoskeletal Disorders 2012, 13:38 http://www.biomedcentral.com/1471-2474/13/38

[25] Lindegård A, Gustafsson M, Hansson GA: Effects of prismatic glasses including optometric correction on head and neck kinematics, perceived exertion and comfort during dental work in the oral cavity-a randomised controlled intervention. Appl Ergon 2012, 43(1): p. 246-253.

[26] Nicholas RA, Feuerstein M, Suchday S: Workstyle and upper-extremity symptoms: a biobehavioral perspective. J Occup Environ Med 2005,47(4): p. 352-361.

[27] Nordander C, Ohlsson K, Akesson I, Arvidsson I, Balogh I, Hansson GA, Stromberg U, Rittner R, Skerfving S: Risk of musculoskeletal disorders among females and males in repetitive/constrained work. Ergonomics 2009, 52(10): p. 1226-1239.

[28] Norman K, Floderus B, Hagman M, Toomingas A, Tornqvist EW: Musculoskeletal symptoms in relation to work exposures at call centre companies in Sweden. Work 2008, 30(2): p. 201-214.

[29] Rempel D, Barr A, Brafman D, Young E: The effect of six keyboard designs on wrist and forearm postures. Appl Ergon 2007, 38(3): p. 293-298

[30] Rempel DM, Krause N, Goldberg R, Benner D, Hudes M, Goldner GU: A randomised controlled trial evaluating the effects of two workstation interventions on upper body pain and incident musculoskeletal disorders among computer operators. Occup Environ Med 2006, 63(5): p. 300-306.

[31] Rothman KJ, Greenland S, Lash TL: Modern epidemiology Philadelphia: Lippincott Williams & Wilkins; 2008.

[32] Roquelaure Y, Ha C, Leclerc A, Touranchet A, Sauteron M, Melchior M,Imbernon E, Goldberg M: Epidemiologic surveillance of upper-extremity musculoskeletal disorders in the working population. Arthritis Rheum 2006, 55(5): p. 765-778.

[33] Sauter SL, Swanson NG: An ecological model of musculoskeletal disorders in office work. In Beyond biomechanics: Psychosocial aspects of musculoskeletal disorders in office work Edited by: Moon SD, Sauter SL 1996: p. 3-21.

[34] Sillanpää J, Huikko S, Nyberg M, Kivi P, Laippala P, Uitti J: Effect of work with visual display units on musculo-skeletal disorders in the office environment. Occup Med 2003, 53(7): p. 443-451.

[35] Stock SR, Fernandes R, Delisle A, Vezina N: Reproducibility and validity of workers' self-reports of physical work demands. Scand J Work Environ Health 2005, 31(6): p. 409-437.

[36] Tornqvist EW, Hagberg M, Hagman M, Risberg EH, Toomingas A: The influence of working conditions and individual factors on the incidence of neck and upper limb symptoms among professional computer users.Int Arch Occup Environ Health 2009, 82(6): p. 689-702.

[37] Tyrer KJ, Greenland S, Lash TL: Modern epidemiology Philadelphia: Lippincott Williams & Wilkins; 2008. Veiersted KB, Westgaard RH: Development of trapezius myalgia among female workers performing light manual work. Scand J Work Environ Health 1993, 19(4): p. 277-283.

[38] Wahlstrom J, Lindegard A, Ahlborg G Jr, Ekman A, Hagberg M: Perceived muscular tension, emotional stress, psychological demands and physical load during VDU work. Int Arch Occup Environ Health 2003, 76(8): p. 584-590.

[39] Wahlstrom J: Ergonomics, musculoskeletal disorders and computer work. Occupational Medicine 2005, 55(3): p. 168-176.

[40] Wahlstrom J, Hagberg M, Toomingas A, Wigaeus Tornqvist E: Perceived muscular tension, job strain, physical exposure, and associations with neck pain among VDU users; a prospective cohort study. Occup Environ Med 2004, 61(6): p. 523-528.

[41] World Health Organization. World Cancer Report 2008. Lyon: International Agency for Research on Cancer;2008

[42] Walker-Bone K, Palmer KT, Reading I, Coggon D, Cooper C: Prevalence and impact of musculoskeletal disorders of the upper limb in the general population. Arthritis Rheum 2004, 51(4): p. 642-651

[43] Zelic, I., Lavrac, N., Najdenov, P., Rener-Primec, Z. (1999). Impact of machine Learning of the Diagnosis and Prognosis of First Cerebral Paroxysm. Machine Learning and Applications: Machine Learning in Medical Applications. Chania, Greece: p. 24-26.

SOCIETY FOR SCIENCE AND EDUCATION
UNITED KINGDOM

TNC TRANSACTIONS ON NETWORKS AND COMMUNICATIONS

VOLUME 3, ISSUE 6
ISSN: 2054 -7420

Resource Allocation Algorithm for Improving Performance of the OFDMA Based Connection Oriented Networks

Md. Nazmus Saadat[1], Borhanuddin Mohd Ali[1], Aduwati Sali[2], Raja Syamsul Azmir Raja Abdullah[2] and Hafizal Mohamad[3]

[1,2]Faculty of Engineering, University Putra Malaysia, Serdang, 43300, Selangor, MY
[3]MIMOS Berhad, Technology Park Malaysia 57000,
nazmus.saadat@yahoo.com, {borhan, aduwati, rsa}@eng.upm.edu.my
hafizal.mohamad@mimos.my

ABSTRACT

To enhance network performance, PHY and MAC layer has direct influence besides other factors as these are major layers of OSI based communication system. One way of enhancing network performance is the managing the radio resources intelligently. As cross layer based systems might be faster responding in case of network resource distribution and due to the spectrum limitation for commercial use, there are active researches in this area that targets to enhance the network users' experience, though RA might be considered as an evergreen topic for all evolving communication systems. This paper aims to focus specifically on how to increase throughput and delay performance leading to overall higher system performance and fairness. We use techniques of graph theoretic tools and optimization mechanism in our solution to improve radio resource allocation. After we optimize the subcarrier allocation using cross layer interaction of mainly MAC and PHY, the final assignment is done along with power allocation to all users. Then we reevaluate each new incoming resource request and use threshold based allocation techniques to cater for more users. Besides showing the performance enhancement we also show the fairness comparison to other existing state of the art research as benchmarking by means of simulation.

Key words: OFDMA, Resource Allocation, Radio Resource, Connection Oriented Networks, Wireless Networks, Algorithms, Graphs, QualNet, Cross Layer.

1 Introduction & Literature:

Various resource allocation algorithms has been proposed based on different opinions on how to save resources and enhance system performance. For example in [1] authors described optimized and suboptimal solution to manage multiuser diversity and resource allocation which has similar objective as we do but differs in approach to the solution. In [2], several cross layer based ideas are discussed and it is clear that cross layer design can bring higher performance for wireless networks comparing to conventional systems. In this paper, our proposed solution also make use of it and comes with better and intelligent algorithm. Besides, there are works on adaptive allocation. Adaptive nature of allocation is important due to that static allocation might not really handle all different situations in huge network loads. For example, in [3], authors defined an adaptive algorithm to solve the OFDMA mapping problem

DOI: 10.14738/tnc.36.1280
Publication Date: 21st November 2015
URL: http://dx.doi.org/10.14738/tnc.36.1280

in IEEE 802.16e networks. Authors showed that with the price of lesser throughput the active time of the SS can be reduced. They have proposed few different mapping algorithms to enhance system performance mainly using the resource mapping efficiency and they showed it by means of simulation tools.

In [4] authors considered highly QoS sensitive applications like multipoint video conferences and interactive videos games etc. and proposed optimum discrete bit loading aiming to satisfy all users. During resource allocation, when allocation of subcarrier gets updated at the starting of a time windows and channel gain is not known accurately at that moment and slow adaptive systems needs to have adaptive algorithms for better performance as per authors. They have formulated proportional resource allocation based on chance constrained programming for such slow adaptive systems that maximizes the average sum rate. Also they claim to maintain Jain's Fairness Index with target probability. The proposed solution is a hybrid of ant colony optimization and support vector machine. However satisfying all users comes to an expense of less number of users to use the network at the same time which might restrict the growth of number of users in the network. Authors in [5] proposed a decoupled solution like [1] but having an iterative and semi-distributed approach to implement a frequency domain scheduler. Their approach implements packet scheduler for all cells and users and interfaces of the wireless network in frequency domain to determine the global resource allocation. In [6] authors proposed an opportunistic scheduling algorithm considering power and subchannel allocation. They formulate the optimization problem targeting maximizing average sum rate for users and also claim to provide QoS requirement. They address non-convexity and coupled optimization same as this paper addresses but in different way to solve it. They also proposed two heuristic algorithms to reduce computational complexity. But the work may not be directly comparable to this paper as they consider device to device communication when planning for resource distribution which is not of the similar aspect as ours. In [8] authors aimed for sum capacity maximization by using MIMO OFDMA structure. They have proposed Lagrange dual based method first. This method is computationally expensive and hence they also proposed sub optimal solution to reduce complexity. However, though MIMO has definite benefits, for this paper we have proposed solutions based on SISO system and our work targets objectives similar to [1] but again our approach to the problem is very different than that of [1]. Due to that it is very close to our focus, we have mainly evaluated and benchmarked against this article comparing our outcomes.

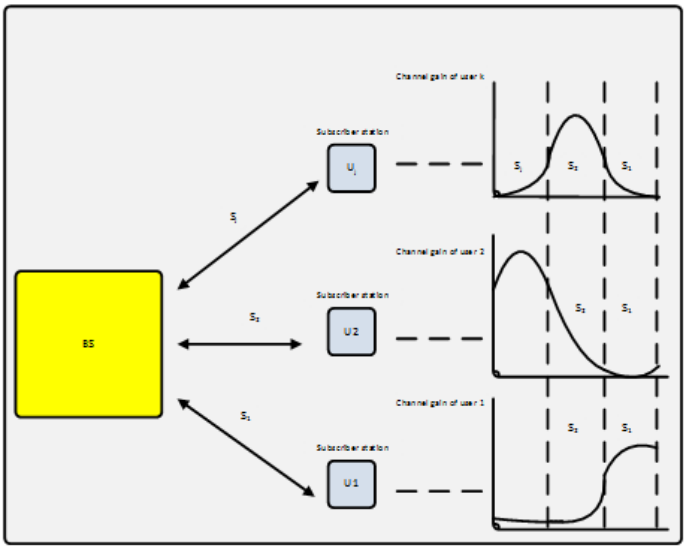

Figure 1: OFDMA based point to multipoint networks

Normally a cell or a site is prepared with its probable load capacity of that specific area. Also the resources starts to be used up incrementally rather than suddenly even though this case is also considered. Hence the necessity of the extra resources comes after the distribution of existing resources. But also, if the system is not ready before finishing of 100% of its resources, it might face a QoS crisis specially in terms of delay when new requests start to pop into the system because optimized resource decision usually are computationally expensive than non-optimized solution. However, most of the existing works focus on instantaneous sum rate or delay improvement or both. This is why we propose to do a long term system wide optimization with our proposed solution model which clearly shows significant improvement in performance and stability. Then we also perform our experimentation based on the proposed solution in a full-fledged network simulation with modeling using cross layer mechanism (Figure 2).

This paper describes the methods to enhance both speed (delay) and volume of data transfer/time slot (throughput), from system wide average performance perspective. As radio resource management (RRM) has direct impact on network performance, this paper proposes an effective solution that can handle higher number of users than that of existing reference systems with support of better QoS in terms of system wide fairness. Here we also consider the problem of fairness in this solution even though maximizing system sum data rate but many times the process shut off the user during scheduling time due to that they don't have good channel gain. We propose a threshold based resource distribution where the system sum data rate is increased but without shutting off current users, rather we propose to use a certain portion of available bandwidth from high rate consuming users by means of threshold calculation algorithm and share with starving users along with adaptive allocation to balance system wide performance. However in the beginning we would show

2 The Proposed Solution with System Model

The system model for the proposed solution is a cross layer model for OFDMA based connection oriented networks. Multilayer communication and contribution to accurate decision making on resource distribution is considered as depicted in the figure 2.

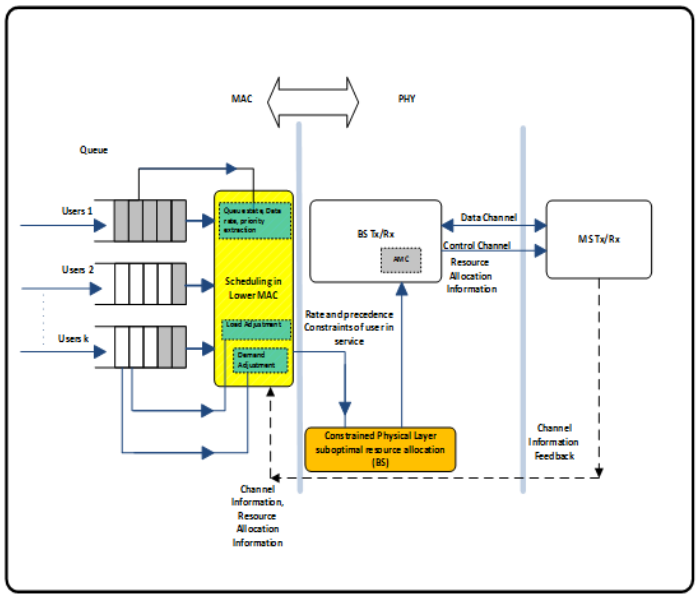

Figure 2: Base cross layer system model for proposed solution

This paper proposes solution for a long term effectiveness and stability for the system. The system model is based on figure 2. This paper introduces a new resource allocation strategy based on threshold optimized distribution and re-allocation approach. Initially, the system allocates resources based on cross layer system model which is adaptive. As the load increases, it triggers a new re-evaluation process based on proposed threshold model and most recent updated history of resource distribution. We consider the system to look into existing connected users' allocation from the history of the system to understand the minimum rate requirement (Rminimum) for current services in place for the user. Usually resources are not 100% occupied on 100% timescale. So the idle queue information is also included into decision making to stop the idle user and use that resource for the one requesting or, for the user currently starving. It may look a bit harsh from fairness perspective from the first look, but it has really good effects on the system performance as we will show by means of simulation based on the mathematical formulation proposed along with the algorithms.

Mathematically, the optimization problem considered here can be formulated based on [1] and shown below:

$$\max_{p_{k,n}\rho_{k,n}} \sum_{k=1}^{K}\sum_{n=1}^{N} \frac{\rho_{k,n}}{N} \log_2\left(1+\frac{p_{k,n}h_{k,n}^2}{N_0\frac{B}{N}}\right) \quad (1)$$

Subject to

$$C_1: \sum_{k=1}^{K}\sum_{n=1}^{N} p_{k,n} \le P_{total},$$

$$C_2: p_{k,n} \ge 0 \; for \; all \; k,n,$$

$$C_3: \rho_{k,n} = \{0,1\} for \; all \; k,n,$$

$$C_4: \sum_{k=1}^{K} \rho_{k,n} = 1 \; for \; all \; n,$$

C_5: $E[T_k] \leq \tau_k$.

Here,

- K is the total user number,
- N denotes the total subchannel number,
- B and P_{total} are the total bandwidth and power.
- $p_{k,n}$ denotes the power that is allocated for user k on the subchannel n
- $\rho_{k,n}$ is to be either 0 or 1, that indicates if user k is using subchannel n.
- fading and channel gain of user k on subcarrier n is $g_{k,n}$, having AWGN or additive white Gaussian noise, $\sigma^2 = N_0 \frac{B}{N}$, and N_0 denotes noise power spectral density [1]
- and its channel to noise ratio for the subchannel, $h_{k,n} = \frac{g_{k,n}^2}{\sigma^2}$
- user k receives the SNR on subcarrier n, $\gamma_{k,n} = p_{k,n} h_{k,n}$
- C4 shows each subchannel can be used by one user only.
- user k has the channel capacity of R_k which is given below:

$$R_k = \sum_{n=1}^{N} \frac{\rho_{k,n}}{N} \log_2 \left(1 + \frac{p_{k,n} h_{k,n}^2}{N_0 \frac{B}{N}} \right) \quad (2)$$

Users bits are modulated in BS into N M-level QAM and then combined using IFFT into OFDMA symbols [34], [35], the subchannel-to-noise ratio using [37] be,

$h_{k,n} \geq 4$ and BER$\leq 10^3$,

and, $BER_{M-QAM}(\gamma_{k,n}) \approx 0.2exp\left[\frac{1.6\gamma_{k,n}}{2^{\gamma_{k,n}}-1}\right]$.

then, solving for number of bits, $r_{k,n}$, we have

$R_{k,n} = \log_2 \left(1 + \frac{\gamma_{k,n}}{\varphi}\right)$,

where, $\varphi = \left(\frac{-\ln(5BER)}{1.6}\right)$, which is a constant (SNR gap) and $H_{k,n} = \frac{h_{k,n}^2}{N_0 \frac{B}{N}}$.

We vary users by high priority users and general users (low priority). Thus if the users are of type high priority users, the rate calculation would be,

$$R_k = R_k + \frac{B}{N} \log_2 \left(1 + \frac{pH_{k,n}}{\varphi_{high}}\right) \quad (3)$$

if the user is of low priority, the rate calculation will be

$$R_k = R_k + \frac{B}{N} \log_2 \left(1 + \frac{pH_{k,n}}{\varphi_{low}}\right) \quad (4)$$

Equation 3.3 and 3.4 will be used to calculate rate for the user during allocation cycle.

- with the Physical layer resource allocation, we include the delay bindings of a user that can be extracted from MAC layer when a request is heard at the MAC in connection oriented networks such as WiMAX. We assume, if E[T_k] is the average system time of user k and τ is its delay bound, the delay requirement of the user k can be formed as C5 considering a M/G/1 queue in a Poisson distribution based system [27]. The value of τ, is inversely proportional to the priority of the user.

To take this into consideration, we introduce an index of the users' delay bound and accordingly sort it according to the index; the lowest delay bound first and subsequently the rest of the index in increasing order. If the same delay bound is found for multiple users, first-in first-out mechanism is considered to serve them.

As the optimization of (2.1) involves both continuous variables $p_{k,n}$ and binary variables $\rho_{k,n}$, it becomes very hard to solve in computing environment. Furthermore, non-linear constraintsgives rise to higher complexities in order to find an optimal solution [1]. If we separate the power and subcarrier allocation in suboptimal manner, the complexity would reduce to almost half, since the number of variables of the objective function reduces to half [1]. So, we use maximum weight matching techniques from graph theory for subcarrier matching and allocation. For power allocation the proposed algorithm in [1] has very low complexity which can be used to get minimized power distribution among users and hence the higher possible values for (3.2). However, power optimization is not the focus of this work even though it can bring definite improvement in performance. For simplicity, we adopt greedy water filling method from [28]. The solution is different in many ways to [1] such as, it considers priority and QoS parameters such as delay whereas [1] does not. Secondly it uses graph theory whereas [1] uses Lagrangian relaxation which may require high computational resource for optimal solution. As subcarrier matching with constraints can be categorized as combinatorial optimization because it needs to find optimal allocation by matching from a finite set of subcarriers and exhaustive search is not feasible as it is expensive in operations. Thus Hungarian Algorithm is used along with the proposed solution. It is also called Kuhn-Munkres Algorithm (KMA) which works on bipartite graph to find a match optimally, that is, it is guaranteed that it would find an optimal solution and this is the reason we adopt this to get the subcarrier of maximum matching during the subcarrier allocation part. Also, it considers queue state of the connected SSs but [1] does not and it has different set of constraints to [1] which is another reason to be distinct as a solution. In this paper the core is of subcarrier allocation, assignment and related issues with detailed design. However, there is a commonality which is that both address the issue of enhancing system throughput but it does it in distinctive ways using the techniques and mechanism described in the next section that provide higher performance of the overall system and this would be demonstrated by simulations in WiMAX based network simulator. In the next part the subcarrier allocation algorithm will be described.

2.1 Subcarrier allocation algorithm

During subcarrier allocation, the first thing that the system will need to see is what is the rate and requirements. We formulate here, assuming B bits per symbol loaded for every subcarrier, if a user requested R bps with subcarrier spacing to be D_f Hertz, the total number of subcarriers to be allocated to the user would be,

$$S = \left\lceil \frac{R}{(BD_f)} \right\rceil$$

There are a few steps involved in the proposed subcarrier allocation algorithm, they are firstly collecting MAC layer information of how many subcarriers is needed by a specific user, labeling users and subcarriers to form bipartite graph, assignment of weight, optimizing the assignment and collecting optimized allocation information. This completes the bit and power allocation. After that this resource allocation information is finally sent to SS through dedicated control channels.

The proposed solution converts the allocation problem into a weighted bipartite matching problem. The matching graph is denoted as G=(U,V,E). U is referred to as subset of users, V is subset of vertices that represents the subcarriers to be assigned, E is the subset that has the set of selected subcarriers, U and V are disjoint subsets. Next we find a matching from U to V on a one-to-one basis. A valid matching is constrained by requirements like C4 in (2.1) which restrict that one subcarrier can be used by one user at a given time, which eliminates interference probability. We need to assign the weight for each edge expressed as w(e). Before assigning the weight, we need to sort the users according to priority and delay bound to meet the delay requirement expressed by C5 to ensure that the serving user can have appropriate QoS. Then after assigning the channel gain as weight w(e) for each edge e∈E, the problem now is converted to constrained weighted bipartite matching problem. After weight assignment, the calculation for matching starts. However, the bipartite graph produced does not provide optimized assignment, which means that the number of subcarrier a user gets, might be higher if we do further optimization on the graph. To get optimal solution for a match, Kuhn-Munkres [29] algorithm (KMA) is used in our solution for highest possible cardinality to achieve highest performance in terms of data rate because for single objective optimization, it is known that KMA can always find the optimal matching for a bipartite graph with O(n3) computational complexity [30]. The KMA is based on the procedure of the Hungarian algorithm [31]. The subcarrier allocation algorithm we came up with which includes matching part using KMA is provided here next.

Assume that,

A = {1, 2, …, N}, the subchannels in set.

S(A)=size of *A.*

N = total number of subchannels.

N_R =*Remaining channels*

R_i = set of user requests, i=1 to M

R_i = {R_1, R_2, …, R_M}.

Last request=R_L,

q = the request of user k for rate, q≠ 0

FS_k = the set for user k consisting of allocated subchannels

Z=Size (FS_k) = total subchannels of FS_k.

R_k = the total allocated rate/capacity for k

The steps of the allocation are as follows:

Start

Initialize:

$\boldsymbol{R_i = 0}$.

1. Sort the users as per the delay bound and priority information received from MAC layer in ascending order, and start processing from top to bottom. Get the number of subcarriers required to serve the current request: assign n_k = Z, for every user and $R_k > q$ and n_k is minimum, for all FS_k.
2. Repeat process 1 and 2 where total of $\sum n_k > S(A)$. $Ri = \{Ri - R_L\}$. R_L not accepted, as it is R while $S(A) <= \sum n_k$. Otherwise, N_R= size of $(A) - \sum n_k$
3. Run KMA for getting optimized FS_k for every admitted k having the number of the subcarriers in step 1, $S(A)$ is unchanged at this stage.
4. For all admitted k and $R_k > q$, update A, *with* $(A - \{FS_k\})$; R with $(R - q)$
5. $R_i = R_{(i+1)}$ if $R_i \neq R_L$
6. When $S(A) \neq 0$, $R \neq \{\}$, $n_k = n_k + 1$. Otherwise, if SFC = 0 then $R = R - R_{Lastone}$.
7. Repeat 1 - 7 while size of (A)> n_k
8. Assign p for each element in $R_i$using Greedy waterfilling
9. Call module **rate_allocation(selected_subcarrier)**

End

//module rate_allocation pseudo code

rate_allocation(selected_subcarrier)

{//start

if user priority == high{

use equation 2.3 to calculate rate assignment

update system of the assignment

}

else if user priority == low{

use equation 2.4 to calculate rate assignment

update system of the assignment

}

} //end

3 Threshold Based Optimal Resource Re-Distribution Algorithms

In this paper we consider a special problem or scenario where the number of users might get high typically higher than what is originally planned. Putting extra BSs is expensive, infeasible and time consuming. We propose a solution to this problem which exploits the idea of greedy type of resource distribution and re-distribution over time. We assume that any user with higher priority enjoys the best possible resource in terms of sub channels and power allocation, and the user has lower need of bandwidth because it already has it more than what it requires. This type of users are easily identifiable from the history of the allocation and also in MAC layer allocation log. However, we put the constraints that if the delay bound of a user (τ_k) is lower than other users in the same type queue, the previous one would be served first if the required power is available and there are enough subcarriers to entertain the request. If available power is not enough, it needs know it can manage it from within the existing resources used or unused. If it does

not get that, the user would be rejected. However, when it needs more subcarrier if there is not enough available, it would start to search for it. This is the point where the algorithm would start to subtract 1 subcarrier from each of the highest rate consuming nodes from the sorted index in the MAC layer as per the proposed formula. This process continues until the highest consumers' rate becomes reduced to threshold maximum (threshold value T_h will be derived in this paper next), and the new users are put under the continuous system flow of assignment and allocation. Finally, when the threshold T_h in (3) is reached, no further re-assignment is done and the user request for resources might be queued or dropped.

3.1 The major steps of the algorithm

3.1.1 Initialization:

Besides system parameters described earlier we need to add few more parameters to run the proposed solution. The new main parameters here that need to be added are threshold values (to be used in the next section) T_h, the set $\{\sigma_i\}_{i=1}^{K}$, where σ indicates the value for user *i* which signifies the proportion of resources fixed for his service as per the service layer agreement (SLA), K is the number of users.

3.1.2 Run distribution:

If the system has enough resources unutilized then this part still would be running the resource allocation algorithm described earlier. However, as soon as the resources are utilized with assumed 100% of the total resources, it starts the re-distribution process as the systems proactively calculates and run algorithm for saving and reusing existing resources described next. This process can start earlier for example when the resources are 50%-80% consumed to reduce computational delay as there will be ample history data of existing users to be used.

3.1.3 Run re-distribution:

This section will start the full optimal solution once the resources are already in use to a full scale. The system will re-examine with the existing user list and its allocation. The system starts the following new process in the system. The solution in paper 4 performs requirement formation and assignment of subcarrier in one phase and power allocation in another phase. However, when the number of users exceeds the limit, and they need to manage subcarriers as well as to know the power availability and required power level for each subcarrier $p_{k,n}$ (from section 4.4), the total maximum power P_{total} is fixed for a BS and it is being used by users already admitted in the system. This process will trigger once the resources reach $\frac{N}{2}$ or $\frac{P_{total}}{2}$ whichever comes first in this case. The reason is that it can get ample time to process the steps below to avoid processing delay that would affect the QoS. At this stage the systems acts like its resources are already exhausted but in reality it still has resources. This heuristic process adds benefits to the system resource management in terms of entertaining more users' request and maintaining the QoS performance in course of time.

Sub Steps of the algorithm for reallocation re-distribution

- Run extra-user accommodation process in case of (total resources)/2 <= (total usage at the moment),
    - Search through all users current allocation information
    - extract current usage information

- ✓ if service queue is idle, remove the connection and delete the whole resource of that connection type from the allocation

o Extract users with 0 requirement, and these would be the ones that already have the highest amount of resources for their SLA. We define a requirement index for all the users indicated by the following equation:

$$R_k^{index} = \begin{cases} q, & R' \leq R_{minimum} \\ 0, & R' > R_{minimum} \end{cases} \quad (5)$$

Where R' is the already allocated resources to the user and $R_{minimum}$ is the required minimum rate for the service currently using, q is defined in paper 4, section 4.3 which is the rate requirement of a new requesting user. We also assume, a user *k* having current rate beyond the $R_{minimum}$ has a necessity of rate request indicated byR_k^{index}.

o Subtract $N^{\oplus}$ subcarrier from each of the highest rate consuming range
- ✓ Follow the new equation of subtracting

$$N_k = \left[N \left(\frac{\sigma_k}{\sum_{i=1}^{k} \sigma_i} \right) - 1 \right] \quad (6)$$

and,

$$N^{\oplus} = \sum_{i=1}^{K} IntegerOf(N_i) \quad (7)$$

Where, k=1, 2, 3, …, K, N^{int} is the nearest rounding, and $\{\sigma_i\}_{i=1}^{K}$the set of constant values as per SLA to provide proportional part of resources for service. N_k indicates deduction of 1 subcarrier from the required total number of subcarrier for his service.

o Determine if

$$\sum N^{\oplus} \geq R_k^{index} \quad (8)$$

- ✓ if this condition is met, then it is enough to serve current rate request, assign it to the requesting user, at the same time distribute required power for bit loading using greedy water-filling.

o if resources get freed anywhere in system, assign first to the users that contributed to the previous process with subcarrier deduction until their previous allocation as per SLA, provided if they are requesting more resources. The reason is that they are usually of higher priority users.

o if more resources are available, keep it as reserved resource to serve new resource request incoming by incrementing resource indicators.

o if resources are available to serve the whole user base, use suboptimal solution.

At this stage we need to know the threshold value and how it is calculated. This is described next.

3.2 Calculation of threshold value Th

To calculate the threshold value T_h, first (2) can be written in terms of data rate as:

$$\boldsymbol{T_h = \frac{R_k}{2}} \quad (9)$$

This depends on the number of subcarriers assigned (F_k in section 4.4.1) to user k, and power assigned to user k is expressed as:

$$\boldsymbol{P_k = \sum_{i=1}^{x} p_{k,n_i}} \quad (10)$$

Where,

$\boldsymbol{P_k}$ is the total power assigned to user k,

$\boldsymbol{p_{k,n_i}}$ is power assigned to subcarrier n of user k and i=1 to x, and

$\boldsymbol{x}$ is the number of subcarriers assigned to user k in set F_k (from section 3.4.1).

Figure 3.8 shows the whole process of the solution, and the dotted box shows the threshold based re-distribution module.

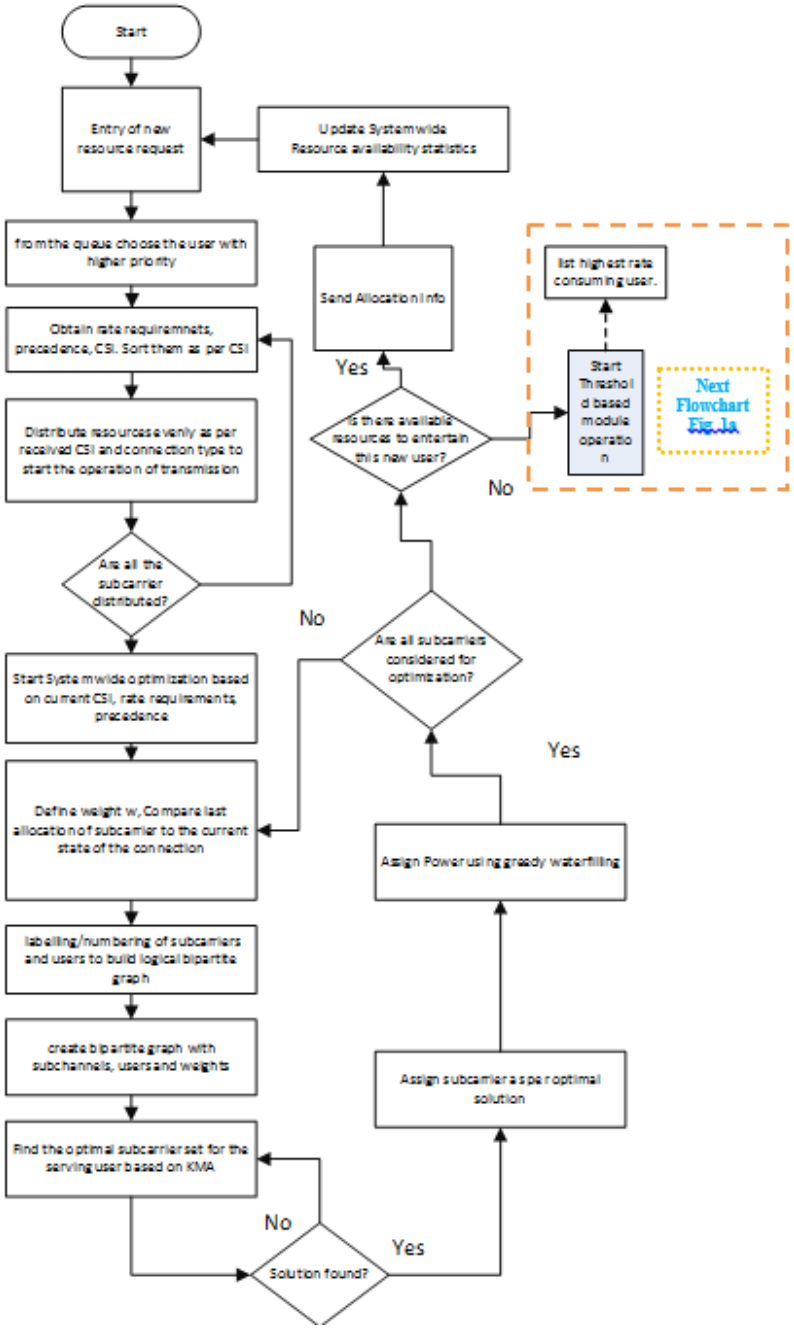

Figure 1: Total algorithm flow of the proposed solution along with threshold based distribution module (added flow chart next due to space)

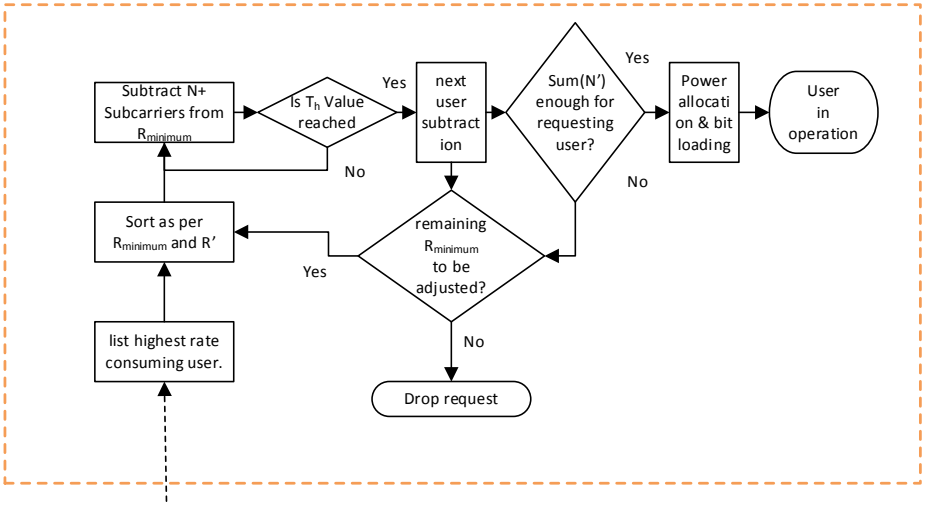

Figure 1a: Th based resource re-distribution module flowchart

4 Performance Evaluation

The results obtained from carrying out several simulation experiments in the current study were examined and evaluated in order to prove the performance of the proposed solution under various conditions. The aim of such experiments is to assess the ability of the proposed solutions and test its effectiveness.

In the following experiments, the threshold based optimal resource reallocation and re-distribution increases the total sum rate and as well as QoS performance. It is achieved by reusing existing subcarriers and power more efficiently to allow low priority nodes to use adequate resources while not affecting the higher priority nodes. It creates system wide better network experience contributing to higher overall sum rate and QoS benefits. To evaluate the performance of the proposed solution, we compare first with Zukang Shen et al. (Ref [1]) under the same conditions here.

5 Simulation and Results

This paper investigates different cases with the simulation. We mark the proposed algorithm to be AORAA in the graphs because the algorithm works in conjunction with AORAA proposed in paper 4, though the process of paper 4 has a number of changes to adopt the proposed algorithms in this paper. To distinguish, paper 4 proposes the optimized subcarrier assignment and allocation algorithm in some details, while paper 5 proposes a threshold based resource balancing algorithm with mathematical formulation that improves the long term network performance.

5.1 Effects of Various Network Load

We implement the steps shown above in QualNet WiMAX simulator (Advanced Wireless Model, Version 1), the results produced shows improvement that we will explore now. However, for smaller number of nodes performance variation is not too much as the resources are enough to support the load and this is why we will show the simulation during benchmarking. Here we start from higher number of nodes contributing to the scenarios so that the improvement gets clearer with the provided graphs.

A. Scenario with 60 nodes

In this scenario there is a maximum of 60 nodes. The base parameters are as those described in paper 4. The plots are presented here for the two algorithms separately and benchmarked with other existing solutions at the later sections.

1. Using reference [1]

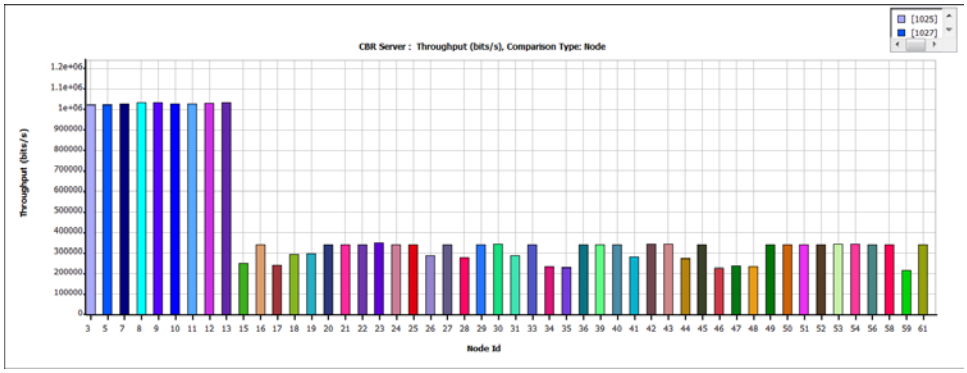

Figure 2: Throughput plot for reference [1] for 60 nodes

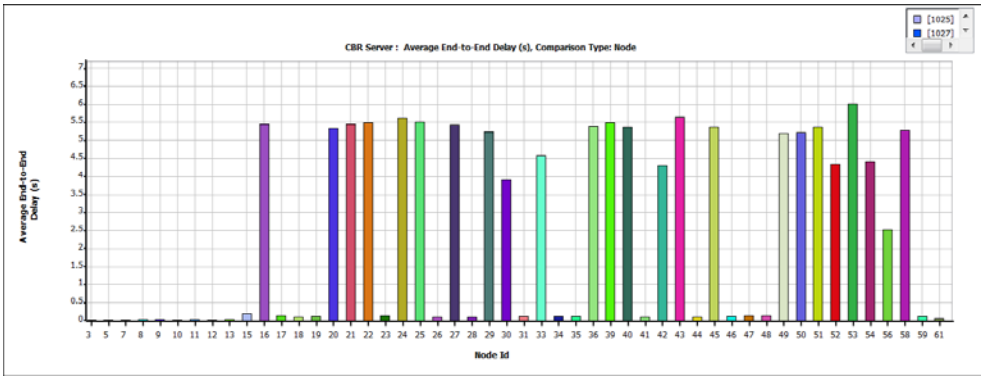

Figure 3: Average end-to-end delay plot for reference [1] for 60 nodes

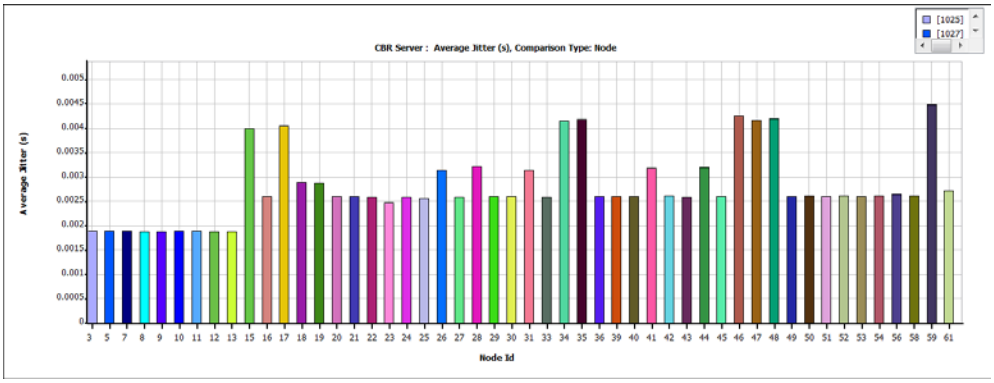

Figure 4: Average jitter for reference [1] for 60 nodes

2. Using AORAA

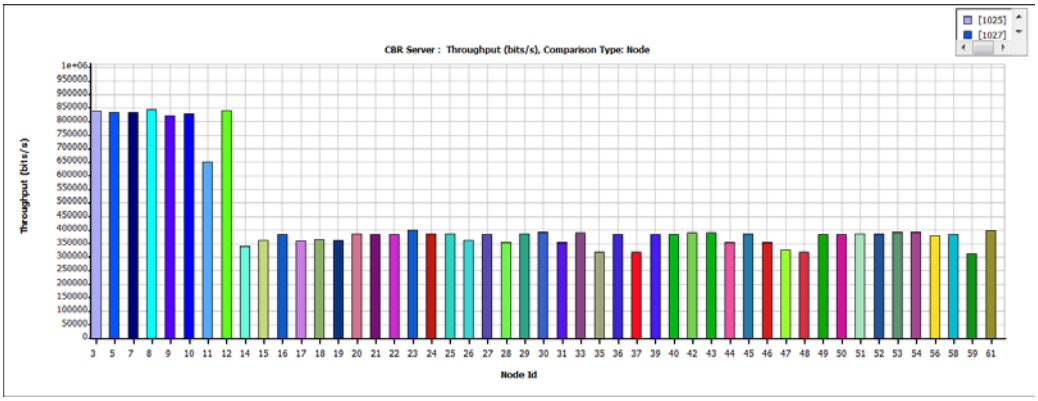

Figure 5: Throughput performance using AORAA for 60 users

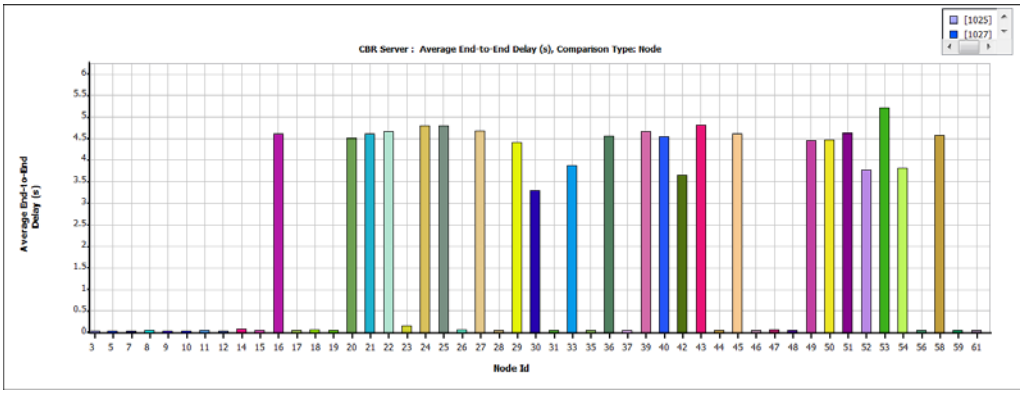

Figure 6: Delay performance with AORAA for 60 users

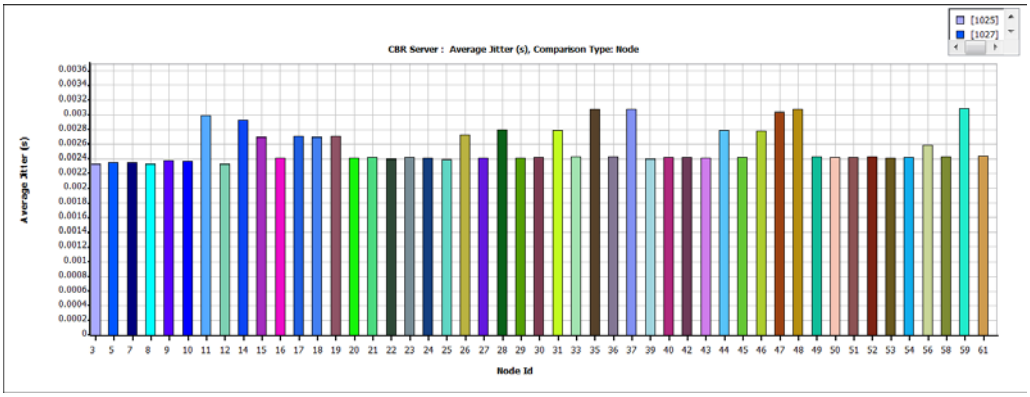

Figure 7: Jitter with AORAA for 60 users

► **Throughput and delay analysis of 60 nodes case**

In case of throughput for reference [1], it is seen that the maximum of 20% nodes with higher priority and requirements have the same throughput which is around 1Mbps whereas the throughput for rest of the 80% nodes are having around 250 Kbps. The delay of the 80 % nodes with lower priority is having average of around 5s. Some of the nodes have delays in millisecond scale. When AORAA uses the throughput of the higher priorities are reduced to around 850Kbps rather than keeping it 1Mbps. The other 80% of the nodes experience throughput of around 350Kbps compared to 250 Kbps in the case of [1]. The delay of

AORAA is also distorted but with the range of 4-4.50 s whereas it was near 5 s in case of reference [1]. This stemmed from the fact that the most disadvantaged nodes would be provided with the share of the resources from the best and highest resource-endowed nodes until the threshold (T_h) value is reached.

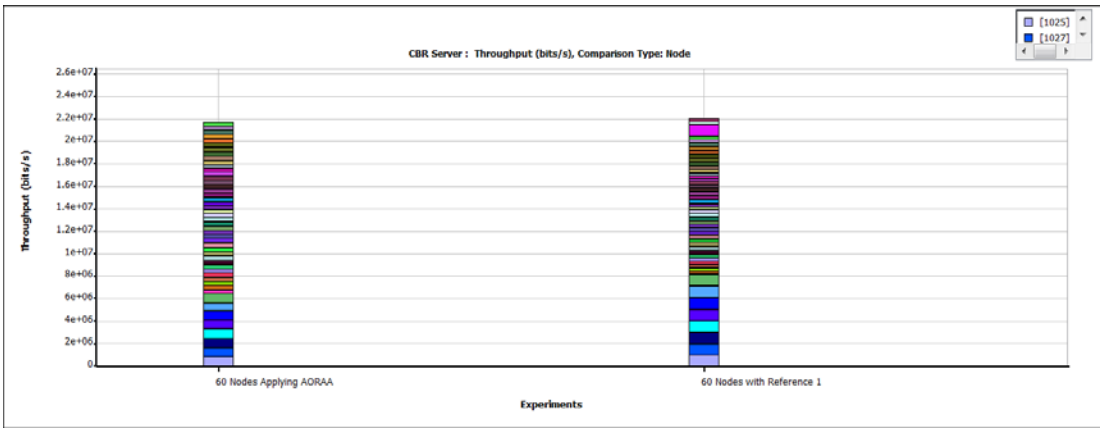

Figure 8: Throughput performance using AORAA and reference [1] for maximum of 60 nodes

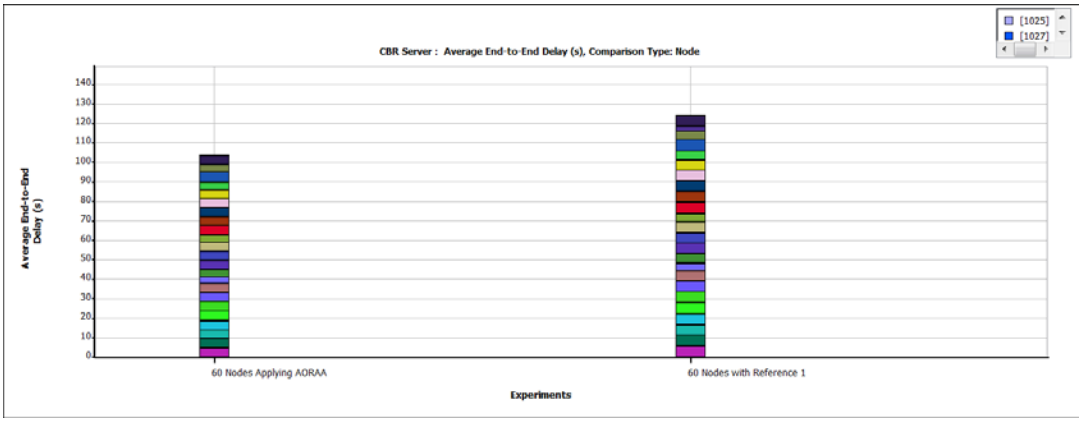

Figure 9: Delay performance using AORAA and reference[1] for maximum of 60 nodes

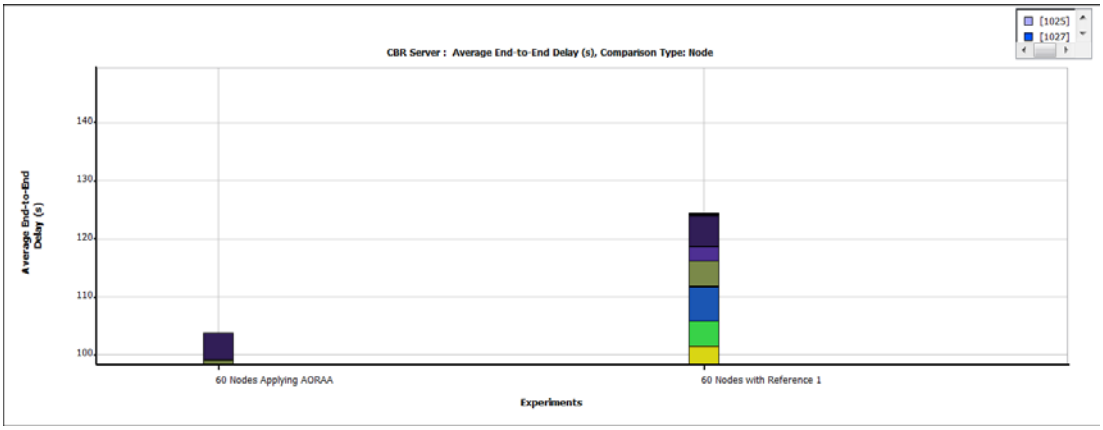

Figure 10: Delay performance using AORAA and reference [1] for maximum of 60 nodes (zoomed)

B. Scenario with 80 nodes

There are a maximum of 80 nodes for this simulation. Like previous scenarios the 20-80 division of priority is followed as before. The following figures show the output from applying reference [1] and AORAA. The comparison is given after few figures below.

1. Using reference [1]

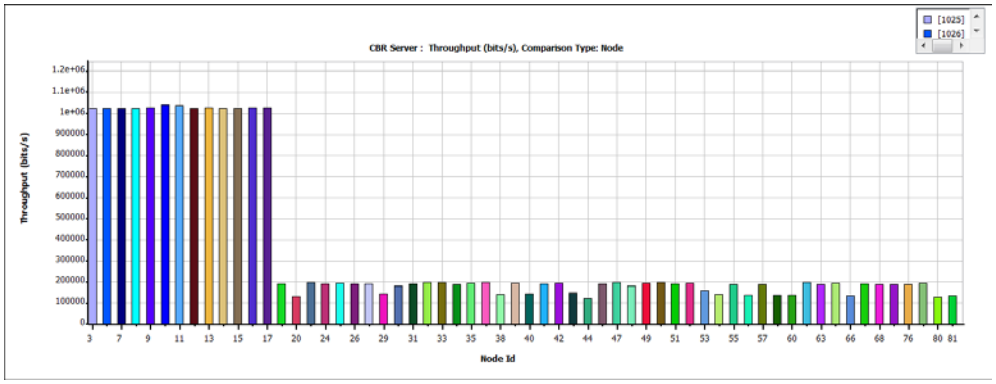

Figure 11: Throughput performance of reference [1] for maximum of 80 users

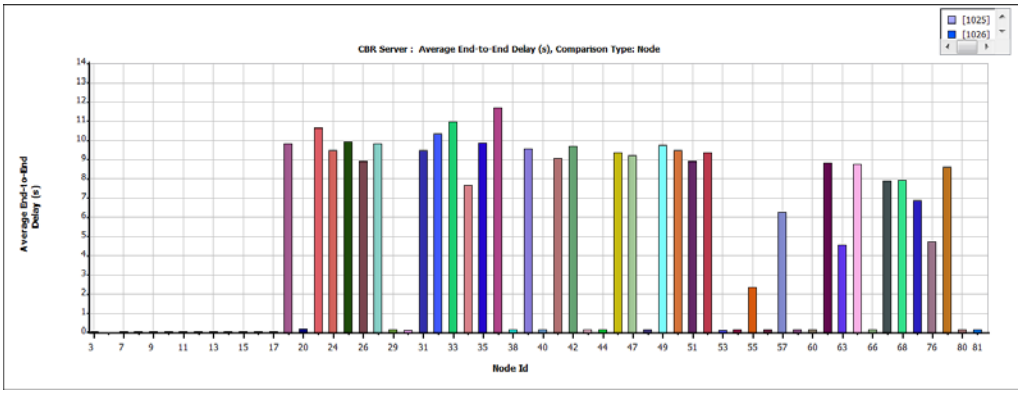

Figure 12: Delay performance of reference [1] for maximum of 80 users

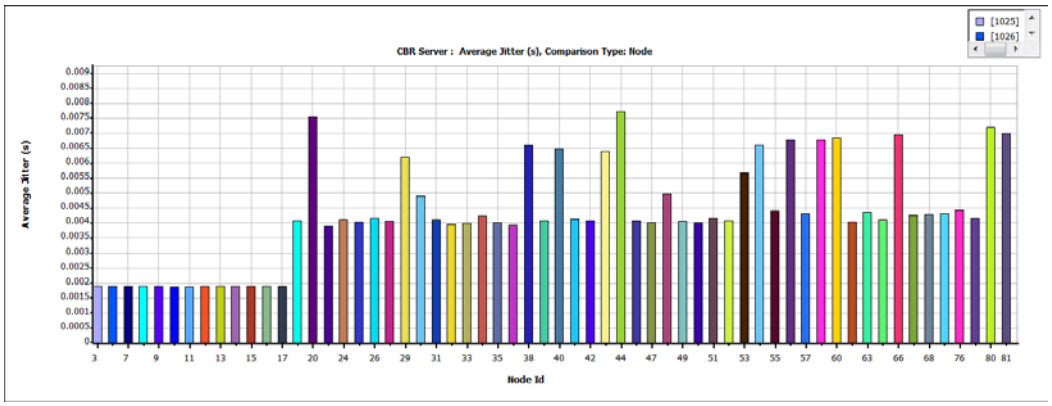

Figure 13: Jitter performance of reference [1] for maximum of 80 users

2. Using AORAA

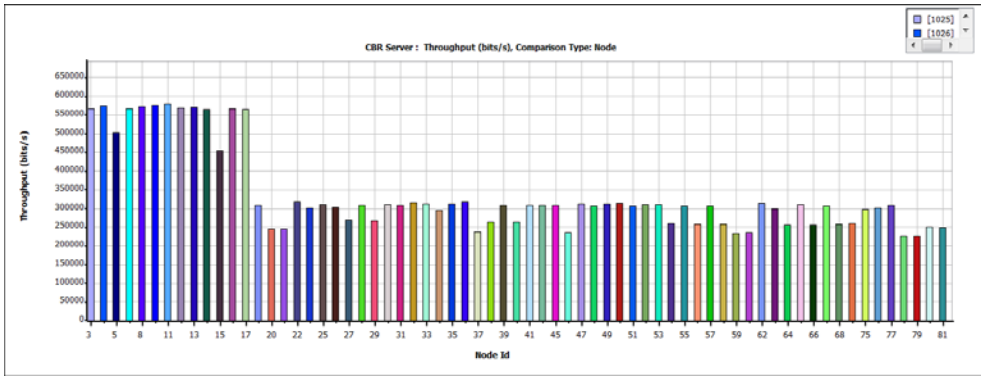

Figure 14: Throughput performance using AORAA on 80 users

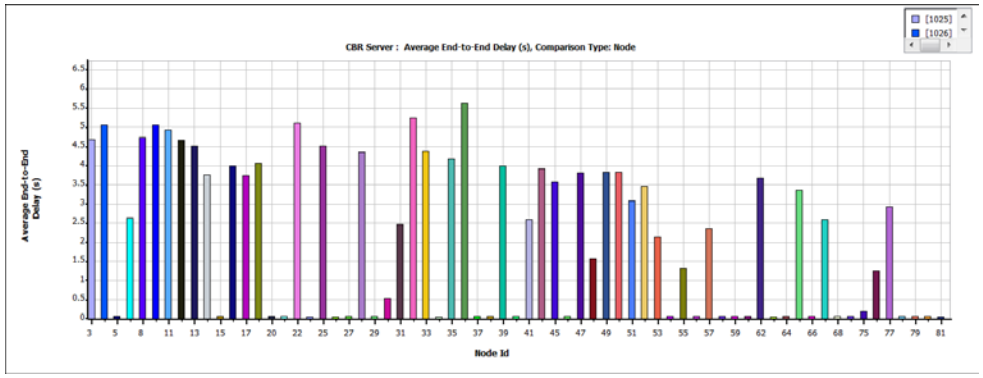

Figure 15: Delay performance using AORAA on 80 users

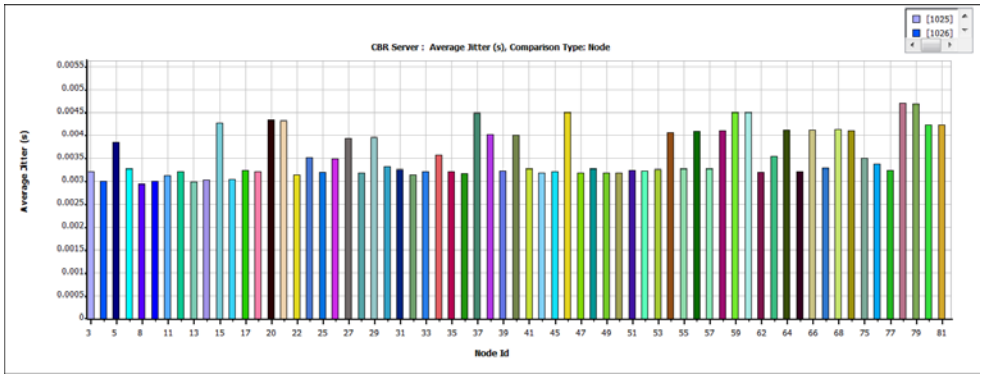

Figure 16: Jitter performance using AORAA on 80 users

► **Throughput and delay analysis of 80 user case:**

In this scenario, the 20% nodes with higher priority get what they should get which is around 1Mbps; and the rest of the 80% of lower priority nodes get the throughput of around 150 Kbps (where each of them should have 512Kbps at the best case). With AORAA, 80% of the nodes with lower priority get around 300Kbps bandwidth which is around double that of reference [1]. Then, for the average end-to-end delay, both cases of AORAA and reference [1], the delay performance is not uniform. But in case of AORAA the 20% high priority nodes suffer some distorted delay as well. However, for the average performance of the

whole system as shown in figures 19, 20. AORAA shows better delay and throughput performance than reference [1].

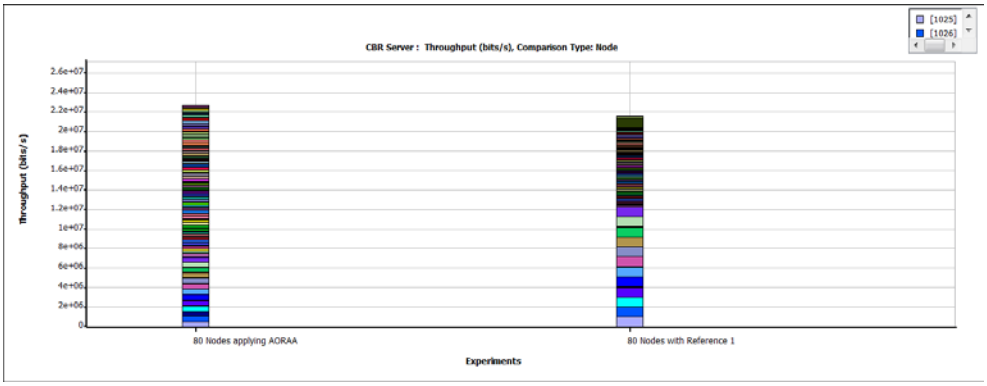

Figure 19: Throughput performance comparison of AORAA and reference [1] for maximum of 80 nodes

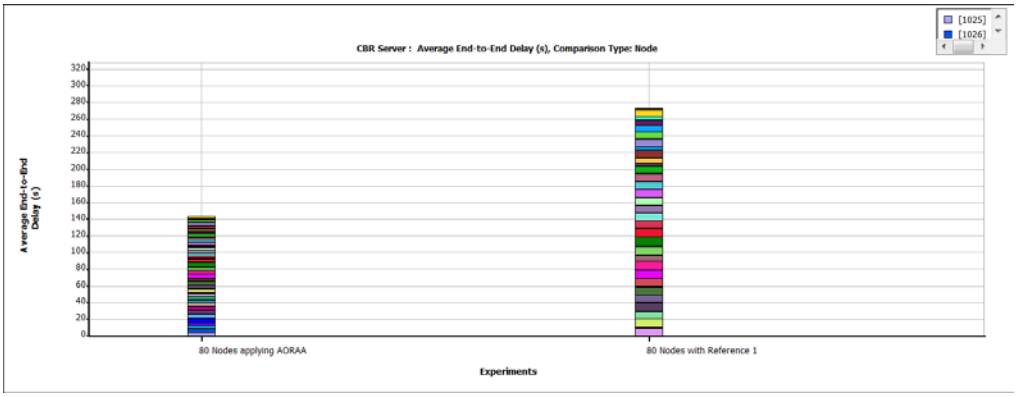

Figure 20: Delay performance comparison of AORAA and reference [1] for maximum of 80 nodes

C. Scenario with 100 nodes

In this scenario, there are a maximum of 100 users considered. This has quite a big effect on the overall system performance, however using the proposed algorithm the enhancements are proved here using the plots below comparing it to reference [1]. The discussion will follow next.

1. Using reference [1]:

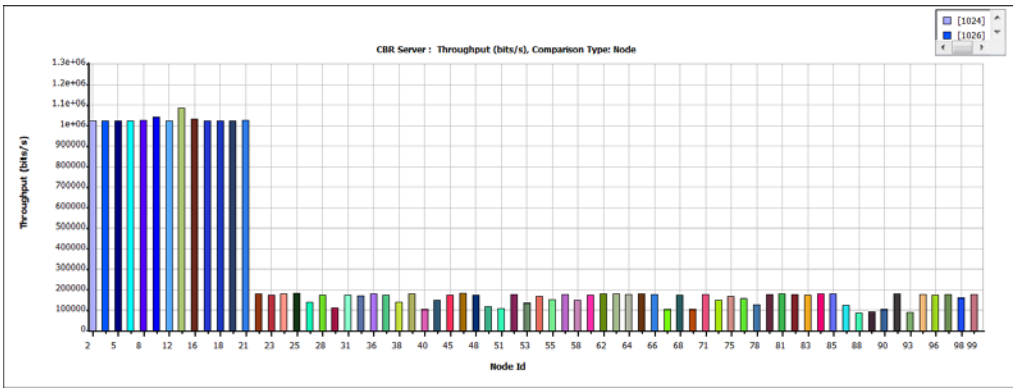

Figure 21: Throughput performance of reference [1] for maximum of 100 users

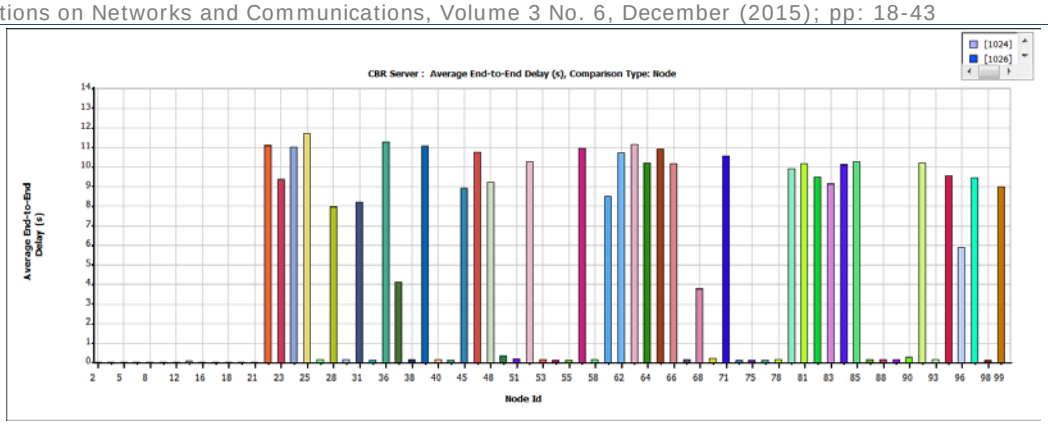

Figure 22: End to end delay performance of reference[1] for maximum of 100 users

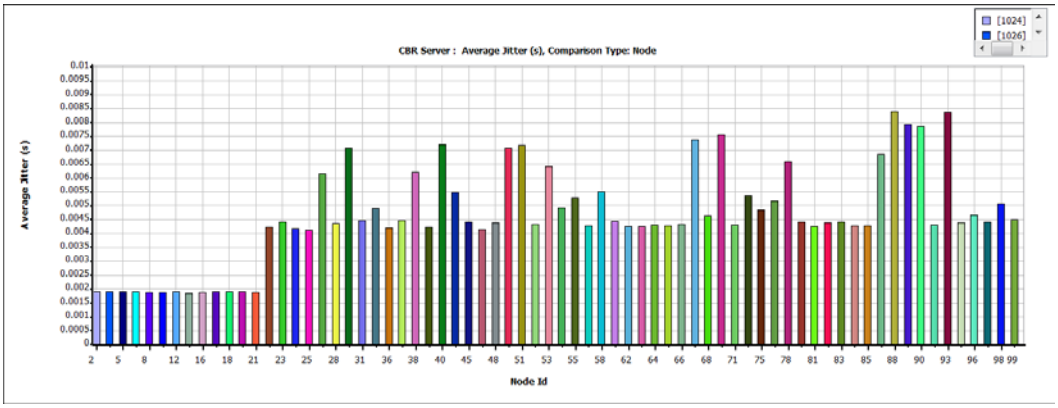

Figure 23: Jitter performance of reference [1] for maximum of 100 users

2. Using AORAA:

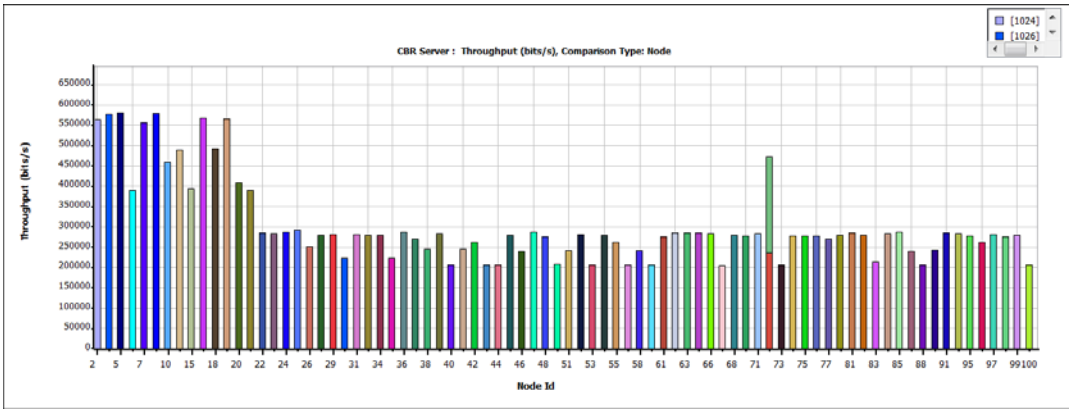

Figure 24: Throughput performance of maximum of 100 nodes using AORAA

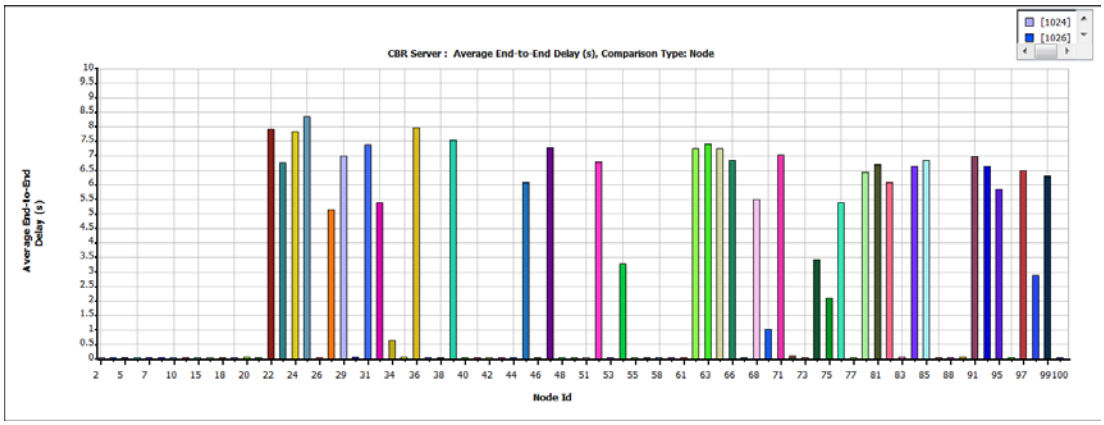

Figure 25: Delay performance of maximum of 100 nodes using AORAA

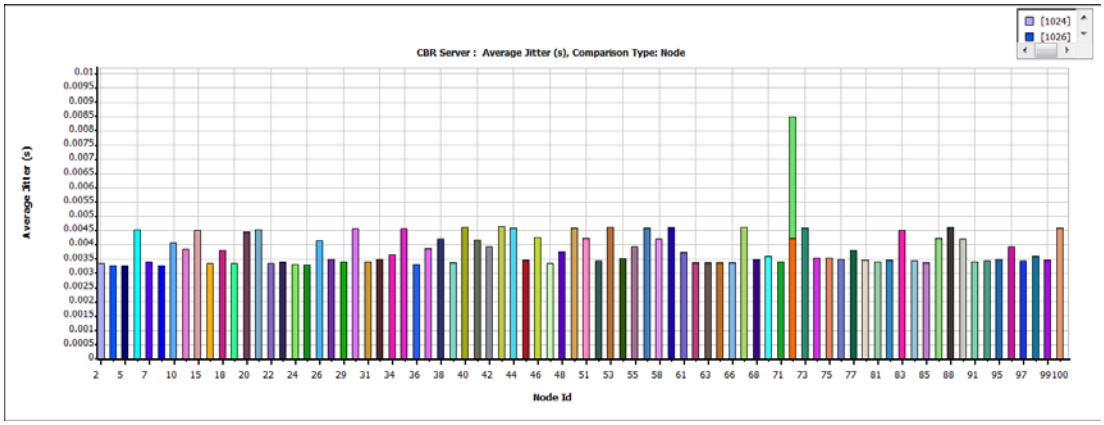

Figure 26: Jitter performance of maximum of 100 nodes using AORAA

► **Analysis of throughput and average end to end delay for 100 nodes:**

The compared values are given in a tabular format next. It is observed that for maximum of 100 nodes, the throughput of AORAA for whole downlink system is around 24.5 Mbps whereas reference [1] has around 22.5Mbps. For the case of delay it is observed that AORAA's average delay is 220s whereas for reference [1] delay is 320s. So it is clear that in both the cases the performance is enhanced.

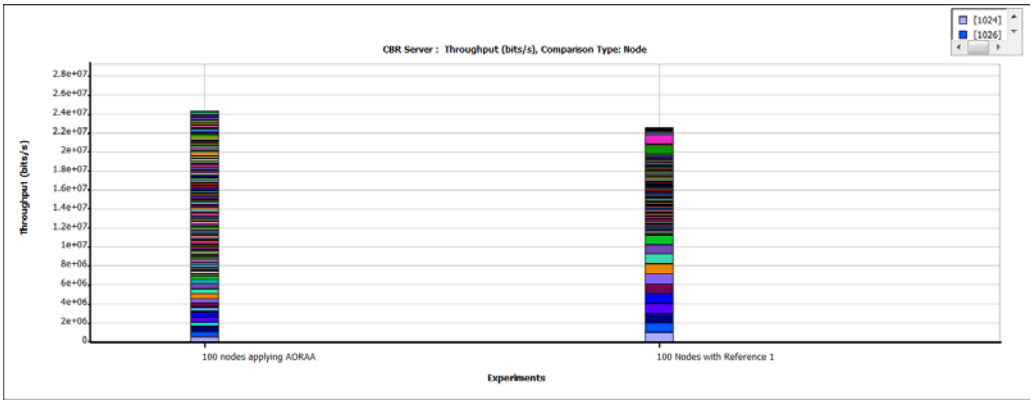

Figure 27: Throughput comparison of AORAA and reference [1] for maximum of 100 nodes

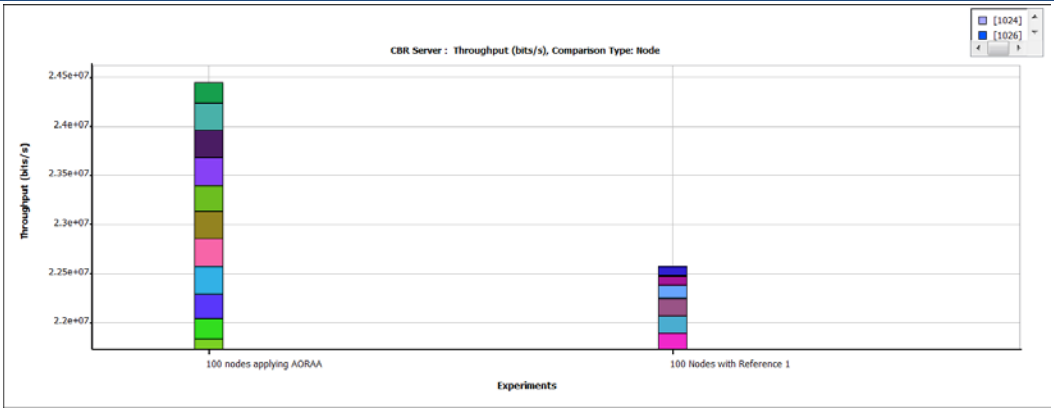

Figure 28: Throughput comparison of AORAA and reference [1] for maximum of 100 nodes (zoomed version of Fig. 27)

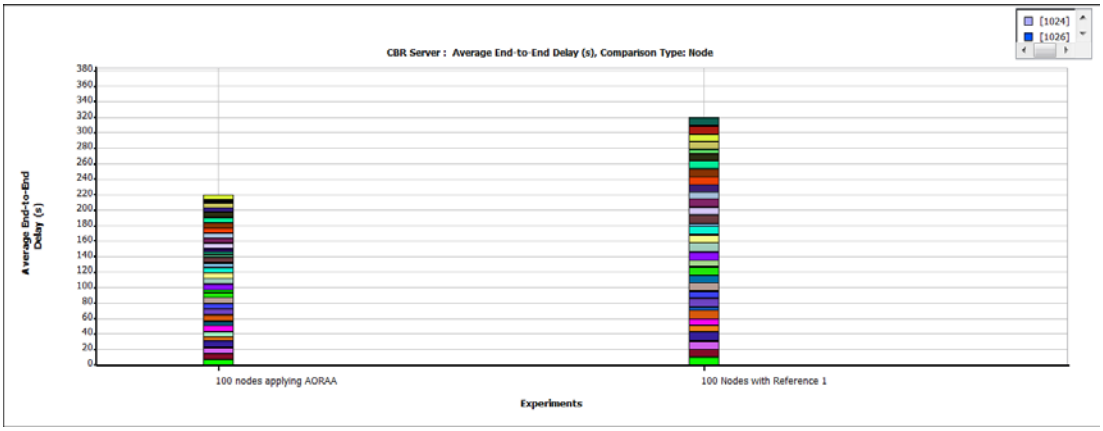

Figure 29: Delay comparison of AORAA and reference [1] for maximum of 100 nodes (total delay of nodes)

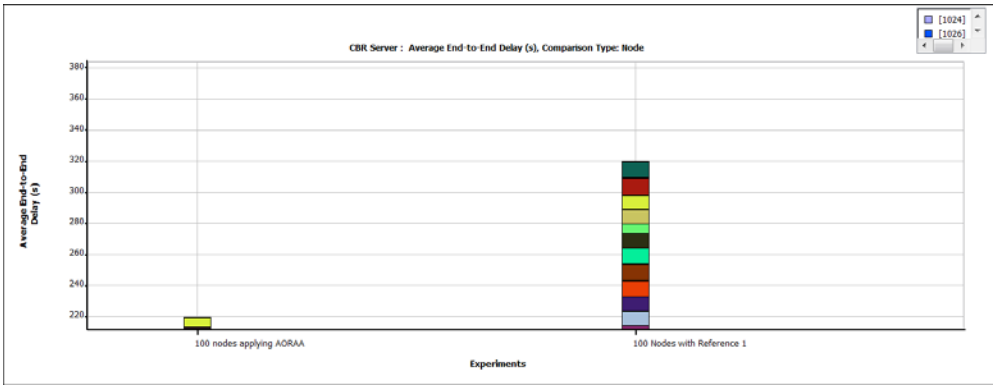

Figure 30: Delay comparison of AORAA and reference [1] for maximum of 100 nodes (zoomed)

D. Comparison of Global Trends of AORAA And Reference [1] for Threshold Based RA

From the plots below it is observed that the throughput increases as long as resources are available and the number of users increase. It happens for both the compared algorithms. Delay also increases the same way for both algorithms. However, by comparison it is shown that AORAA enhances the overall

system performance in terms of throughput and delay over reference [1]. Also it could be seen that this happens mostly when the number of users are increasing, this is when AORAA acts to balance the system.

1) AORAA

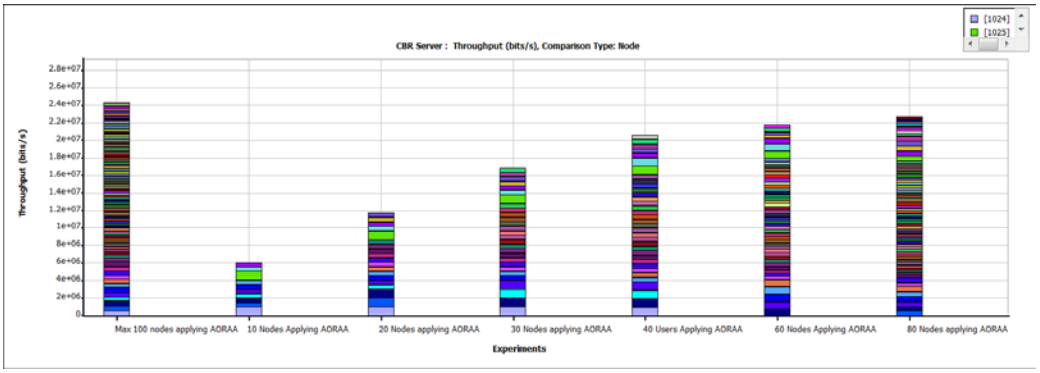

Figure 31: Trend of throughput for AORAA for different load

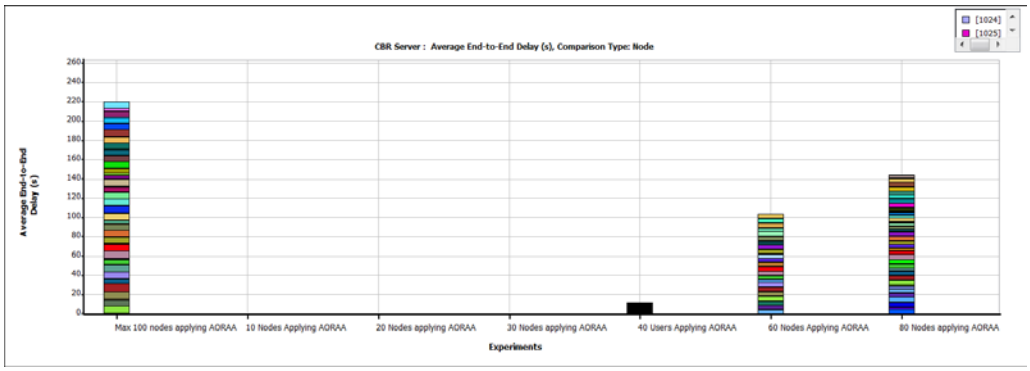

Figure 32: Trend for average end to end delay for AORAA (100 nodes at left most)

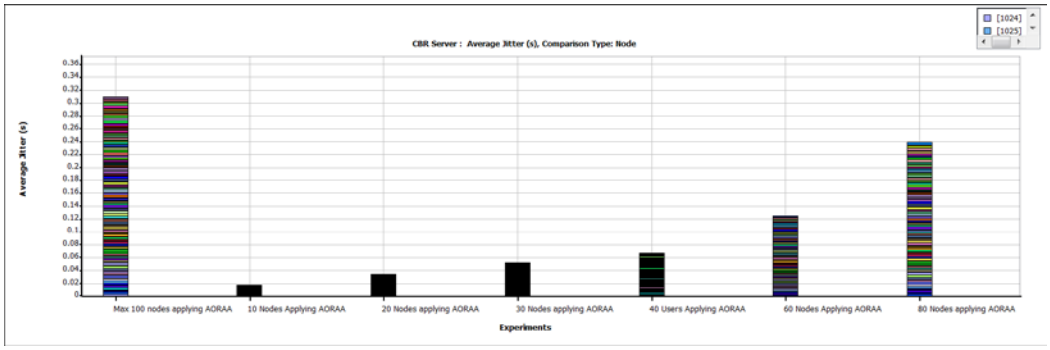

Figure 33: Jitter trend for AORAA (left most is the 100 nodes)

2) REFERENCE [1]

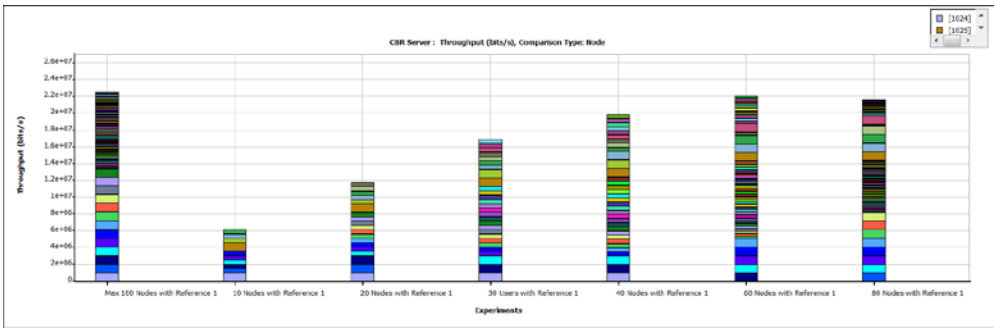

Figure 34: Throughput performance trend for reference [1]

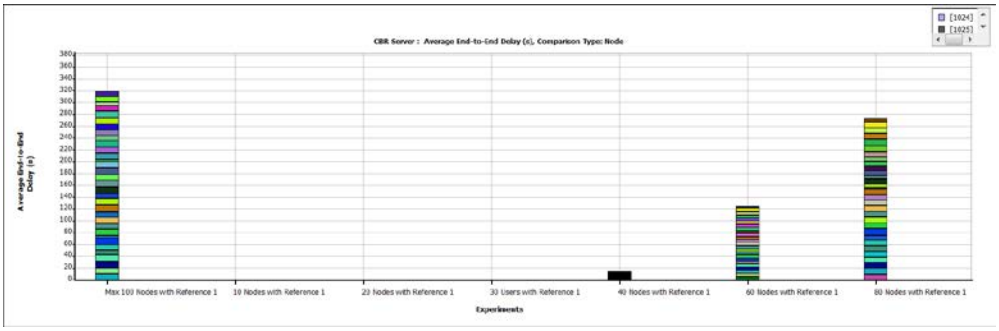

Figure 35: Delay performance trend for reference [1]

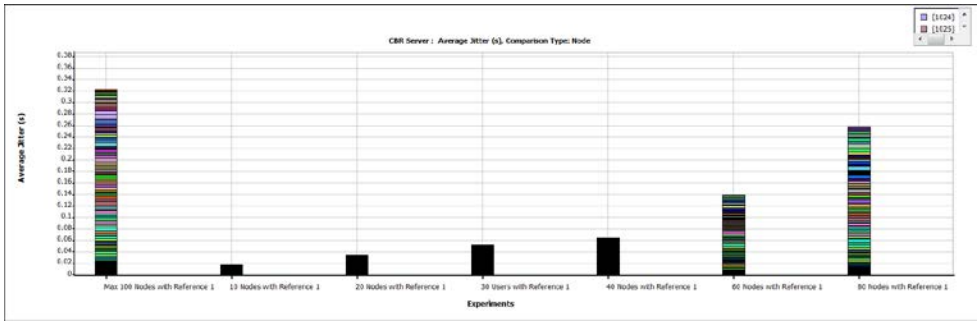

Figure 36: Jitter performance trend for reference [1]

6 Fairness Comparison and Algorithm Complexity

We need to compare fairness of the algorithm as well because this is an important performance parameter in a scheduling algorithm. In this section, we evaluate Jain's fairness index. On a whole fairness is reduced as more load is added to the same existing resources which has happened to all the comparing algorithms in figure 37. However, with the same condition, we will observe which one is performing better. It could be observed that threshold based AORAA achieves higher fairness value in the form of Jain's fairness index till around drop zone as marked in figure 37. Then it drops for some time and then increases than before for higher number of user. This is attributed to the threshold-based logic of the proposed solution. At that point it behaves a bit unfairly because it redistributes a portion of the high resource-consuming nodes to the starving nodes due to higher load on the system. Then it raises again in

the raising zone shown in the same figure. Whereas, fairness of ref[1] drops almost linearly and the fairness index is most of the time lower than the proposed solution. The algorithm complexity is at most $O(n^3)$. It provides optimal solution for subcarrier matching and guarantees to find matching in every cycle which results in higher throughput. In contrast Z. Shen et al. [1], cannot guarantee optimality and thus have performance gap, to guarantee same as proposed solutions, it requires O(n!) which is much higher comparing to our solution

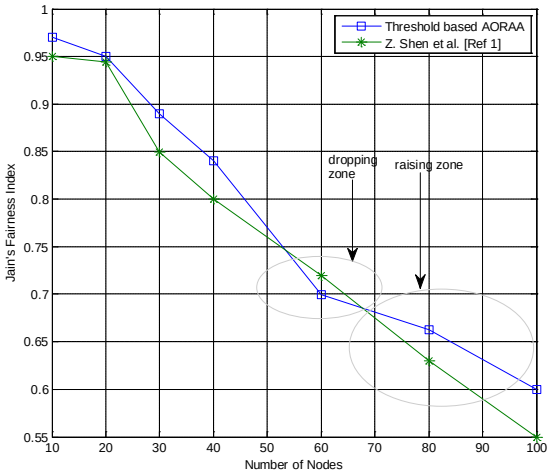

Figure 37: Fairness comparison using Jain's fairness index.

7 Conclusion

This paper described the proposed system AORAA for subcarrier allocation, threshold based optimized reallocation and re-distribution of user resource granting. This is to enhance network performance focusing mainly on system sum data rate or throughput and QoS metrics, especially delay and jitter. This has been simulated and compared to reference work [1]. After calculating the average performance metrics, we show that the proposed solution performs 31.9% higher for throughput and 23% better for delay performance. However we intend to implement the system on 4G and forthcoming 5G networks and it is left as near future work.

REFERENCES

[1] Zukang Shen ; Wireless Networking & Commun. Group, Univ. of Texas, Austin, TX, USA; Andrews, J.G. ; Evans, B.L., "Adaptive resource allocation in multiuser OFDM systems with proportional rate constraints", Wireless Communications, IEEE Transactions on (Volume:4, Issue: 6).

[2] Loutfi Nuaymi, "WiMAX: Technology for Broadband Wireless Access", ISBN: 978-0-470-02808-7, Wiley, 2007.

[3] Jian Zhu ; Sch. of Electr. & Comput. Eng., Georgia Inst. of Technol., Atlanta, GA, USA ; Bing, B. ; Ye Geoffrey Li ; Jun Xu ,"An adaptive subchannel allocation algorithm for OFDM-based wireless home networks.", Consumer Communications and Networking Conference, 2004. CCNC 2004.

[4] ProfNizar Zorba, Charalambos Skianis and Christos Verikoukis, "Cross Layer Designs In Wlan Systems".

[5] Sofoklis A. Kyriazakos George T. Karetsos, "Practical radio resource management for wireless systems", The Artech House Universal Personal Communications Series.

[6] Vasileios D. Papoutsis, Ioannis G. Fraimis, and Stavros A. Kotsopoulos, "A Novel Fairness-Aware Resource Allocation Scheme in Multiuser SISO-OFDMA Downlink", International Journal of Vehicular Technology Volume 2010 (2010), Article ID 432762

[7] J. Jang and K. B. Lee, "Transmit power adaptation for multiuser OFDM systems," IEEE Journal on Selected Areas in Communications, vol. 21, no. 2, pp. 171–178, 2003.

[8] G. Li and H. Liu, "On the optimality of the OFDMA network," IEEE Communications Letters, vol. 9, no. 5, pp. 438–440, 2005.

[9] S. Boyd and L. Vandenberghe, Convex Optimization, Cambridge University Press, Cambridge, UK, 2004.

[10] H. Rohling and R. Gruenheid, "Performance comparison of different multiple access schemes for the downlink of an OFDM communication system," in Proceedings of the 47th IEEE Vehicular Technology Conference (VTC '97), pp. 1365– 1369, Phoenix, Fla, USA, May 1997.

[11] C. Y. Wong, R. S. Cheng, K. B. Letaief, and R. D. Murch, "Multiuser OFDM with adaptive subcarrier, bit, and power allocation," IEEE Journal on Selected Areas in Communications, vol. 17, no. 10, pp. 1747–1758, 1999.

[12] G. Zhang, "Subcarrier and bit allocation for real-time services in multiuser OFDM systems," in Proceedings of the IEEE International Conference on Communications, pp. 2985–2989, Paris, France, June 2004.

[13] G. Yu, Z. Zhang, Y. Chen, J. Shi, and P. Qiu, "A novel resource allocation algorithm for real-time services inmultiuser OFDM systems," in Proceedings of the 63rd IEEE Vehicular Technology Conference (VTC '06), pp. 1156–1160, Melbourne, Australia, May 2006.

[14] D. Kivanc, G. Li, and H. Liu, "Computationally efficient bandwidth allocation and power control for OFDMA," IEEE Transactions on Wireless Communications, vol. 2, no. 6, pp. 1150–1158, 2003.

[15] C. Y. Wong, C. Y. Tsui, R. S. Cheng, and K. B. Letaief, "A real-time sub-carrier allocation scheme for multiple access downlink OFDM transmission," in Proceedings of the 50th IEEE Vehicular Technology Conference (VTC '99), vol. 2, pp. 1124–1128, Amsterdam, The Netherlands, September 1999.

[16] Q. Wang, J. Xu, and Z. Bu, “Proportional-fair bit and power adaptation in multiuser OFDM systems,” in Proceedings of the 17th IEEE International Symposium on Personal, Indoor andMobile Radio Communications, pp. 1–4, Helsinki, Finland, September 2006.

[17] W. Rhee and J. M. Cioffi, “Increase in capacity of multiuser OFDM system using dynamic subchannel allocation,” in Proceedings of the 51st IEEE Vehicular Technology Conference (VTC ’00), pp. 1085–1089, Tokyo, Japan, May 2000.

[18] Z. Shen, J. G. Andrews, and B. L. Evans, “Adaptive resource allocation in multiuser OFDM systems with proportional rate constraints,” IEEE Transactions on Wireless Communications, vol. 4, no. 6, pp. 2726–2736, 2005.

[19] I. C. Wong, Z. Shen, B. L. Evans, and J. G. Andrews, “A low complexity algorithm for proportional resource allocation in OFDMA systems,” in Proceedings of IEEE Workshop on Signal Processing Systems Design and Implementation, pp. 1–6, Austin, Tex, USA, October 2004.

[20] S. Sadr, A. Anpalagan, and K. Raahemifar, “Suboptimal rate adaptive resource allocation for downlink OFDMA systems,” International Journal of Vehicular Technology, vol. 2009, Article ID 891367, 10 pages, 2009.

[21] C. Mohanram and S. Bhashyam, “A sub-optimal joint subcarrier and power allocation algorithm for multiuser OFDM,” IEEE Communications Letters, vol. 9, no. 8, pp. 685–687, 2005.

[22] Y. J. Zhang and K. B. Letaief, “Multiuser adaptive subcarrierand- bit allocation with adaptive cell selection for OFDM systems,” IEEE Transactions on Wireless Communications, vol.3, no. 5, pp. 1566–1575, 2004.

[23] Z.Mao and X.Wang, “Efficient optimal and suboptimal radio resource allocation in OFDMA system,” IEEE Transactions on Wireless Communications, vol. 7, no. 2, Article ID 4450806, pp. 440–445, 2008.

[24] K. A. D. Teo, Y. Otani, and S. Ohno, “Adaptive subcarrier allocation for multi-user OFDM system,” IEICE Transactions on Fundamentals of Electronics, Communications and Computer Sciences, vol. E89-A, no. 11, pp. 3131–3137, 2006.

[25] Y. Ma, “Rate maximization for downlink OFDMA with proportional fairness,” IEEE Transactions on Vehicular Technology, vol. 57, no. 5, pp. 3267–3274, 2008.

[26] A. Biagioni, R. Fantacci, D.Marabissi, and D. Tarchi, “Adaptive subcarrier allocation schemes for wireless OFDMA systems in wimax networks,” IEEE Journal on Selected Areas in Communications, vol. 27, no. 2, Article ID 4769396, pp. 217– 225, 2009.

[27] I. Kim, H. L. Lee, B. Kim, and Y. H. Lee, “On the use of linear programming for dynamic subchannel and bit allocation in multiuser OFDM,” in Proceedings of the IEEE Global Telecommunications Conference (GLOBECOM ’01), pp. 3648–3652, San Antonio, Calif, USA, November 2001.

SOCIETY FOR SCIENCE AND EDUCATION
UNITED KINGDOM

TNC TRANSACTIONS ON NETWORKS AND COMMUNICATIONS

VOLUME 3, ISSUE 6
ISSN: 2054 -7420

Genetic Algorithm based Approach to Enhance Network Performance in Multi-rate WLANs

Qiang Ma, Abdullah Al-Dhelaan and Mznah Al-Rodhaan
Department of Computer Science, College of Computer & Information Sciences
King Saud University, Riyadh, Saudi Arabia
qiang.ma@student.ksu.edu.sa;{dhelaan,rodhaan@ksu.edu.sa}

ABSTRACT

In a multi-rate 802.11 WLAN environment, the users' fairness and network throughput is a trade-off problem. Although there are many valuable research papers related to this optimization problem, up to date, none of those researches could offer a rational, clearly designed mathematical model which can be easily and widely implemented using the well known AI algorithms. Thus our research aims to fill such gap. In this paper we define the problem as an informed search NP-hard problem in a practical scenario, and then we will propose a new intuitive simplified mathematical model called Simplified Coefficient of Variation (SCV), by using Genetic Algorithm to implement the SCV model, through controlling the power of Access Points to optimize and enhance the performance of the network. The simulation gives excellent results that indicate our model is efficient and superior to existing method. After the experiment analysis, we use software SAS to further reveal the relationships of three indicators to illustrate the essence of our algorithm and an existing algorithm.

Keywords: Power Control; SCV; Genetic Algorithm; Optimization; Cost Function; Coefficient of Variation.

1 Introduction

The rapid development of the Internet and the progress of wireless technology are making wireless networks play an increasingly important role in many areas. This is particularly true for the IEEE 802.11 wireless local area network (WLAN) technology. With its development, the increasing demands of service quality and a sharp rise in the number of user groups, the problem has become heavily concentrated in some places such as offices, meeting rooms and other crowded places. In this case, many access points may be allocated, but without an overall channel or power planning and this will result in a large amount of co-channel interference, load imbalance, and network throughput decline, which will degrade the user experience. As it is one of the hot spots in the wireless area, research institutions, academic institutions, and commercial companies have developed many valuable solutions to solve the problems of WLAN, but those solutions cannot be applied easily.

Currently, most research on WLAN technology is mainly focused on the following two aspects:

a) Wireless channel planning. Through different methods, the limited channel resources will be reasonably assigned to all access points (APs) to make it possible to reduce co-channel interference and network overhead in order to improve overall network throughput.

DOI: 10.14738/tnc.36.1625
Publication Date: 28st November 2015
URL: http://dx.doi.org/10.14738/tnc.36.1625

b) Power control to achieve load balancing. Power control mainly uses the proportional relationship of AP signal strength and the power of the AP selected by the user accessing the wireless network, increasing or decreasing the power to adjust the signal strength of the AP. It thus changes the access topology of the user-AP in the network in order to reduce the scheduling overhead, improve load balance etc.

This article considers both aspects above. The rest of the paper is organized as follows: related work is discussed in Section 2. Section 3 shows the motivation. As background knowledge, a brief introduction of genetic algorithm will be given in Section 4, and then we start to explain our new model SCV and apply the Genetic Algorithm. The simulation modeling using Matlab is explained in Section 5. After this, we analyze the results using the statistics software SAS in Section 6 and finally give conclusions in Section 7.

2 Related Work

According to IEEE 802.11, a high-density WLAN deployment environment offers a short distance between APs and users. In this case, each user will connect with the AP by the strongest received signal strength indicator (RSSI) by default. We know that the users are not uniformly distributed in an area, which makes some APs connect more users than the other APs. This will produce the load imbalance problem, as some APs are hungry while some APs are overloaded. This situation results in unfair use of resources.

As a part of our research, the basic solution has been introduced in [1]. In order to improve the Quality of Service, the authors in [2] provided an enhanced method called DCF which providing weighted fairness among multiple priority classes in 802.11-based WLAN to properly control the transmission probability of nodes. The method was expected to achieve not only the weighted fairness but also maximize the system throughput and minimize the frame delay at the same time.

The authors in [3] proposed an Improved Power Control MAC (IPCM) protocol which improves the throughput and yields energy saving. The protocol adopted optimal transmission power to send all kinds of packets in order to save the energy, which also made spatial reuse of the wireless channels, and achieved the maximum throughput compared to the other schemes.

The authors in [4] introduced three strategies which were Dirty Paper Coding (DPC) strategy, Noise strategy, and Opportunistic Interference Cancellation (OIC) strategy. Then they compared the achievable rates of the three strategies. Also they proposed corresponding optimal power control algorithms for each strategy. The simulation results showed that the proposed algorithms can dramatically improve the transmission rate of cognitive user.

The popular 802.11 MAC protocol provides equal transmission chances to all users, which may achieve throughput-based fairness if all users have the same frame size during a cycle [5]-[8]. Recent studies have shown that time-based fairness is much better than throughput-based fairness in multi-rate WLANs [9].

So far, we have two fairness criteria factors that are widely used in network management: proportional fairness [7] which allocates bandwidth to users in proportion to their bit rates to maximize the sum of the bandwidth utilities of the users, and max-min fairness [10] which allocates throughput as equally as possible through maximizing the minimum throughput. Proportional fairness and time-based fairness are equivalent in multi-rate WLANs when all users have the same weight [11]. The equivalence of max-min fairness and throughput-based fairness under the same condition (integral association) was proved in [12].

The authors in [13] proposed a new algorithm called Power Control for AP (PCAP) to optimize the network utility by maximizing the average and minimizing the variance of the AP utility, the result directly maximized the "throughput" as its target, and then the author started to calculate the "J" (Jain's fairness index [14]). The author did not mention the "J" at the beginning, though the result showed significant improving of trade-off. We will analyze the relationship between these two variables.

According to IEEE802.11, AP transmission powers can be changed in an allowable range, this technique is called power control. Some previous studies, such as [15]-[16], have assumed that the user-AP associated topology will not change when adjusting the power of APs, so this assumption is not the reality. On the contrary, some papers have noticed this phenomenon and developed techniques called cell breathing [17].

A variable polyhedron genetic algorithm (GA) is proposed in [18], which not only provides an AP service availability guarantee but also yields a near-optimal beacon range for each AP when the number of evolutions is large enough.

The authors in [19] proposed an algorithm that transformed the problem into a monotonic optimization problem. It is solved with geometric programming [20], but it is not suitable for the low Signal to Interference Ratio (SIR) case.

In [21], the authors proposed a centralized algorithm called Non-Linear Approximation Optimization for Proportional Fairness to derive the user-AP association via relaxation, and gave a distributed heuristic called Best Performance First; which provides an AP selection criterion for new comers.

In [22], the authors jointly considered the channel allocation and AP association, aims to maximize the system performance in terms of throughput and fairness. They introduced two penalty functions to relax the constraints, and a discrete particle swarm optimization algorithm to solve the problem.

In [23], to solve the fairness problem in Wireless Mesh Networks (WMNs), the authors proposed a probabilistic approach to provide proportional fairness without solving global non-linear and non-concave optimization. Their Simulation result shows that the proposed solution is better than the standard IEEE 802.11s based EDCA MAC in terms of fairness and throughput.

Similarly in [24], the authors proposed a novel channel assignment algorithm (CAA) to mitigate co-channel interference in Multi-radio Multi-channel (MRMC) wireless mesh networks (WMNs); which is called Topology controlled Interference-aware Channel-assignment Algorithm (TICA). This algorithm uses topology control based on power control to assign channels so that co-channel interference is minimized, network throughput is maximized, and network connectivity is guaranteed. In further, they proposed algorithm using two-way interference-range edge coloring, called Enhanced TICA (e-TICA), which improves the fairness among flows in the network.

In this paper, the contributions are modeling and analysis. The contributions are listed as follows: (a). we describe the "trade-off" using "J of user" and "J of AP", which refer to the fairness of users and fairness of APs respectively, then we study these two variables and derive our simplified coefficient of variation (SCV) model, which is a clear mathematical function to solve such trade-off problem. This is the core contribution of our paper. (b). we define the problem as an informed search NP-hard problem and apply Genetic Algorithm to solve the SCV model. (**c).** we use multi-channel allocation to improve the

transmission rate. **(d).** we use Statistical Analysis System (SAS) for analysis to reveal the relationships of three indicators and the essence of algorithms. **(e).** SCV opens a door for many AI algorithms; it is a bridge between Network & AI.

3 Motivation

3.1 The Essence of PCAP: Throughput

From our SAS analysis in Fig.3, three indicators (Juser: J of user; Jap: J of AP; Tpt: relative Throughput) show that J of AP can represent Throughput (value>0.8, so it is highly linear related). Through our Statistics calculation, PCAP focus on J of AP only, which means it only focus on Throughput. This is a deficiency of Target Function design, which is not well reflecting our topic.

3.2 The Essence of SCV

The problem is defined as a NP-hard problem since we apply a practical scenario that includes 20 APs, each AP has 10 levels of power, so the state space of the problem will be 10^{20}, making it neither solvable nor verifiable in polynomial time, which makes it a NP-hard.

From the computation theory, we know that we cannot get an accurate solution. Compared with other NP-hard problems such as TSP (Traveling Salesman Problem), we get some heuristic methods. Since existing models are complicated by using a definition of utility and disturbed by many parameters such as channel gain, those models are not clear enough to apply informed search techniques, so first we need to build a clear, simplified model SCV, and then apply the Genetic Algorithm to solve the model.

Since our topic is: “J of user (fairness of users) & Throughput”, which means to make balance between these two parameters. Obviously the two parameters have different units, then we have to convert the “Throughput” to “J of AP” (already explained, it can represent Throughput, with high linear relation).

Then our SCV offers a new designed target function: F=(1/Jusers-1)+ ω(1/Japs-1), which reflects the balance of two parameters (J of user & Throughput), and we will rewrite to get its final form f.

4 Genetic Algorithm

The genetic algorithm is an adaptive strategy and a global optimization technique [25]. It is an evolutionary algorithm and belongs to the broader study of evolutionary computation.

The genetic algorithm is inspired by population genetics (including heredity and gene frequencies), and its evolution is at the population level, as well as the understanding of the structure (such as chromosomes, genes, and alleles) and mechanisms (such as recombination and mutation). Individuals of a population contribute their genetic material (called the genotype) in proportion to the suitability of their expressed genome (called their phenotype) to their environment in the form of offspring. The next generation is created through a procedure of mating that involves recombination of two individual genomes in the population with the introduction of random copying errors (called mutations). This iterative procedure may result in an improved adaptive fit between the phenotypes of individuals in a population and the environment.

The goal of the genetic algorithm is to maximize the payoff of candidate solutions in the population against a cost function from the problem domain. The strategy of the genetic algorithm is to repeatedly employ surrogates for the recombination and mutation genetic mechanisms in the population of candidate

solutions, where the cost function (also known as objective or fitness function) applied to a decoded representation of a candidate governs the probabilistic contributions a given candidate solution can make to the subsequent generation of candidate solutions.

Simple Genetic Algorithm:

```
{
   initialize population;
   evaluate population;
   while Termination Criteria Not Satisfied
   {
      select parents for reproduction;
      perform recombination and mutation;
      evaluate population;
   }
}
```

5 Model Design and Simulation

Now we are going to explain our SCV model and apply it in Genetic Algorithm.

5.1 The Way APs Attract Users

The user will select the strongest received signal strength indicator (RSSI) as default. In the model [26], $RSSI = aP / X^{\alpha}$ where "a" is a constant factor, "P" is received power, "X" is distance between user and selected AP, while "α" has different value in different scenarios, generally between 1.6 and 6.5 [27]. The formula only determines the association matrix of User-AP. In practice, the general power range of the AP is 10dBm ~ 30dBm, i.e. 1mw ~ 1w, here we adopt α =3 for indoor case. From the formula, the value of "a" does not affect the association results, to simplify the mathematical form, we take $a=1$, so our model adopts a simplified form:

$$RSSI = P / X^{3} \tag{1}$$

5.2 Study the SINR[r_{ij}] of the User[i]

Assuming the user[i] connects to AP[j], the power of AP[j] is P_j. Wherein "g" are channel gains, A_i is a set of all APs within the same channel of AP[j]. N_{0j} is an additive white Gaussian noise generated by AP[j].

$$r_{ij} = \frac{g_{ij} p_j}{\sum_{k \in A_i \cap k \neq j} g_{ik} p_k + N_{0j}} \tag{2}$$

It is worth noting that N_{0j} can be adjusted to an exact value [28]-[29]. So we can set a constant μ>0,

$$\mu = \frac{g_{ij}}{\sum_{k \in A_i \cap k \neq j} g_{ik} p_k + N_{0j}} \tag{3}$$

5.3 Study the Relationship between User[i]'s Transmission Rate v_i and Its SINR [r_{ij}]

Table 1. v_i - r_{ij} relationship

r_{ij} (dB)	6-7.8	7.8-9	9-10.8	10.8-17	17-18.8	18.8-24	24-24.6	24.6-
v_i(Mbps)	6	9	12	18	24	36	48	54

From Table 1 in [13], we see the monotonically increasing relationship between the two variables. Here we might assume that two variables meet the linear relationship as an approximation, $v_i=\beta r_{ij}$, β >0 is a constant of proportionality. Then connect this to (2) and (3) we have: $v_i=\beta r_{ij}=\beta\mu p_j=\lambda p_j$ (4)

So λ is a constant: $\lambda=\beta\mu$ (5)

5.4 Study the Effective Speed of v_i

Let N[j] denote the total number of users which connect with AP[j]. Because the users are time based share the chance of AP[j], so the effective speed of v_i is:

$$\overline{v_i}=\frac{\lambda p_j}{N[j]} \tag{6}$$

From this formula we know that it is better to decrease the N[j], and increase the p_j and λ.

5.5 Study the AP'S Power

According to the simulation result in [13], we know that usually 10 levels of AP power will be enough to achieve a good result. Therefore, in our model, p_{max} and p_{min} have relationship as following:

$p_{max}/p_{min}=10$, p_{max} will be the basis of calculation, since we need to increase the p_j, so the 10 power levels are in Table 2.

Table 2. Level-value relationship

level	1	2	...	10
value	p_{min}	$2p_{min}$	...	$10p_{min}$

Note here the unit of power is "mw", not "dBm". Since $P_j=P_{min}l_j$ (l_j=1,2...10), note that l_j denotes the level of AP power, so the formula (6) can be rewritten as follows:

$$\overline{v_i}=\frac{\lambda p_{min} l_j}{N[j]}=\lambda p_{min}\frac{l_j}{N[j]} \tag{7}$$

Let M be the total number of users and N be the total number of APs. From statistics we know that the expectation of $\overline{V}_i$ for all users is denoted as $E(\overline{V}_i)$, and variance of $\overline{V}_i$ for all users is denoted as $S^2(\overline{V}_i)$. We have the following (i=1,2,…M; j=1,2,…N):

$$E(\overline{v_i}) = \lambda p_{\min} E(\frac{l_j}{N[j]}) \tag{8}$$

$$S^2(\overline{v_i}) = (\lambda p_{\min})^2 S^2(\frac{l_j}{N[j]}) \tag{9}$$

Let b[i] denote the average transmission speed from user[i] to AP[j], we have b[i]= $\overline{V}_i$. Moreover, let U[j] denote the transmission speed from the AP[j] to backbone. The Expectation of b[i] is denoted as: $E(b[i])$, and Variance of b[i] is denoted as: $S^2(b[i])$, and Expectation of U[j] is denoted as: $E(U[j])$, and Variance of U[j] is denoted as: $S^2(U[j])$, so continue we have formulas as following:

$$E(b[i]) = E(\overline{v_i}) = \lambda p_{\min} E(\frac{l_j}{N[j]}) \tag{10}$$

$$S^2(b[i]) = S^2(\overline{v_i}) = (\lambda p_{\min})^2 S^2(\frac{l_j}{N[j]}) \tag{11}$$

$$E(U[j]) = E(\sum_{user[i]\to AP[j]} b[i]) = E(\lambda p_{\min} N[j] \frac{l_j}{N[j]}) = \lambda p_{\min} E(l_j) \tag{12}$$

$$S^2(U[j]) = S^2(\sum_{user[i]\to AP[j]} b[i]) = S^2(\lambda p_{\min} N[j] \frac{l_j}{N[j]}) = (\lambda p_{\min})^2 S^2(l_j) \tag{13}$$

Let cvusers denote the coefficient of variation of transmission speed of all users and cvAPs denote the coefficient of variation of transmission speed of all APs, we have:

$$\text{cvusers}^2 = \frac{S^2(b[i])}{E^2(b[i])} = \frac{(\lambda p_{\min})^2 S^2(\frac{l_j}{N[j]})}{(\lambda p_{\min})^2 E^2(\frac{l_j}{N[j]})} = \frac{S^2(\frac{l_j}{N[j]})}{E^2(\frac{l_j}{N[j]})} = \frac{M \sum_{i=1, b[i]\to AP[j]}^{M} \frac{l_j^2}{N^2[j]}}{(\sum_{j=1}^{N} l_j)^2} - 1 \tag{14}$$

$$= \frac{M \sum_{j=1}^{N} \frac{l_j^2}{N[j]}}{(\sum_{j=1}^{N} l_j)^2} - 1 = \frac{1}{J_{users}} - 1$$

$$cvAPs^2 = \frac{S^2(U[j])}{E^2(U[j])} = \frac{(\lambda p_{\min})^2 S^2(l_j)}{(\lambda p_{\min})^2 E^2(l_j)} = \frac{S^2(l_j)}{E^2(l_j)} = \frac{N \sum_{j=1}^{N} l_j^2}{(\sum_{j=1}^{N} l_j)^2} - 1 = \frac{1}{J_{APs}} - 1 \tag{15}$$

Note, here we adopt the definition of J in [13], where we have $J_x = (\sum_{i=1}^{n} x_i)^2 \Big/ n \sum_{i=1}^{n} x_i^2$, above is the relationship between J and the square of coefficient of variation.

5.6 Cost Function f Construction

According to our topic, we need a function that can describe the tradeoff between fairness of users and throughput of network. In [13], the algorithm is divided into two steps: increase average value and decrease variance value of AP utility to increase throughput of network. They are equal to decreasing $_{cvAPs}$ or $cvAPs^2$. So increasing J of users is equal to decreasing cvusers^2.

Let F denote a target function as follows: $F = \text{cvusers}^2 + \omega(cvAPs^2)$, ω is weight proportion factor, it is very important reflecting our requirement how to make the balance between fairness and throughput, it is a quantifiable indicator.

Here we do some mathematical derivation to illustrate how we get a reasonable value of ω. Considering the static grouping problem: m numbers are average divided by n groups, therefore each group has m/n numbers. Given that the expectation of total numbers is σ, and their variance is s^2, so for group[i] we have:

$$E(group[i]) = E(\sum_{number[j]\in group[i]} number[j]) = \sum_{number[j]\in group[i]} E(number[j]) = \frac{m}{n}\sigma$$

$$S^2(group[i]) = S^2(\sum_{number[j]\in group[i]} number[j]) = \sum_{number[j]\in group[i]} S^2(number[j]) = \frac{m}{n}s^2$$

$$cvnumbers^2 = \frac{s^2}{\sigma^2}$$

$$cvgroups^2 = \frac{S^2(group[i])}{E^2(group[i])} = \frac{\frac{m}{n}s^2}{(\frac{m}{n})^2\sigma^2} = \frac{1}{\frac{m}{n}}\frac{s^2}{\sigma^2} = \frac{1}{\frac{m}{n}}cvnumbers^2 \tag{16}$$

So it means $cvgroups^2$ is much smaller than $cvnumbers^2$, comparing this example to our function "F", in function "F" we should amplify the small part since two parts have relationship. So we decide to give value to ω, let $\omega = M/N$.

$$F = \text{cvusers}^2 + \omega(cvAPs^2) = \frac{M\sum_{j=1}^{N}\frac{l_j^2}{N[j]}}{(\sum_{j=1}^{N}l_j)^2} - 1 + \frac{M}{N}(\frac{N\sum_{j=1}^{N}l_j^2}{(\sum_{j=1}^{N}l_j)^2} - 1) = M\frac{(\sum_{j=1}^{N}\frac{l_j^2}{N[j]} + \sum_{j=1}^{N}l_j^2)}{(\sum_{j=1}^{N}l_j)^2} - (1+\frac{M}{N}) = Mf - (1+\frac{M}{N}) \tag{17}$$

Wherein:

$$f = \frac{(\sum_{j=1}^{N}\frac{l_j^2}{N[j]} + \sum_{j=1}^{N}l_j^2)}{(\sum_{j=1}^{N}l_j)^2} = \frac{\sum_{j=1}^{N}(l_j^2(1+\frac{1}{N[j]}))}{(\sum_{j=1}^{N}l_j)^2} \tag{18}$$

Note that M and N are constants as defined before. M is total number of users, N is total number of APs. When "F" goes to minimum, it is equal to "f" goes to minimum. So (18) will be our simplified target function, to achieve the purpose of the tradeoff between Fairness (users) and Throughput (network).

5.7 Throughput

From formula (12) we know that:

$$Throughput_{real} = \sum_{j=1}^{N} U[j] = \lambda p_{\min} \sum_{j=1}^{N} l_j = \lambda p_{\min} Throughput_{relative} \tag{19}$$

$$Throughput_{relative} = \sum_{j=1}^{N} l_j \tag{20}$$

Since the λp_{min} is constant， we use $Throughput_{relative}$ to represent $Throughput_{real}$.

5.8 Genetic Algorithm Design and Simulation

In this part we are going to place a total number of N=20 APs on a 4 by 5 grid, with each AP on a grid point. The coverage area of each AP can across the whole area. The distance between two adjacent APs is set to 100 meters. The maximum transmit power of each AP is set to 20dBm (100mw), and so according to our model, the minimum transmission power of each AP is set to 100/10=10mw=10dBm.

We arrange M=200 users random distributed in the whole area. According to [30], a separation of four channels can be used without reducing the performance, so the possibilities could be opened to channels 1, 5, 9 and 13. In this paper we decide to use these channels in order to get a bigger $Throughput_{real}$.

Let $AP_j \rightarrow Ci$ denote AP_j using channel i, we use 1, 5, 9, 13 these channels to configure the network as in Table 3.

Table 3. AP-Channel relationship

$AP_1 \rightarrow C1$	$AP_2 \rightarrow C9$	$AP_3 \rightarrow C1$	$AP_4 \rightarrow C9$	$AP_5 \rightarrow C1$
$AP_6 \rightarrow C5$	$AP_7 \rightarrow C13$	$AP_8 \rightarrow C5$	$AP_9 \rightarrow C13$	$AP_{10} \rightarrow C5$
$AP_{11} \rightarrow C9$	$AP_{12} \rightarrow C1$	$AP_{13} \rightarrow C9$	$AP_{14} \rightarrow C1$	$AP_{15} \rightarrow C9$
$AP_{16} \rightarrow C13$	$AP_{17} \rightarrow C5$	$AP_{18} \rightarrow C13$	$AP_{19} \rightarrow C5$	$AP_{20} \rightarrow C13$

a. Chromosome Coding: the whole path from AP_1 to AP_{20} is denoted as a Chromosome, and each element is denoted as a Gene, the value of Gene is the level of AP's power. In Table 4. Where $ge_{ij} = 1, 2, ...10$

Table 4. Chromosome Coding

Chro\Gene	1	…	j	…	20
$Chro_i$	ge_{i1}	…	ge_{ij}	…	ge_{i20}

b. Fitness Function is f in (18), since all parameters' values in algorithm can affect the result of the calculation, the following parameters' values are better after repeated tests.

C=50; denotes the total number of generations.
Ps=0.6; denotes the probability of selection operation.
Pc=0.9; denotes the probability of crossover operation.
Pm=0.1; denotes the probability of mutation operation.

6 Result Analysis

The solution of Genetic Algorithm has many parameters. Since all parameters' values in algorithm can affect the result of the calculation, we need to run multiple times on the same data and same parameters, and select the best, average, or representative results, also search for the more suitable parameters' values. Here we use $Throughput_{relative}$ to represent $Throughput_{real}$. We know that the maximum of $Throughput_{relative}$ is: $10 \times 20 = 200$, but it will never be achieved, at least because of users' distribution.

The simulation results show in the following figures. Generally, in genetic algorithm, when the best individuals of each generation are saved then the simulation result will converge. According to fitness function, we save enough best chromosomes and phase out those worst ones, therefore, each parameter is convergent, since random factors exist in algorithm, so there is slight vibration around the horizontal line.

From the Figure 1& Figure 2 we can see there are totally 52 generations in the experiment. We select the best path in each generation and calculate the values of those indicators in this path, then plot these values for all 52 generations. In Fig.1, max J of user denotes the maximum fairness value of users in that generation, max J of AP denotes the maximum fairness value of APs in that generation. In Figure 2, max Throughput of network denotes the maximum value of $Throughput_{relative}$ in that generation, min cost of f denotes the minimum value of the function in (18).

From the Fig.1, at the 21st generation, the biggest J of user is almost equal to 0.84, and corresponding J of AP is almost equal to 0.99, while in the Fig.2, at the 21st generation the $Throughput_{relative}$ is almost equal to 169, since its maximum value is 200, then the throughput of the network is almost equal to 169/200≈85% of the network bandwidth. Moreover the cost of f in 21st generation is 0.057. So from the figures, the administrator may choose this generation to configure the network.

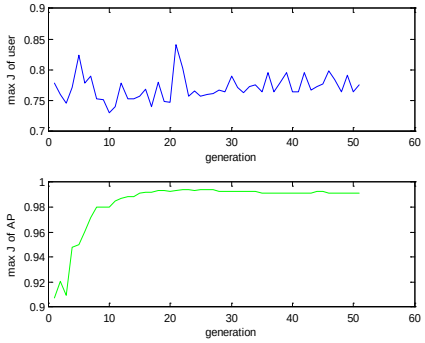

Figure 1. {max J of user, max J of AP}-generation plot

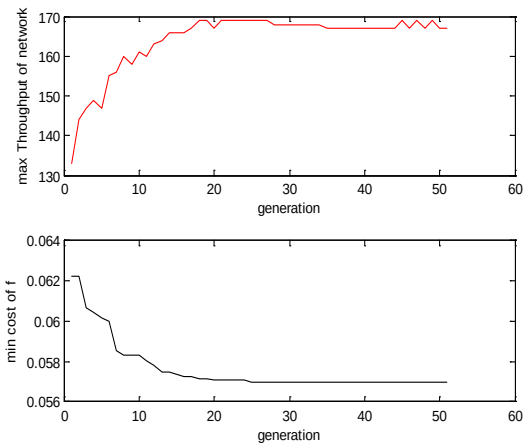

Figure 2. {max Throughput of network, min cost of f}-generation plot

SAS Analysis: we use the samples from experimental data to study the correlation coefficients among these indicators. Wherein Juser denotes J of user, Jap denotes J of AP, Tpt denotes $Throughput_{relative}$, cost denotes the value of function f in (18).

Pearson Correlation Coefficients, N = 326 Prob > |r| under H0: Rho=0				
	cost	Tpt	Jap	Juser
cost cost	1.00000	-0.80950 <.0001	-0.94339 <.0001	-0.31595 <.0001
Tpt Tpt	-0.80950 <.0001	1.00000	0.80200 <.0001	0.17151 0.0019
Jap Jap	-0.94339 <.0001	0.80200 <.0001	1.00000	0.11425 0.0392
Juser Juser	-0.31595 <.0001	0.17151 0.0019	0.11425 0.0392	1.00000

Figure 3. correlation coefficients.

Figure 3 shows that at alpha=0.05 significance level, all the p-values are less than 0.05, so we reject the H_0, and accept H_1 that these variables are linearly related, wherein the Tpt-(Jap, Juser) have highly significant linear correlations, while correlations of Jap-Juser is weak. We compared the degree of concentration of those data points in Fig.4 and Fig.5. It is clear that data points are more concentrated in Fig.5. This means the linear correlation of Tpt-Jap is much higher than the linear correlation of Tpt-Juser, which also proves the effectiveness of SCV model (coefficient of Tpt-Jap>0.8, Tpt-Juser=0.17, so it is more effective to use J of AP whereas not J of user to represent the Throughput).

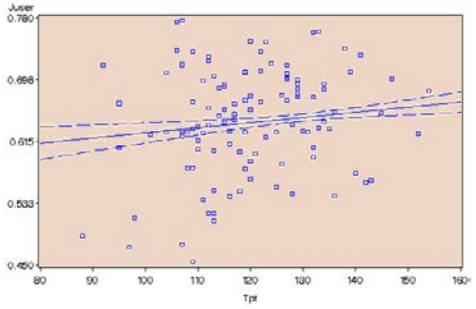

Figure 4. Tpt-Juser linear regressions

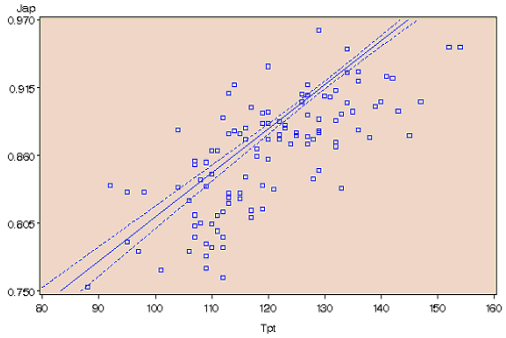

Figure 5. Tpt-Jap linear regression

Comparison Analysis:

Table 5. The Statistics of the Results

Algorithm	Average AP Utility ($\overline{U^a}$)	AP Utility Variance (σ_u)	Total Network Utility	Jain's Fairness Index	Average Power (dBm)
PCAP	3.82×10^9	2.98×10^9	117.42	0.90	17.15
MARL	2.67×10^9	5.00×10^9	102.30	0.85	17.28
SR	1.46×10^9	12.80×10^9	99.66	0.75	18.06
SSF	1.11×10^9	27.31×10^9	79.59	0.37	20.00

Here we want to compare our solution with PCAP in [13], we can see the above Table 5 from [13],

since we use different definitions to denote throughput of AP and throughput of network, we have to use the indirect method to illustrate some issues.

According to [13], we can transfer and calculate their J of AP:

$$cvAPs^2 = \frac{S^2(U[j])}{E^2(U[j])} = \frac{\log(2.98\times10^9)}{(\log(3.82\times10^9))^2} = 0.1 = \frac{1}{J_{APs}} - 1 \quad (21)$$

So their $J_{APs} = 0.9 = J_{users}$ (22)

And we have: $U \le n\log(\overline{U^a}) = 20\log(3.82\times10^9) = 191.64 = U_{\max}$ (23)

Then their throughput percentage of network bandwidth is:

$$U_{network\cdot utility} / U_{\max} = 117.42 / 191.64 \approx 61.3\% \quad (24)$$

In [13], the authors set 300 users and 16 APs (the other 4 APs actually became useless under their assumption).

We select average case in Fig.1, at the 30th generation, the J of user is almost equal to 0.79, and corresponding J of AP is almost equal to 0.99, the $Throughput_{relative}$ is almost equal to 168, since its maximum value is 200 as mentioned before, then the throughput of the network is equal to 168/200=84% of the network bandwidth. And the corresponding cost of f is almost equal to 0.057.

In Figure 1, our J of AP is superior to theirs in (22). From the throughput point of view, our throughput percentage of network bandwidth is 84%>61.3% in (24), so our method is better than PCAP. But from the fairness of users(J of user) point of view, PCAP is better than ours since 0.79<0.9 in (22).

According to (17), we convert (22) into our function F, we have:

$$F_{PCAP} = [(1/J_{users}) - 1] + (M/N)[(1/J_{APs}) - 1] = [(1/0.9) - 1] + (300/16)[(1/0.9) - 1] = 2.17 \quad (25)$$

$$F_{SCV} = Mf - (1 + M/N) = 200\times0.057 - (1 + 200/20) = 0.4 \quad (26)$$

So the overall performance depends on the requirement of administrators, what indicator they most concern. Here we define the value of "F" as the overall performance criteria of algorithm, note smaller "F" is better then from (25) and (26) we know that our SCV model is much better than PCAP. The above comparison analysis result is in Table 6.

Table 6. Comparison Result

	PCAP	SCV-gen
J of user (↑win)	0.9	0.79
J of AP (↑win)	0.9	0.99
Throughput % (↑win)	61.3%	84%
Function "F" value (↓win)	2.17	0.4

Theoretically, our design of target function "F" in (17) is more simple and rational than PCAP algorithm, since we joint consider the J of user and Throughput (represented by J of AP), we regard them as two variables to reflect our topic. While the target of PCAP is the Throughput, the author used two sub-algorithms to achieve J of AP only, and then got their by-product: J of user.

Technically, our SCV math model is a door that leads this problem to AI algorithms. The clear target function "F" is easy to be applied to other AI algorithms, while PCAP cannot

7 Conclusions

The objective of this paper is to improve the trade-off between user fairness (J of user) and network throughput(represented by J of AP) via power control in multi-rate WLANs.

In this article, we first construct a new simplified model called SCV. The goal of the model is to derive a target function "F" (17) and its simplified form " f " (18) as our key foundation. Then we use Genetic Algorithm to solve our model, we conduct a simulation in Matlab. After that we give analysis of our SCV model and simulation results which confirm that our model is efficient and superior to PCAP in some aspects and overall performance under a new criteria of algorithm designed for such specific problem. In addition, based on the data samples from the state space, we use SAS to conduct correlationship analysis mainly among three indicators, and reveal their relationships.

SCV opens a door for many AI algorithms to apply in this problem, it is a bridge between Network & AI.

Our future work is to derive a more accurate target function, and adjust the values of parameters to find more suitable combination so that to improve the results. Also we are working on other AI solutions based on SCV model.

ACKNOWLEDGMENT

The authors extend their appreciation to the Deanship of Scientific Research at King Saud University for funding this work through research group no. RGP-264.

REFERENCES

[1]. Qiang Ma, Abdullah Al-Dhelaan, Mznah Al-Rodhaan, "Using Genetic Algorithm to Improve Tradeoff between Fairness and Throughput in Multi-Rate WLANs", Proc. 8th WSEAS International Conference on Circuits, Systems and Signals (CSS'15), Michigan State University, USA, September 2015.

[2]. Jain-Shing Liu, "AchievingWeighted Fairness in IEEE 802.11-based WLANs: Models and Analysis", WSEAS Transactions on Communications, Issue 6, vol. 7, June 2008.

[3]. Yaser Mahmood, A. Hamid, D. K. Lobiyal. "Improved Power Control MAC Protocol for wireless Ad Hoc Networks", WSEAS Transactions on Communications, Issue 1, vol. 10, January 2011.

[4]. Qian Hu, Zhenzhou Tang, "Study on Power and Rate Control Algorithm for Cognitive Wireless Networks", WSEAS Transactions on Communications, Issue 4, vol. 9, April 2010.

[5]. G. Tan, J. Guttag, "Time-based fairness improves performance in multi-rate WLANs", Proc. Usenix Annual Technical Conf., 2004, pp. 23–23.

[6]. M. Heusse, F. Rousseau, G. Berger Sabbatel, A. Duda, "Performance anomaly of 802.11b", Proc. IEEE INFOCOM, 2003, pp. 836– 843.

[7]. F. P. Kelly, "Charging and rate control for elastic traffic", European Trans. Telecommun., vol. 8, no. 1, 1997.

[8]. A. Banchs, P. Serrano, H. Oliver, “Proportional fair throughput allocation in multi-rate IEEE 802.11e wireless LANs”, Wireless Networks, vol. 13, no. 5, pp. 649–662, 2007.

[9]. A. V. Babu, L. Jacob, “Performance analysis of IEEE 802.11 multi-rate WLANs: time based fairness vs throughput based fairness”, Proc. IEEE Int. Conf. on Wireless Networks, Comm. and Mobile Compu., pp. 203–208. 2005.

[10]. D. Bertsekas, R. Gallager, “Data Networks”, Prentice-Hall, 1987.

[11]. W. Li, Y. Cui, S. Wang, X. Cheng, “Approximate optimization for proportional fair AP association in multi-rate WLANs”, Proc. 5th Int. Conf. WASA, 2010, pp. 36–46.

[12]. Y. Bejerano, S. J. Han, L. E. Li, “Fairness and load balancing in wireless LANs using association control”, IEEE/ACM Trans. Network., vol. 15, no. 3, pp. 560–573, 2007.

[13]. Wei Li, Yong Cui, Xiuzhen Cheng, Mznah A. Al Rodhaan, Abdullah Al Dhelaan, “Achieving Proportional Fairness via AP Power Control in Multi-Rate WLANs”, IEEE Transactions on Wireless Comm., vol. 10, no. 11, November 2011.

[14]. R. Jain, D. M. Chiu, W. R. Hawe, “A quantitative measure of fairness and discrimination for resource allocation in shared computer system”, Digital Equipment, Tech. Dec-Tr-301, 1984.

[15]. V. P. Mhatre, K. Papagiannaki, F. Baccelli, “Interference mitigation through power control in high density 802.11 WLANs”, Proc. IEEE INFOCOM, pp. 535–543, 2007.

[16]. V. Hasu, V. Koivo, “Fair transmission rate allocation: a power control feasibility approach”, Proc. IEEE ICCS, pp. 1–5, 2006.

[17]. Y. Bejerano, S. J. Han, “Cell breathing techniques for load balancing in wireless LANs”, IEEE Trans. Mobile Computing, vol. 8, no. 6, 2009.

[18]. Shengling Wang, Jianhui Huang, Xiuzhen Cheng, Biao Chen, “Coverage adjustment for load balancing with an AP service availability guarantee in WLANs”, Wireless Networks, April 2014, vol 20, Issue 3, pp. 475-491.

[19]. L. P. Qian, Y. Jun, “Monotonic optimization for non-concave power control in multiuser multicarrier network systems”, Proc. IEEE INFOCOM, 2009, pp. 172–180.

[20]. M. Chiang, C. W. Tan, D. P. Palomar, D. O’Neill, D. Julian, “Power control by geometric programming”, IEEE Trans. Wireless Commun., vol. 6, no. 7, pp. 2640–2651, 2007.

[21]. Wei Li, Shengling Wang, Yong Cui, Xiuzhen Cheng, Ran Xin, Mznah A. Al-Rodhaan, Abdullah Al-Dhelaan, “AP Association for Proportional Fairness in Multirate WLANs”, IEEE/ACM Trans. on Networking, vol. 22, no. 1, February 2014.

[22]. Xiaohui Chen, Wenqing Cheng, Wei Yuan, Wei Liu, Jing Xu, "Joint Optimization of Channel Allocation and AP Association in Variable Channel-width WLANs", 2013 IEEE Wireless Communications and Networking Conference: MAC.

[23]. Sandip Chakraborty, Pravati Swain, Sukumar Nandi, "Proportional fairness in MAC layer channel access of IEEE 802.11s EDCA based wireless mesh networks", Ad Hoc Networks, 2013, vol.11 (1).

[24]. Aizaz U Chaudhry, Nazia Ahmad, Roshdy HM Hafez, "Improving throughput and fairness by improved channel assignment using topology control based on power control for multi-radio multi-channel wireless mesh networks", EURASIP Journal on Wireless Comm. and Networking, 2012, vol.2012 (1), pp.1-25.

[25]. Jason Brownlee, "Clever Algorithms: Nature Inspired Programming Recipes", LuLu, first edition, January 2011, ISBN: 978-1-4467-8506.

[26]. DING Xiaole, LI Fenghua, LI Hewu, JIANG Yong, WU Jianping, "Dynamic load balancing mechanism in WLAN Based on Power Control and Location Information", Journal of Xiamen University(Natural Science), vol.46, Sup 2, Nov. 2007.

[27]. Andrea Goldsmith, "Wireless Communications", Stanford University, 2004.

[28]. Yin Zhongqiu, Shi Chunhe, Chen Mingsheng, Liu Shuzhong, "A White and Gaussian White Noise Generator with Adjustable Parameters", Fire Control and Command Control, 2008.08.

[29]. Wang Pengyu, Zhai Lili, Shi Jufeng, "Design of Gaussian White Noise Generator with Adjustable Parameters Based on FPGA", Shipboard Electronic Countermeasure, doi: 10.3969/j.issn.1673-9167.2013.04.029

[30]. Eduard Garcia Villegas, Elena López-Aguilera, Rafael Vidal, Josep Paradells, "Effect of adjacent-channel interference in IEEE 802.11 WLANs", Cognitive Radio Oriented Wireless Networks and Communications, 2007. 2nd International Conference, doi:10.1109/crowncom.2007.4549783.

SOCIETY FOR SCIENCE AND EDUCATION
UNITED KINGDOM

TNC TRANSACTIONS ON NETWORKS AND COMMUNICATIONS

VOLUME 3, ISSUE 6
ISSN: 2054 -7420

Effects of Diffraction Propagation at 24GHz Spectrum Band

[1]Femi-Jemilohun O.J and [2]Walker S.D
[1]Ekiti State University, Ado Ekiti, Nigeria;
[2]School of Computer Science and Electronic Engineering, University of Essex, United Kingdom.
dunnifj@gmail.com; stuwal@essex.ac.uk

ABSTRACT

The experimental measurement results of fast and slow signal fading due to corner diffraction characteristics of newly opened 100MHz bandwidths in the 24GHz spectrum for wireless communication is presented in this work. Two distinct regions are noticeable in the curve depicting these characteristics; a linear curve for the diffraction angles above 5 degrees, and a logarithmic curve for diffraction angles below 5 degrees. This feature being in agreement with what other research findings in similar working environment but at lower spectrum, as well as specifications by fundamental theory, points out the tremendous potential of this unlicensed 100MHz bandwidth for communication system for high and efficient delivery capacity especially in non-line of sight and obstructed transmission.

Keywords: Diffraction Propagation; slow and fast fading; Millimeter Waves; Non-Line-of-Sight; Exponential growth.

1 Introduction

The exponential growth in devices that require gigabits data rates application has taken over the classical microwave frequencies. This is heralded by the millimeter wave bands with huge unlicensed bandwidth capable of few gigabits data rates with high spatial reuse. The millimeter wave at 60GHz was the first candidate to provide such requirement for the gigabit multimedia application services, nevertheless, the atmospheric conditions effect on this band has confined it to strictly LoS propagation and a small space environment. A great opportunity and way out from this technical challenge was discovered in the newly opened 100MHz bandwidth window in the 24GHz band allocated for unlicensed usage in the wireless communication. This band has be found to perform acceptably in the NLoS propagations such as hallway and corridors as well as across offices in modern building [1, 2]. It is technologically unfeasible to achieve LoS propagation to all wireless service users, therefore, optimization and effective utilization of system capacity requires reaching many users as much as possible hence means of adequate signal transmission in the Non-line of sight nodes are crucial. Two major propagation techniques for sufficient wireless network services to consumers outside the LoS of the propagating antennas are diffraction and reflection. Among the two, the latter is a better means (reduced attenuation) for received signal prediction at any given time, especially when the diffracting angle is small. The measurement in this work evaluates the additional attenuation when 24GHz radio wave bends around an object

DOI: 10.14738/tnc.36.1712
Publication Date: 17st December 2015
URL: http://dx.doi.org/10.14738/tnc.36.1712

Diffraction occurs at the edge of an impenetrable body that is large compared to wavelength of radio wave. In addition to reflection and multipath propagation that assist the signal transmission in the indoor environment, diffraction propagation results in wave propagation in the geometrical shadow region behind obstacles. It is an important propagation mechanism to be addressed as the effect of such may cause a tangible multipath propagation under both LoS and NLoS. A linear equation describes the diffraction curve with the angle of diffraction greater than 5 degrees while a logarithmic equation describes that of angle less than 5 degrees [3] [4].

2 Fast and Slow/ Small and Large Scale Fading

The prominent applications of millimeter wave in the NLoS environments results in the fading of the received power which are classified as small and large scale fading represented as:

$$P_{inst}(d) = P_{large}(d) + P_{small}(d) \quad \text{(dB)} \tag{1}$$

Where the large scale fading determines the average characteristics of the channel due to free space path loss and the shadowing effects of large object and the small scale fading estimates the signal change in a local area of a few wavelength distance. The large scale fading is characterized by log-distance model as follows:

$$PL_{dB} = UL_{d_0} + 10nlog\left(\frac{d}{d_0}\right) + X_\sigma \tag{2}$$

Where PL_{dB} is the average pathloss between transmission links, UL_{d_0} is the reference path loss at d_0=1m for indoor propagation, n is the path loss exponent and d is the separation between transmitter and receiver in meters, X_σ is a zero-mean Gaussian randomly distributed variable with standard deviation σ.

One of the major causes of small scale fading is the interaction of the complex impulse-response details acquired within a limited bandwidth. Doppler spread shows that the coherence can lead to the transmission channel variation over time due to motion of objects or persons in the propagation environment or movement of the transmission links which will result in spectrum broadening. The coherence time is given by:

$$T_{Coh} = \frac{1}{2f_D} \tag{3}$$

The presence of directional antenna in the propagation devices used in this experiment minimized this fading contribution by its spatial filtering feature and increase the coherence time [5]

3 Diffraction Signal Propagation Enhancement

“Research works have mostly focused on reflection and transmission characteristics of various building materials at millimeter waves and have largely neglected their rough surface scattering characteristics which cause angular dispersion in the received signal. In the LoS applications, the presence of a building can cause shadowing or conversely, provide an alternate ray path to beam form along. Past research works for corner diffraction have focused on cellular applications at 28 and 40 GHz, and diffraction from metal and wooden wedges at 60 GHz. In addition to the diffraction from building corners, the columns, window frames, etc. on building surfaces are expected to give significant contributions to the received signal. The knowledge of where the relevant scaterers on the surface are, can speedup beam-finding times

and enhance performance" [6]. Limited work has been done in the 60 GHz band, while little or none has been found in the new 100MHz bandwidth provided in the 24GHz band for communications networks. This work serves to fill this gap by investigating the enhanced performance of millimeter (24GHz) wave in NLoS due to diffraction propagation.

"Diffraction can influence the received power in indoor environments, especially in areas that are heavily shadowed. Though according to [7] , diffraction does not constitute a relevant propagation mechanism already at mm-waves in their investigation with 60GHz, and therefore concluded that, since diffraction losses increase with frequency, this mechanism can be neglected for propagation prediction in the THz range but the results of this work shows that diffraction propagation at 24GHz enhanced the received power. This as depicted in the results will facilitate the effective and optimum utilization of such network in the office as well as nlos environments.

The advantage of a commercially-available 24GHz point-to-point link wireless system (Ubiquiti airFiber) was utilized in this work, this wireless system uses either horn or parabolic dish antennas [8][9][10]. This system featured both multiple-input/multiple-output (MIMO) technologies, dynamically variable signal constellations together with adaptive time/frequency multiplexing, while both frequency and time division multiplexing are used in hybrid form: HDD; the combination of the best features of both TDD and FDD (e.g. interference-reduction and flexible band-planning) [11][12] enhances the realization of the specified 1.4Gbps delivery as established by the results of the real-time application measurements conducted earlier . It is well-known that mm-wave links have intrinsically smaller Fresnel zones, as a guide, 60% of this zone should be unobstructed [13], otherwise it is deemed as NLoS as in the indoor environment. 24GHz point-to-point link used in these experiments had a narrow beam width of 3.5 degrees hence an obstruction smaller than the wavelength of the transmitted signal would cause scattering while a rough surface would diffuse the radio signal in all directions [14].

4 Methodology and Experimental Setup

The experimental set up shown in Figure 1 consists of the 24GHz point-to-point link with maximum transmitter output power of 20dBm. It has delivery capacity of 1.4Gbps using the HDD in bidirectional mode at 6X64 QAM modulations scheme (highest) and is backward compatible to lower modulation scheme of QPSK through the automatic rate adaptation to accommodate low signal transmission. The feature enables a link pair to sustain up to 142.5 dB path loss when switched to basic QPSK modulation mode. Full duplex transmission is used with slight different carrier frequency of 24.1 and 24.2GHz; a bandwidth of 100MHz [12]. The transmitting and the receiving terminals have an antenna gain of 33dBi each. For the experimental measurement, both antennas were mounted on tripods 1.7m above the floor level, and connected to PCs for signal transmission monitoring. A board was arranged in between the links to provide an edge/obstruction to allow diffraction propagation from the source to the receiving terminal. The diagrammatical representation of the transmission links is shown in Figure 2.

Figure 1: Diffraction Propagation experimental Set Up

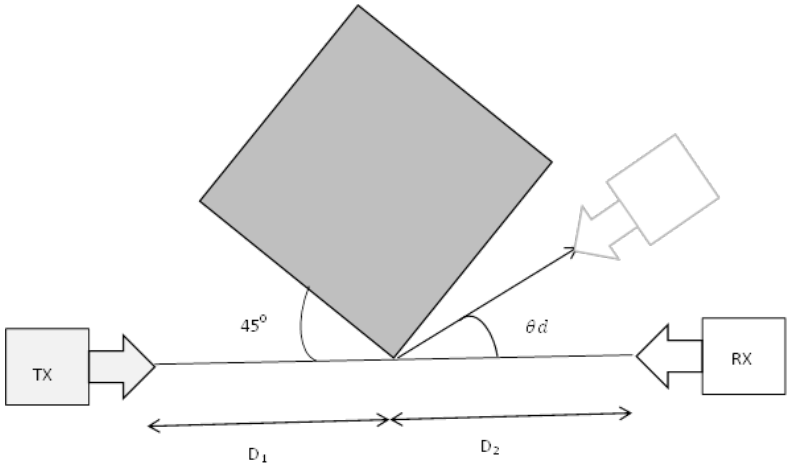

Figure 2: Corner edge propagation measurement Setup

5 Results and discussion

The 3.5 degrees bore sight of 24GHz transceiver is significant. The divergence of the Radiation Pattern is confined within a narrow spread even in the clustered and potentially diffractive scenario where this experiment was conducted. This aided the transmitted signal to focus and concentrated the transmitted power to the receiving terminal with little or no waste along the signal path, hence impressive results were achieved with increase in the diffraction propagation angles. The terminals were initially set at LoS to each other and latter, the edge of a board was arranged to provide obstruction of signal on the transmission path. The receiver links was rotated around the obstruction edge at 5 degree step for reception until total fading was achieved at 45 degrees shadowing created by the board. The curves of the signal attenuation and the different angles of diffraction are presented in figures 3-5. Also on the curve of the diffraction propagation loss, is the free space path loss of the device for comparison purpose.

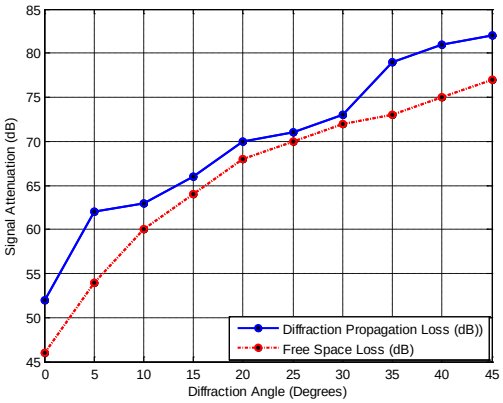

Figure 3: Signal Attenuation at different angles of diffraction and Free Space path loss

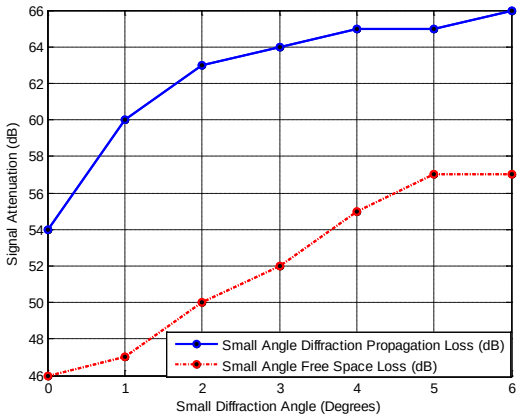

Fig 4: Signal Attenuation at small angles of diffraction Propagation and Free space Path loss

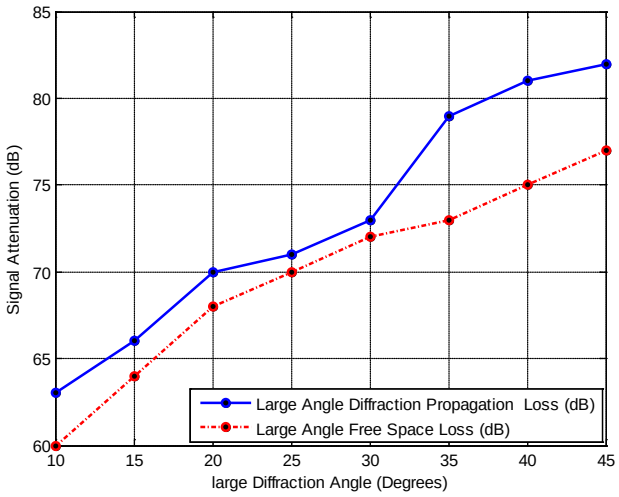

Figure 5: Signal Attenuation at Large angles of diffraction Propagation and Free space path loss

6 Conclusion

The enhanced signal transmission in an obstructed environment as revealed by the experimental results of this work shows that the integration of directional antennas in millimeter wave WLAN systems enhances the system performance by increasing the capacity and extending the angular range of reception. In out experiments interference was mitigated and multipath effects were equalized to achieve high data rate at reasonably diffraction angles. It is can be concluded that wireless networks can now compare favorably with their wired counterparts for gigabit data rate delivery required by the numerous consumer applications in the office and obstructed environments, while security is enhanced due to the antenna directivity, focusing the signal transmission with increased gain while suppressing interference towards the targeted user. The tremendous advantages in this newly opened frequency spectrum at 24Ghz can be tapped into for the realization of fast and seamless high throughput transmission needed for the fast growing ubiquitous wireless and internet applications.

REFERENCES

[1]. O.J Femi-Jemilohun and S. D. Walker, "Pathloss Prediction Models for Corridor Propagation at 24GHz," Transactions on Networks and Communications, vol. 2, pp. 84-94, 2014.

[2]. O.J Femi-Jemilohun, T. Quinlan, S Barc, and S.D Walker, "An Experimental Investigation into GbE Wireless data Communication at 24GHz in Non-Line-of-Sight and Multi-Path Rich environments," Antenna and Wireless Propagation Letters IEEE, vol. 13, pp. 1219-1222, 2014.

[3]. M. Jacob, S. Priebe, R. Dickhoff, T. Kleine-Ostmann, T. Schrader, and T. Kurner, "Diffraction in mm and sub-mm Wave Indoor Propagation Channels," Microwave Theory and Techniques, IEEE Transactions on, vol. 60, pp. 833-844, 2012.

[4]. P. A. Tenerelli, "Diffraction by Building Corners at 28 Ghz: Measurements and Modeling," Citeseer, 1998.

[5]. P.F.M Smulders "Statistical Characterisation of 60GHz Indoor Radio Channells" IEEE Transaction of Antenna and Propagatio, vol 57, 2009.

[6]. J. Medbo, etal "Channel Modelling for the Fifth Generation Mobile Communications "

[7]. H. D. Schotten and M. A. Uusitalo (Editors), “Intermediate description of the spectrum needs and usage principles,” Deliverable D5.1, V1.0, ICT-317669, METIS project, 30th August 2013.

[8]. S. Kavanagh, “An introduction to 24GHz,” Kitohener Waterloo Amateur Radio Club, 2001.

[9]. A. C. T. Workings, “Hardware and solution for the broadband wireless industry,” Altius Communication Technology Workings Electronic Article, 2013.

[10]. J. Laskar, S. Pinel, D. Dawn, S. Sarkar, B. Perumana, and P. Sen, “The next wireless wave is a millimeter wave,” Microwave Journal, vol. 50, no. 8, p. 22, 2007.

[11]. S. Yun, S. Park, Y. Lee, D. Park, Y. Kim, K. Kim, and C. G. Kang, “Hybrid division duplex system for next-generation cellular services,” Vehicular Technology, IEEE Transactions on Vehicular Technology, vol. 56, no. 5, pp. 3040–3059, 2007.

[12]. Y. J. Sang, J. M. Park, S.-L. Kim, and K. S. Kim, “An overlaid hybrid-division duplex OFDMA system with multihop transmission.,” ETRI Journal, vol. 33, no. 4, 2011.

[13]. Digi, “Application note xst-an010a,” Digi, p. 6, 2012.

[14]. J. Zyren and A. Petrick, “Tutorial on basic link budget analysis,” Application Note AN9804, Harris Semiconductor, 1998.

SOCIETY FOR SCIENCE AND EDUCATION
UNITED KINGDOM

TNC TRANSACTIONS ON NETWORKS AND COMMUNICATIONS

VOLUME 3, ISSUE 6
ISSN: 2054 -7420

RFID Tags Detectors Stability Analysis Under Delayed Schottky Diode's Internal Elements in Time

Ofer Aluf, Netanya, Israel

ABSTRACT — **In this article, we discuss the crucial subject of stability analysis of RFID tag detectors under Schottky diodes internal time delay elements. The Schottky diode detector demodulates the signal and sends the data on to the digital circuit of the TAG; this is the so-called "wake up" signal. A simple RFID TAG receiver block diagram includes input antenna signal with series resistance, inductor (choke), Schottky diode, and output capacitor. Due to the Schottky parasitic delay, there is a stability issue in analyzing detector operation. We define τ_1, τ_2 as delays in time respectively for a Schottky equivalent circuit. We first consider those two delays in time that are not equal ($\tau_1 \neq \tau_2$)then the other three cases τ_1=τ and $\tau_2 = 0$, τ_2=τ and $\tau_1 = 0$, τ_1=τ and τ_2=τ. The RFID receiver detector time delay equivalent circuit can be represent as delayed differential equations that depend on variable parameters and delays. The article illustrates certain observations, and analyzes local bifurcations of an appropriate arbitrary scalar delayed differential equation. All of that for optimization of an RFID receiver detector equivalent circuit parameters analysis to get the best performance.**

Index Terms: RFID video receiver, Schottky diode, Delay Differential Equations (DDE), Stability, Bifurcation, Orbit.

I. INTRODUCTION

In this article, we discuss the crucial and useful subject of stability analysis of RFID tag detectors under Schottky diodes internal time delay elements. In RFID systems, the reader or interrogator sends a modulated RF signal that is received by the TAG. The Schottky diode detector demodulates the signal and sends the data on to the digital circuits of the TAG. The reader stops sending modulated data and illuminates the TAG with continuous wave (CW) or an un-modulated signal. The TAG's FSK encoder and switch driver, switch the load placed on the TAG's antenna from one state to another, causing the radar cross section of the TAG to be changed. For incoming RF small signal from the RFID reader to the TAG, we can use Schottky diode which represented by a linear equivalent circuit. Rj is the junction resistance (Rv or video resistance) of the diode, where RF power is converted into video voltage output. For maximum output, all the incoming RF voltage should ideally appear across Rj. Cj is the junction capacitance

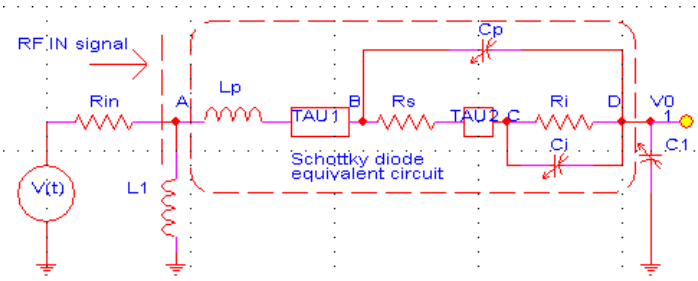

Fig. 1. RFID TAG receiver detector equivalent circuit.

of the diode chip itself. It is a parasitic element which shorts out the junction resistance, shunting RF energy to the series resistance Rs. Rs is a parasitic resistance representing losses in the diode's bond wire, the bulk silicon at the base of the chip and other loss mechanisms. RF voltage appearing across Rs results in power lost as heat. Lp and Cp are package parasitic inductance and capacitance, respectively. The package parasitic inductance Lp has a parasitic delay element in time (τ_1). The resistance losses in the diode's bond wire have a parasitic delay element in time (τ_2). $V(t)$ represents the RFID tag antenna voltage in time, incoming RF small signal from RFID reader [1] [2]. We consider ideal delay lines (TAU1, TAU2).

$$V_{\tau_1} \to \varepsilon_1; V_{\tau_1} \to \varepsilon_2; \varepsilon_1, \varepsilon_2 \ll \varepsilon \tag{1}$$

II. RFID TAG RECEIVER DETECTOR EQUIVALENT CIRCUIT DIFFERENTIAL EQUATIONS AND FIXED POINTS

$$\begin{aligned} &\tfrac{V(t)-V_A}{R_{in}} = I_{R_{in}}; I_{R_{in}} = I_{L_1} + I_{L_P}; V_{\tau_1} \to \varepsilon_1 \\ &V_{\tau_1} \to \varepsilon_2; \varepsilon_1, \varepsilon_2 \ll \varepsilon > 0; V_A - V_B = L_P \tfrac{dI_{L_P}}{dt} \end{aligned} \tag{2}$$

$$\begin{aligned} &I_{L_P} = I_{C_P} + I_{R_S}; I_{R_S} = \tfrac{V_B - V_C}{R_S}; V_A = L_1 \tfrac{dI_{L_1}}{dt} \\ &I_{C_P} = C_P \tfrac{d(V_B - V_D)}{dt}; I_{R_j} = \tfrac{V_C - V_D}{R_j} \end{aligned} \tag{3}$$

$$\begin{aligned} &I_{C_j} = C_j \tfrac{d(V_C - V_D)}{dt}; I_{R_S} = I_{R_j} + I_{C_j} \\ &I_{C_1} = C_1 \tfrac{dV_D}{dt}; I_{C_1} = I_{C_P} + I_{R_j} + I_{C_j} \end{aligned} \tag{4}$$

$$\begin{aligned} &\tfrac{dV_D}{dt} = \tfrac{I_{C_1}}{C_1}; I_{C_j} = C_j \tfrac{d(V_C - V_D)}{dt} = C_j [\tfrac{dV_C}{dt} - \tfrac{dV_D}{dt}] \\ &I_{C_j} = C_j [\tfrac{dV_C}{dt} - \tfrac{dV_D}{dt}] \end{aligned} \tag{5}$$

DOI: 10.14738/tnc.36.1653
Publication Date: 17st December 2015
URL: http://dx.doi.org/10.14738/tnc.36.1653

$$I_{C_P} = C_P\frac{d(V_B-V_D)}{dt} = C_P[\frac{dV_B}{dt} - \frac{dV_D}{dt}] = C_P[\frac{dV_B}{dt} - \frac{I_{C_1}}{C_1}]$$
$$\frac{V(t)-V_A}{R_{in}} = I_{R_{in}} = I_{L_1} + I_{L_P} \tag{6}$$

$$\frac{V(t)}{R_{in}} - \frac{L_1}{R_{in}}\frac{dI_{L_1}}{dt} = I_{L_1} + I_{L_P}; I_{R_{in}} = I_{L_1} + I_{L_P}$$
$$I_{L_1} = I_{R_{in}} - I_{L_P} = \frac{V(t)-V_A}{R_{in}} - I_{L_P} \tag{7}$$

$$\frac{V(t)}{R_{in}} - \frac{L_1}{R_{in}}\frac{d}{dt}[\frac{V(t)-V_A}{R_{ip}} - I_{L_P}] = I_{L_1} + I_{L_P} = I_{R_{in}}$$
$$I_{C_P} = C_P[\frac{dV_B}{dt} - \frac{I_{L_P}}{C_1}] \tag{8}$$

$$I_{R_j} = \frac{V_C-V_D}{R_j}; I_{R_j}R_j = V_C - V_D; I_{C_j} = C_j\frac{d(V_C-V_D)}{dt}$$
$$I_{R_j}R_j = C_j\frac{d(I_{R_j}R_j)}{dt} = C_jR_j\frac{dI_{R_j}}{dt} \tag{9}$$

$$I_{L_P} = I_{C_P} + I_{R_S} \Rightarrow I_{C_P} = I_{L_P} - I_{R_S}$$
$$I_{C_1} = I_{C_P} + I_{R_j} + I_{C_j} = I_{L_P} - I_{R_S} + I_{R_j} + I_{C_j} \tag{10}$$

$$I_{R_S} = I_{R_j} + I_{C_j} \Rightarrow I_{C_1} = I_{L_P} - I_{R_S} + I_{R_j} + I_{C_j}$$
$$I_{C_1} = I_{L_P} - (I_{R_j} + I_{C_j}) + I_{R_j} + I_{C_j} = I_{L_P} \tag{11}$$

$$I_{R_{in}} = \frac{V(t)-V_A}{R_{in}} = \frac{V(t)}{R_{in}} - \frac{1}{R_{in}}L_1\frac{dI_{L_1}}{dt}$$
$$I_{R_{in}} = \frac{1}{R_{in}}[V(t) - L_1\frac{dI_{L_1}}{dt}]$$
$$I_{L_1} = I_{R_{in}} - I_{L_P}; I_{C_P} = I_{L_P} - I_{R_S} \tag{12}$$

$$I_{C_1} = I_{L_P}; I_{R_S} = I_{R_j} + I_{C_j}; I_{C_j} = C_j[\frac{dV_C}{dt} - \frac{I_{C_1}}{C_1}]$$
$$I_{C_j} = C_j\frac{d}{dt}[I_{R_j}R_j] = C_jR_j\frac{dI_{R_j}}{dt} \tag{13}$$

$$I_{C_P} = C_P[\frac{dV_B}{dt} - \frac{I_{C_1}}{C_1}]; V_A - V_B = L_P\frac{dI_{L_P}}{dt}$$
$$L_1\frac{dI_{L_1}}{dt} - V_B = L_P\frac{dI_{L_P}}{dt}; V_B = L_1\frac{dI_{L_1}}{dt} - L_P\frac{dI_{L_P}}{dt} \tag{14}$$

$$\frac{dV_B}{dt} = L_1\frac{d^2I_{L_1}}{dt^2} - L_P\frac{d^2I_{L_P}}{dt^2}; I_{C_P} = C_P[\frac{dV_B}{dt} - \frac{I_{C_1}}{C_1}]$$
$$I_{C_P} = C_P[L_1\frac{d^2I_{L_1}}{dt^2} - L_P\frac{d^2I_{L_P}}{dt^2} - \frac{I_{C_1}}{C_1}] \tag{15}$$

$$I_{L_1} = I_{R_{in}} - I_{L_P} = \frac{V(t)-V_A}{R_{in}} - I_{L_P}$$
$$I_{L_1} = \frac{V(t)}{R_{in}} - \frac{L_1}{R_{in}}\frac{dI_{L_1}}{dt} - I_{L_P}$$
$$I_{C_P} = I_{L_P} - I_{R_S}; I_{C_1} = I_{L_P} \tag{16}$$

$$I_{L_1} = \frac{V(t)}{R_{in}} - \frac{L_1}{R_{in}}\frac{dI_{L_1}}{dt} - I_{L_P}$$
$$\frac{dI_{L_1}}{dt} = \frac{1}{R_{in}}\frac{dV(t)}{dt} - \frac{L_1}{R_{in}}\frac{d^2I_{L_1}}{dt^2} - \frac{dI_{L_P}}{dt} \tag{17}$$

$$\frac{L_1}{R_{in}}\frac{d^2I_{L_1}}{dt^2} = \frac{1}{R_{in}}\frac{dV(t)}{dt} - \frac{dI_{L_P}}{dt} - \frac{dI_{L_1}}{dt}$$
$$\frac{d^2I_{L_1}}{dt^2} = \frac{1}{L_1}\frac{dV(t)}{dt} - \frac{R_{in}}{L_1}\frac{dI_{L_P}}{dt} - \frac{R_{in}}{L_1}\frac{dI_{L_1}}{dt} \tag{18}$$

$$I_{R_S} = I_{R_j} + I_{C_j}; \frac{V_B-V_C}{R_S} = I_{R_j} + I_{C_j}$$
$$I_{C_j} = I_{R_S} - I_{R_j}; I_{C_j} = C_jR_j\frac{dI_{R_j}}{dt}$$
$$I_{R_S} - I_{R_j} = C_jR_j\frac{dI_{R_j}}{dt} \tag{19}$$

$$I_{C_P} = C_P[\frac{dV(t)}{dt} - R_{in}\frac{dI_{L_P}}{dt}$$
$$-R_{in}\frac{dI_{L_1}}{dt} - L_P\frac{d^2I_{L_P}}{dt^2} - \frac{I_{C_1}}{C_1}] \tag{20}$$

$$I_{L_P} - I_{R_S} = C_P[\frac{dV(t)}{dt} - R_{in}\frac{dI_{L_P}}{dt} - R_{in}\frac{dI_{L_1}}{dt}$$
$$-L_P\frac{d^2I_{L_P}}{dt^2} - \frac{I_{C_1}}{C_1}] \tag{21}$$

$$I_{C_1} = I_{L_P}; I_{L_P} - I_{R_S} = C_P[\frac{dV(t)}{dt} - R_{in}\frac{dI_{L_P}}{dt}$$
$$-R_{in}\frac{dI_{L_1}}{dt} - L_P\frac{d^2I_{L_P}}{dt^2} - \frac{I_{L_P}}{C_1}] \tag{22}$$

$$I_{R_S} = \frac{V_B-V_C}{R_S}; V_B - V_C = I_{R_S}R_S$$
$$I_{C_P} = C_P\frac{d(V_B-V_D)}{dt}; \frac{I_{C_P}}{C_P} = \frac{d}{dt}(V_B - V_D)$$
$$V_B - V_D = \frac{1}{C_P}\int I_{C_P}dt \tag{23}$$

$$I_{C_j} = C_j\frac{d(V_C-V_D)}{dt} \Rightarrow \frac{I_{C_j}}{C_j} = \frac{d(V_C-V_D)}{dt}$$
$$V_C - V_D = \frac{1}{C_j}\int I_{C_j}dt \tag{24}$$

$$(*)\, V_B - V_D = \frac{1}{C_P}\int I_{C_P}dt \tag{25}$$

$$(**)\, V_C - V_D = \frac{1}{C_j}\int I_{C_j}dt \tag{26}$$

$$(*)-(**)\quad V_B - V_C = \frac{1}{C_P}\int I_{C_P}dt - \frac{1}{C_j}\int I_{C_j}dt$$
$$I_{R_S}R_S = \frac{1}{C_P}\int I_{C_P}dt - \frac{1}{C_j}\int I_{C_j}dt \tag{27}$$

$$I_{R_S}R_S = \frac{1}{C_P}\int I_{C_P}dt - \frac{1}{C_j}\int I_{C_j}dt$$
$$R_S\frac{dI_{R_S}}{dt} = \frac{1}{C_P}I_{C_P} - \frac{1}{C_j}I_{C_j} \tag{28}$$

$$R_S\frac{dI_{R_S}}{dt} = \frac{1}{C_P}I_{C_P} - \frac{1}{C_j}I_{C_j}$$
$$R_S\frac{dI_{R_S}}{dt} = \frac{1}{C_P}(I_{L_P} - I_{R_S}) - \frac{1}{C_j}(I_{R_S} - I_{R_j}) \tag{29}$$

$$R_S\frac{dI_{R_S}}{dt} = \frac{1}{C_P}(I_{L_P} - I_{R_S}) - \frac{1}{C_j}(I_{R_S} - I_{R_j})$$
$$R_S\frac{dI_{R_S}}{dt} = \frac{1}{C_P}I_{L_P} + \frac{1}{C_j}I_{R_j} - I_{R_S}(\frac{1}{C_P} + \frac{1}{C_j}) \tag{30}$$

$$R_S\frac{dI_{R_S}}{dt} = \frac{1}{C_P}I_{L_P} + \frac{1}{C_j}I_{R_j} - I_{R_S}(\frac{1}{C_P} + \frac{1}{C_j})$$
$$\frac{dI_{R_S}}{dt} = \frac{1}{R_SC_P}I_{L_P} + \frac{1}{R_SC_j}I_{R_j}$$
$$-I_{R_S}(\frac{1}{R_SC_P} + \frac{1}{R_SC_j}) \tag{31}$$

We define

$$Y = I_{L_P} \Rightarrow \frac{dI_{R_S}}{dt} = \frac{1}{R_SC_P}Y + \frac{1}{R_SC_j}I_{R_j}$$
$$-I_{R_S}(\frac{1}{R_SC_P} + \frac{1}{R_SC_j}) \tag{32}$$

$$\frac{V(t)}{R_{in}} - \frac{L_1}{R_{in}}\frac{dI_{L_1}}{dt} = I_{L_1} + I_{L_P}$$
$$\frac{V(t)}{R_{in}} - I_{L_1} - I_{L_P} = \frac{L_1}{R_{in}}\frac{dI_{L_1}}{dt}$$
$$\frac{V(t)}{L_1} - \frac{R_{in}}{L_1}I_{L_1} - \frac{R_{in}}{L_1}I_{L_P} = \frac{dI_{L_1}}{dt} \tag{33}$$

$$I_{L_P} - I_{R_S} = C_P[\frac{dV(t)}{dt} - R_{in}\frac{dI_{L_P}}{dt} - R_{in}\frac{dI_{L_1}}{dt}$$
$$-L_P\frac{d^2I_{L_P}}{dt^2} - \frac{I_{L_P}}{C_1}] \tag{34}$$

$$I_{L_P} - I_{R_S} = C_P[\frac{dV(t)}{dt} - R_{in}\frac{dI_{L_P}}{dt}$$
$$-R_{in}(\frac{V(t)}{L_1} - \frac{R_{in}}{L_1}I_{L_1} - \frac{R_{in}}{L_1}I_{L_P})$$
$$-L_P\frac{d^2I_{L_P}}{dt^2} - \frac{I_{L_P}}{C_1}] \tag{35}$$

$$I_{L_P} - I_{R_S} = C_P[\frac{dV(t)}{dt} - R_{in}\frac{dI_{L_P}}{dt} - \frac{R_{in}V(t)}{L_1} + \frac{R_{in}^2}{L_1}I_{L_1} + \frac{R_{in}^2}{L_1}I_{L_P} - L_P\frac{d^2I_{L_P}}{dt^2} - \frac{I_{L_P}}{C_1}] \quad (36)$$

$$-I_{L_P} + I_{R_S} + C_P\frac{dV(t)}{dt} - C_PR_{in}\frac{dI_{L_P}}{dt} - \frac{C_PR_{in}V(t)}{L_1} + C_P\frac{R_{in}^2}{L_1}I_{L_1} + C_P\frac{R_{in}^2}{L_1}I_{L_P} - C_PL_P\frac{d^2I_{L_P}}{dt^2} - \frac{C_PI_{L_P}}{C_1} = 0 \quad (37)$$

$$-C_PL_P\frac{d^2I_{L_P}}{dt^2} - C_PR_{in}\frac{dI_{L_P}}{dt} + I_{L_P}[C_P\frac{R_{in}^2}{L_1} - \frac{C_P}{C_1} - 1] + I_{R_S} + C_P\frac{R_{in}^2}{L_1}I_{L_1} - \frac{C_PR_{in}V(t)}{L_1} + C_P\frac{dV(t)}{dt} = 0 \quad (38)$$

We define:

$$Y = I_{L_P}; X = \frac{dI_{L_P}}{dt}; \frac{dX}{dt} = \frac{d^2I_{L_P}}{dt^2}$$
$$\frac{dY}{dt} = \frac{dI_{L_P}}{dt} = X \quad (39)$$

Then we get the expression:

$$-C_PL_P\frac{dX}{dt} - C_PR_{in}X + Y[C_P\frac{R_{in}^2}{L_1} - \frac{C_P}{C_1} - 1] + I_{R_S} + C_P\frac{R_{in}^2}{L_1}I_{L_1} - \frac{C_PR_{in}V(t)}{L_1} + C_P\frac{dV(t)}{dt} = 0 \quad (40)$$

$$C_PL_P\frac{dX}{dt} = -C_PR_{in}X + Y[C_P\frac{R_{in}^2}{L_1} - \frac{C_P}{C_1} - 1] + I_{R_S} + C_P\frac{R_{in}^2}{L_1}I_{L_1} - \frac{C_PR_{in}V(t)}{L_1} + C_P\frac{dV(t)}{dt} \quad (41)$$

$$\frac{dX}{dt} = -\frac{R_{in}}{L_P}X + Y[\frac{R_{in}^2}{L_1L_P} - \frac{1}{C_1L_P} - \frac{1}{C_PL_P}] + I_{R_S}\frac{1}{C_PL_P} + \frac{R_{in}^2}{L_1L_P}I_{L_1} - \frac{R_{in}V(t)}{L_1L_P} + \frac{1}{L_P}\frac{dV(t)}{dt} \quad (42)$$

$$\frac{dY}{dt} = X; \frac{dI_{L_1}}{dt} = \frac{V(t)}{L_1} - \frac{R_{in}}{L_1}I_{L_1} - \frac{R_{in}}{L_1}Y$$
$$\frac{dI_{R_j}}{dt} = \frac{1}{C_jR_j}I_{R_S} - \frac{1}{C_jR_j}I_{R_j} \quad (43)$$

$$\frac{dI_{R_S}}{dt} = \frac{1}{R_SC_P}Y + \frac{1}{R_SC_j}I_{R_j} - I_{R_S}\frac{1}{R_S}(\frac{1}{C_P} + \frac{1}{C_j}) \quad (44)$$

We have five variables in our system: $X, Y, I_{L_1}, I_{R_j}, I_{R_S}$ and we can represent our system as the following set of differential equations matrix representation.

$$\Xi_{11} = -\frac{R_{in}}{L_P}; \Xi_{12} = \frac{R_{in}^2}{L_1L_P} - \frac{1}{C_1L_P} - \frac{1}{C_PL_P}$$
$$\Xi_{12} = \frac{1}{L_P}(\frac{R_{in}^2}{L_1} - \frac{1}{C_1} - \frac{1}{C_P}); \Xi_{13} = \frac{R_{in}^2}{L_1L_P}; \Xi_{14} = 0 \quad (45)$$

$$\begin{pmatrix} \frac{dX}{dt} \\ \frac{dY}{dt} \\ \frac{dI_{L_1}}{dt} \\ \frac{dI_{R_j}}{dt} \\ \frac{dI_{R_S}}{dt} \end{pmatrix} = \begin{pmatrix} \Xi_{11} & \cdots & \Xi_{1n} \\ \vdots & \ddots & \vdots \\ \Xi_{m1} & \cdots & \Xi_{mn} \end{pmatrix}_{n=m=5} \begin{pmatrix} X \\ Y \\ I_{L_1} \\ I_{R_j} \\ I_{R_S} \end{pmatrix} + \begin{pmatrix} -\frac{R_{in}}{L_1L_P} \\ 0 \\ \frac{1}{L_1} \\ 0 \\ 0 \end{pmatrix} V(t) + \begin{pmatrix} \frac{1}{L_P} \\ 0 \\ 0 \\ 0 \\ 0 \end{pmatrix} \frac{dV(t)}{dt} \quad (46)$$

$$\Xi_{15} = \frac{1}{C_PL_P}; \Xi_{21} = 1; \Xi_{22} = \Xi_{23} = \Xi_{24} = \Xi_{25} = 0$$
$$\Xi_{31} = 0; \Xi_{32} = -\frac{R_{in}}{L_1}; \Xi_{33} = -\frac{R_{in}}{L_1} \quad (47)$$

$$\Xi_{34} = \Xi_{35} = 0; \Xi_{41} = \Xi_{42} = \Xi_{43} = 0$$
$$\Xi_{44} = -\frac{1}{C_jR_j}; \Xi_{45} = \frac{1}{C_jR_j}; \Xi_{51} = 0; \Xi_{52} = \frac{1}{R_SC_P} \quad (48)$$

$$\Xi_{53} = 0; \Xi_{54} = \frac{1}{R_SC_j}; \Xi_{55} = -\frac{1}{R_S}(\frac{1}{C_P} + \frac{1}{C_j}) \quad (49)$$

We consider RFin signal

$$V(t) = A_0 + f(t) \quad (50)$$

$$V(t) = A_0 + f(t); |f(t)| < 1 \,\&\, A_0 \gg |f(t)| \quad (51)$$

$$V(t)|_{A_0 \gg |f(t)|}; V(t)|_{A_0 \gg |f(t)|} = A_0 + f(t) \approx A_0 \quad (52)$$

$$\frac{dV(t)}{dt}|_{A_0 \gg |f(t)|} = \frac{df(t)}{dt} \to \varepsilon \quad (53)$$

We can present our matrix representation: $\varepsilon \to 0$. Due to parasitic delay elements in Schottky equivalent circuit, τ_1 for the current flow through Schottky diode's package parasitic inductance (L_P) and τ_2 for the current flow through Schottky diode's parasitic resistance (R_S), we get the following transformation [3] [4].

$$Y(t) = I_{L_P}(t) \to Y(t-\tau_1) = I_{L_P}(t-\tau_1)$$
$$I_{R_S}(t) \to I_{R_S}(t-\tau_2) \quad (54)$$

and $X(t) = \frac{dI_{L_P}(t)}{dt}; I_{L_1}(t); I_{R_j}(t)$. We consider no delay effects on $\frac{dY}{dt} = \frac{dI_{L_P}}{dt}; \frac{dI_{R_S}}{dt}$. To find equilibrium points (fixed points) of the RFID tag detector, we define

$$\lim_{t\to\infty} Y(t-\tau_1) = Y(t); \lim_{t\to\infty} I_{L_P}(t-\tau_1) = I_{L_P}(t)$$
$$\lim_{t\to\infty} I_{R_S}(t-\tau_2) = I_{R_S}(t) \quad (55)$$

$$\begin{pmatrix} \frac{dX}{dt} \\ \frac{dY}{dt} \\ \frac{dI_{L_1}}{dt} \\ \frac{dI_{R_j}}{dt} \\ \frac{dI_{R_S}}{dt} \end{pmatrix} = \begin{pmatrix} \Xi_{11} & \cdots & \Xi_{1n} \\ \vdots & \ddots & \vdots \\ \Xi_{m1} & \cdots & \Xi_{mn} \end{pmatrix}_{n=m=5} \begin{pmatrix} X \\ Y \\ I_{L_1} \\ I_{R_j} \\ I_{R_S} \end{pmatrix} + \begin{pmatrix} -\frac{R_{in}}{L_1L_P} \\ 0 \\ \frac{1}{L_1} \\ 0 \\ 0 \end{pmatrix} A_0 + \varepsilon \quad (56)$$

In equilibrium points (fixed points)

$$\frac{dY}{dt} = \frac{dI_{L_P}}{dt} = 0; \frac{dI_{R_S}}{dt} = 0 \,\forall\, t \gg \tau_1, t \gg \tau_2$$
$$\exists (t-\tau_1) \approx t, (t-\tau_2) \approx t, t \to \infty \quad (57)$$

We get five equations:

$$-\frac{R_{in}}{L_P}X^*+Y^*[\frac{R_{in}^2}{L_1L_P}-\frac{1}{C_1L_P}-\frac{1}{C_PL_P}] +I^*_{R_S}\frac{1}{C_PL_P}+\frac{R_{in}^2}{L_1L_P}I^*_{L_1}-\frac{R_{in}V(t)}{L_1L_P}+\frac{1}{L_P}\frac{dV(t)}{dt}=0 \quad (58)$$

$$X^*=0;\frac{V(t)}{L_1}-\frac{R_{in}}{L_1}I^*_{L_1}-\frac{R_{in}}{L_1}Y^*=0 \quad \frac{1}{C_jR_j}I^*_{R_S}-\frac{1}{C_jR_j}I^*_{R_j}=0 \quad (59)$$

$$\frac{1}{R_sC_P}Y^*+\frac{1}{R_sC_j}I^*_{R_j}-I^*_{R_s}(\frac{1}{C_P}+\frac{1}{C_j})=0 \quad (60)$$

Since $X^*=0$ then

$$Y^*[\frac{R_{in}^2}{L_1L_P}-\frac{1}{C_1L_P}-\frac{1}{C_PL_P}]+I^*_{R_S}\frac{1}{C_PL_P} +\frac{R_{in}^2}{L_1L_P}I^*_{L_1}-\frac{R_{in}V(t)}{L_1L_P}+\frac{1}{L_P}\frac{dV(t)}{dt}=0 \quad (61)$$

$$\frac{V(t)}{L_1}-\frac{R_{in}}{L_1}I^*_{L_1}-\frac{R_{in}}{L_1}Y^*=0\Rightarrow Y^*=\frac{V(t)}{R_{in}}-I^*_{L_1} \quad (62)$$

$$\frac{1}{R_SC_P}(\frac{V(t)}{R_{in}}-I^*_{L_1})+\frac{1}{R_SC_j}I^*_{R_j} -I^*_{R_S}\frac{1}{R_S}(\frac{1}{C_P}+\frac{1}{C_j})=0 \quad (63)$$

$$(\frac{V(t)}{R_{in}}-I^*_{L_1})[\frac{R_{in}^2}{L_1L_P}-\frac{1}{C_1L_P}-\frac{1}{C_PL_P}] +I^*_{R_S}\frac{1}{C_PL_P}+\frac{R_{in}^2}{L_1L_P}I^*_{L_1}-\frac{R_{in}V(t)}{L_1L_P}+\frac{1}{L_P}\frac{dV(t)}{dt}=0 \quad (64)$$

We get three equations:

$$\frac{1}{C_jR_j}I^*_{R_S}-\frac{1}{C_jR_j}I^*_{R_j}=0 \quad (65)$$

$$\frac{1}{R_SC_P}(\frac{V(t)}{R_{in}}-I^*_{L_1})+\frac{1}{R_SC_j}I^*_{R_j} -I^*_{R_S}\frac{1}{R_S}(\frac{1}{C_P}+\frac{1}{C_j})=0 \quad (66)$$

$$(\frac{V(t)}{R_{in}}-I^*_{L_1})[\frac{R_{in}^2}{L_1L_P}-\frac{1}{C_1L_P}-\frac{1}{C_PL_P}]+I^*_{R_S}\frac{1}{C_PL_P} +\frac{R_{in}^2}{L_1L_P}I^*_{L_1}-\frac{R_{in}V(t)}{L_1L_P}+\frac{1}{L_P}\frac{dV(t)}{dt}=0 \quad (67)$$

$$\frac{1}{C_jR_j}I^*_{R_S}-\frac{1}{C_jR_j}I^*_{R_j}=0\Rightarrow I^*_{R_j}=I^*_{R_S} \quad (68)$$

We get two equations:

$$\frac{1}{R_SC_P}(\frac{V(t)}{R_{in}}-I^*_{L_1})+\frac{1}{R_SC_j}I^*_{R_S} -I^*_{R_S}\frac{1}{R_S}(\frac{1}{C_P}+\frac{1}{C_j})=0 \quad (69)$$

$$(\frac{V(t)}{R_{in_2}}-I^*_{L_1})[\frac{R_{in}^2}{L_1L_P}-\frac{1}{C_1L_P}-\frac{1}{C_PL_P}]+I^*_{R_S}\frac{1}{C_PL_P} +\frac{R_{in}^2}{L_1L_P}I^*_{L_1}-\frac{R_{in}V(t)}{L_1L_P}+\frac{1}{L_P}\frac{dV(t)}{dt}=0 \quad (70)$$

By mathematic manipulation, we get the following two equations:

$$\frac{V(t)}{R_{in}}-I^*_{L_1}-I^*_{R_S}=0\Rightarrow I^*_{R_S}=\frac{V(t)}{R_{in}}-I^*_{L_1} \quad (71)$$

$$I^*_{L_1}(\frac{1}{C_1}+\frac{1}{C_P})+I^*_{R_S}\frac{1}{C_P} +V(t)\{\frac{1}{R_{in}}[\frac{R_{in}^2}{L_1}-\frac{1}{C_1}-\frac{1}{C_P}]-\frac{R_{in}}{L_1}\}+\frac{dV(t)}{dt}=0 \quad (72)$$

We define for simplicity:

$$\Omega=\frac{1}{R_{in}}[\frac{R_{in}^2}{L_1}-\frac{1}{C_1}-\frac{1}{C_P}]-\frac{R_{in}}{L_1} \quad (73)$$

$$I^*_{R_S}=\frac{V(t)}{R_{in}}-I^*_{L_1};I^*_{L_1}(\frac{1}{C_1}+\frac{1}{C_P})+I^*_{R_S}\frac{1}{C_P} +V(t)\Omega+\frac{dV(t)}{dt}=0 \quad (74)$$

$$I^*_{L_1}(\frac{1}{C_1}+\frac{1}{C_P})+(\frac{V(t)}{R_{in}}-I^*_{L_1})\frac{1}{C_P} +V(t)\Omega+\frac{dV(t)}{dt}=0 \quad I^*_{L_1}\frac{1}{C_1}+V(t)[\frac{1}{R_{in}C_P}+\Omega]+\frac{dV(t)}{dt}=0 \quad (75)$$

$$I^*_{L_1}\frac{1}{C_1}+V(t)[\frac{1}{R_{in}C_P}+\Omega]+\frac{dV(t)}{dt}=0 \quad I^*_{L_1}=-C_1\{V(t)[\frac{1}{R_{in}C_P}+\Omega]+\frac{dV(t)}{dt}\} \quad (76)$$

$$I^*_{R_S}=\frac{V(t)}{R_{in}}+C_1\{V(t)[\frac{1}{R_{in}C_P}+\Omega]+\frac{dV(t)}{dt}\} =V(t)\{\frac{1}{R_{in}}+C_1[\frac{1}{R_{in}C_P}+\Omega]\}+C_1\frac{dV(t)}{dt} \quad (77)$$

$$\Omega_1=\frac{1}{R_{in}}+C_1[\frac{1}{R_{in}C_p}+\Omega];I^*_{R_S}=V(t)\Omega_1+C_1\frac{dV(t)}{dt} \quad (78)$$

$$I^*_{R_j}=I^*_{R_S}\Rightarrow I^*_{R_j}=V(t)\Omega_1+C_1\frac{dV(t)}{dt};X^*=0 \quad (79)$$

$$Y^*=\frac{V(t)}{R_{in}}-I^*_{L_1} \quad Y^*=V(t)\{\frac{1}{R_{in}}+C_1[\frac{1}{R_{in}C_P}+\Omega]\}+C_1\frac{dV(t)}{dt} \quad (80)$$

We can summery our system fixed points in the next tables:

Fixed point coordinates $E^*(X^*,Y^*,I^*_{L_1},I^*_{R_j},I^*_{R_S})$	Fixed points expression $V(t)=A_0+f(t)$ $\lvert f(t)\rvert<1;A_0\gg\lvert f(t)\rvert$
X^*	0
Y^*	$V(t)\{\frac{1}{R_{in}}+C_1[\frac{1}{R_{in}C_P}+\Omega]\}+C_1\frac{dV(t)}{dt}$
$I^*_{L_1}$	$-C_1\{V(t)[\frac{1}{R_{in}C_p}+\Omega]+\frac{dV(t)}{dt}\}$
$I^*_{R_j}$	$V(t)\Omega_1+C_1\frac{dV(t)}{dt}$
$I^*_{R_S}$	$V(t)\{\frac{1}{R_{in}}+C_1[\frac{1}{R_{in}C_p}+\Omega]\}+C_1\frac{dV(t)}{dt}$

Table. 1a. RFID tag receiver detector system fixed points.

Fixed point coordinates $E^*(X^*,Y^*,I^*_{L_1},I^*_{R_j},I^*_{R_S})$	$V(t)\lvert_{A_0\gg\lvert f(t)\rvert}=A_0+f(t)\approx A_0$ $\frac{dV(t)}{dt}\lvert_{A_0\gg\lvert f(t)\rvert}=\frac{df(t)}{dt}\to\varepsilon$
X^*	0
Y^*	$A_0\{\frac{1}{R_{in}}+C_1[\frac{1}{R_{in}C_P}+\Omega]\}$
$I^*_{L_1}$	$-C_1A_0[\frac{1}{R_{in}C_P}+\Omega]$
$I^*_{R_j}$	$A_0\Omega_1$
$I^*_{R_S}$	$A_0\{\frac{1}{R_{in}}+C_1[\frac{1}{R_{in}C_P}+\Omega]\}$

Table. 1b. RFID tag receiver detector system fixed points.

III. RFID TAG RECEIVER DETECTOR STABILITY ANALYSIS UNDER DELAY VARIABLES IN TIME

We can check our RFID tag receiver detector system stability for the following cases.

$$(A)\,\tau_1=\tau;\tau_2=0\,(B)\,\tau_1=0;\tau_2=\tau\,(C)\,\tau_1=\tau_2=\tau \quad (81)$$

Stability analysis: The standard local stability analysis about any one of the equilibrium points of the RFID tag detector system consists in adding to coordinate $[X,Y,I_{L_1},I_{R_j},I_{R_S}]$ arbitrarily small increments of exponential form $[x,y,i_{L_1},i_{R_j},i_{R_s}]e^{\lambda t}$ and retaining the first order terms in $X,Y,I_{L_1},I_{R_j},I_{R_S}$. The system of five homogeneous equations leads to a polynomial characteristic equation in the eigenvalues. The polynomial characteristic equations accept by set the below currents and currents derivative with respect to time into RFID tag detector system equations. RFID tag detector system fixed values with arbitrarily small increments of exponential form $[x,y,i_{L_1},i_{R_j},i_{R_s}]e^{\lambda t}$ are: $j=0$ (first fixed point), $j=1$ (second fixed point), $j=2$ (third fixed point), etc.

$$\begin{array}{l} X(t)=X^{(j)}+xe^{\lambda t};Y(t)=Y^{(j)}+ye^{\lambda t} \\ Y(t-\tau_1)=Y^{(j)}+ye^{\lambda(t-\tau_1)} \\ I_{L_1}(t)=I_{L_1}^{(j)}+i_{L_1}e^{\lambda t} \end{array} \quad (82)$$

$$\begin{array}{l} I_{R_j}(t)=I_{R_j}^{(j)}+i_{R_j}e^{\lambda t};I_{R_S}(t)=I_{R_S}^{(j)}+i_{R_S}e^{\lambda t} \\ I_{R_S}(t-\tau_2)=I_{R_S}^{(j)}+i_{R_S}e^{\lambda(t-\tau_2)} \end{array} \quad (83)$$

We choose these expressions for ourselves $X(t),Y(t),I_{L_1}(t),I_{R_j}(t),I_{R_S}(t)$ as a small displacement $[x,y,i_{L_1},i_{R_j},i_{R_S}]$ from the RFID tag detector system fixed points in time $t=0$.

$$\begin{array}{l} X(t=0)=X^{(j)}+x;Y(t=0)=Y^{(j)}+y \\ I_{L_1}(t=0)=I_{L_1}^{(j)}+i_{L_1};I_{R_j}(t=0)=I_{R_j}^{(j)}+i_{R_j} \end{array} \quad (84)$$

$$I_{R_S}(t=0)=I_{R_S}^{(j)}+i_{R_S} \quad (85)$$

For $\lambda<0,t>0$ the selected fixed point is stable otherwise $\lambda>0,t>0$ is unstable. Our system tends to the selected fixed point exponentially for $\lambda<0,t>0$ otherwise go away from the selected fixed point exponentially. Eigenvalue λ parameter is established if the fixed point is stable or unstable; additionally, his absolute value $|\lambda|$ establishes the speed of flow toward or away from the selected fixed point (Yuri, 1995; Jack and Huseyin, 1991) [5] [6]. The speeds of flow toward or away from the selected fixed point for Schottky detector system currents and currents derivatives with respect to time are as follow.

$$\begin{array}{l} \frac{dX(t)}{dt}=\lim\limits_{\Delta t\to\infty}\frac{X(t+\Delta t)-X(t)}{\Delta t} \\ =\lim\limits_{\Delta t\to\infty}\frac{X^{(j)}+xe^{\lambda(t+\Delta t)}-[X^{(j)}+xe^{\lambda t}]}{\Delta t} \\ =\lambda xe^{\lambda t} \end{array} \quad (86)$$

$$\begin{array}{l} \frac{dY(t)}{dt}=\lim\limits_{\Delta t\to\infty}\frac{Y(t+\Delta t)-Y(t)}{\Delta t} \\ =\lim\limits_{\Delta t\to\infty}\frac{Y^{(j)}+ye^{\lambda(t+\Delta t)}-[Y^{(j)}+ye^{\lambda t}]}{\Delta t} \\ =\lambda ye^{\lambda t} \end{array} \quad (87)$$

$$\begin{array}{l} \frac{dI_{L_1}(t)}{dt}=\lambda i_{L_1}e^{\lambda t};\frac{dI_{R_j}(t)}{dt}=\lambda i_{R_j}e^{\lambda t} \\ \frac{dI_{R_S}(t)}{dt}=\lambda i_{R_S}e^{\lambda t};\frac{dY(t-\tau_1)}{dt}=\lambda ye^{\lambda t}e^{-\lambda\tau_1} \end{array} \quad (88)$$

$$\frac{dI_{R_S}(t-\tau_2)}{dt}=\lambda i_{R_S}e^{\lambda t}e^{-\lambda\tau_2} \quad (89)$$

First, we take Schottky detector variable $X,Y,I_{L_1},I_{R_j},I_{R_s}$ differential equations and adding to coordinate $[X,Y,I_{L_1},I_{R_j},I_{R_s}]$ arbitrarily small increments of exponential terms $[x,y,i_{L_1},i_{R_j},i_{R_s}]e^{\lambda t}$ and retaining the first order terms in $x,y,i_{L_1},i_{R_j},i_{R_s}$ $(V(t)\to\varepsilon;\frac{dV(t)}{dt}\to\varepsilon)$

$$\begin{array}{l} E^*(X^*,Y^*,I_{L_1}^*,I_{R_j}^*,I_{R_S}^*)=(0,0,0,0,0) \\ X^{(j=0)}=0;Y^{(j=0)}=0;I_{L_1}^{(j=0)}=0 \\ I_{R_j}^{(j=0)}=0;I_{R_S}^{(j=0)}=0 \end{array} \quad (90)$$

$$\begin{array}{l} \lambda_1=-\frac{R_{in}}{L_P}+\frac{y}{x}[\frac{R_{in}^2}{L_1L_P}-\frac{1}{C_1L_P}-\frac{1}{C_PL_P}] \\ +\frac{i_{R_S}}{x}\frac{1}{C_PL_P}+\frac{R_{in}^2}{L_1L_P}\frac{i_{L_1}}{x} \\ \lambda_2=\frac{x}{y};\lambda_3=-\frac{R_{in}}{L_1}-\frac{R_{in}}{L_1}\frac{y}{i_{L_1}} \end{array} \quad (91)$$

$$\begin{array}{l} \lambda_4=\frac{1}{C_jR_j}\frac{i_{R_S}}{i_{R_j}}-\frac{1}{C_jR_j} \\ \lambda_5=\frac{1}{R_SC_P}\frac{y}{i_{R_S}}+\frac{1}{R_SC_j}\frac{i_{R_j}}{i_{R_S}}-\frac{1}{R_S}(\frac{1}{C_P}+\frac{1}{C_j}) \end{array} \quad (92)$$

We consider

$$\begin{array}{l} \frac{y}{x}\approx 1;\frac{i_{R_S}}{x}\approx 1;\frac{i_{L_1}}{x}\approx 1;\frac{x}{y}\approx 1;\frac{y}{i_{L_1}}\approx 1 \\ \frac{i_{R_S}}{i_{R_j}}\approx 1;\frac{y}{i_{R_S}}\approx 1;\frac{i_{R_j}}{i_{R_S}}\approx 1 \end{array} \quad (93)$$

$$\begin{array}{l} \lambda_1=\frac{2R_{in}^2}{L_1L_P}-[\frac{1}{C_1L_P}+\frac{R_{in}}{L_P}];\lambda_2=1 \\ \lambda_3=-\frac{2R_{in}}{L_1}<0;\lambda_4=0;\lambda_5=0 \end{array} \quad (94)$$

$$\frac{2R_{in}^2}{L_1L_P}>[\frac{1}{C_1L_P}+\frac{R_{in}}{L_P}] \quad (95)$$

$$\begin{array}{l} \frac{2R_{in}^2}{L_1L_P}>[\frac{1}{C_1L_P}+\frac{R_{in}}{L_P}] \\ \frac{2R_{in}^2}{L_1}>\frac{1+R_{in}C_1}{C_1}\Rightarrow\lambda_1>0 \end{array} \quad (96)$$

$$\frac{2R_{in}^2}{L_1}<\frac{1+R_{in}C_1}{C_1}\Rightarrow\lambda_1<0 \quad (97)$$

$$\frac{2R_{in}^2}{L_1}=\frac{1+R_{in}C_1}{C_1}\Rightarrow\lambda_1=0 \quad (98)$$

We can see that our fixed point is a saddle node. We define $Y(t-\tau_1)=Y^{(j)}+ye^{\lambda(t-\tau_1)};I_{R_S}(t-\tau_2)=I_{R_S}^{(j)}+i_{R_S}e^{\lambda(t-\tau_2)}$ then we get five delayed differential equations with respect to coordinates $[X,Y,I_{L_1},I_{R_j},I_{R_s}]$ arbitrarily small increments of exponential$[x,y,i_{L_1},i_{R_j},i_{R_s}]e^{\lambda t}$. We consider no delay effects on $\frac{dY(t)}{dt};\frac{dI_{R_S}(t)}{dt}$. We get the following equations:

Time (t)	$\lambda < 0$
$t = 0$	$X(t=0) = X^{(j)} + x; Y(t=0) = Y^{(j)} + y$ $I_{L_1}(t=0) = I_{L_1}^{(j)} + i_{L_1}$ $I_{R_j}(t=0) = I_{R_j}^{(j)} + i_{R_j}$ $I_{R_S}(t=0) = I_{R_S}^{(j)} + i_{R_S}$
$t > 0$	$X(t) = X^{(j)} + xe^{-\lvert\lambda\rvert t}; Y(t) = Y^{(j)} + ye^{-\lvert\lambda\rvert t}$ $I_{L_1}(t) = I_{L_1}^{(j)} + i_{L_1}e^{-\lvert\lambda\rvert t}$ $I_{R_j}(t) = I_{R_j}^{(j)} + i_{R_j}e^{-\lvert\lambda\rvert t}$ $I_{R_s}(t) = I_{R_s}^{(j)} + i_{R_s}e^{-\lvert\lambda\rvert t}$
$t > 0$ $t \to \infty$	$X(t\to\infty) = X^{(j)}; Y(t\to\infty) = Y^{(j)}$ $I_{L_1}(t\to\infty) = I_{L_1}^{(j)}; I_{R_j}(t\to\infty) = I_{R_j}^{(j)}$ $I_{R_S}(t\to\infty) = I_{R_S}^{(j)}$

.

Table. 2a. RFID tag receiver detector system variables for negative eigenvalue ($\lambda < 0$).

.

Time (t)	$\lambda > 0$
$t = 0$	$X(t=0) = X^{(j)} + x; Y(t=0) = Y^{(j)} + y$ $I_{L_1}(t=0) = I_{L_1}^{(j)} + i_{L_1}$ $I_{R_j}(t=0) = I_{R_j}^{(j)} + i_{R_j}$ $I_{R_S}(t=0) = I_{R_S}^{(j)} + i_{R_S}$
$t > 0$	$X(t) = X^{(j)} + xe^{\lvert\lambda\rvert t}; Y(t) = Y^{(j)} + ye^{\lvert\lambda\rvert t}$ $I_{L_1}(t) = I_{L_1}^{(j)} + i_{L_1}e^{\lvert\lambda\rvert t}$ $I_{R_j}(t) = I_{R_j}^{(j)} + i_{R_j}e^{\lvert\lambda\rvert t}$ $I_{R_s}(t) = I_{R_s}^{(j)} + i_{R_s}e^{\lvert\lambda\rvert t}$
$t > 0$ $t \to \infty$	$X(t\to\infty) = xe^{\lvert\lambda\rvert t}; Y(t\to\infty) = ye^{\lvert\lambda\rvert t}$ $I_{L_1}(t\to\infty) = i_{L_1}e^{\lvert\lambda\rvert t}$ $I_{R_j}(t\to\infty) = i_{R_j}e^{\lvert\lambda\rvert t}$ $I_{R_S}(t\to\infty) = i_{R_s}e^{\lvert\lambda\rvert t}$

.

Table. 2b. RFID tag receiver detector system variables for negative eigenvalue ($\lambda > 0$).

$$\begin{array}{l}\lambda xe^{\lambda t} = -\frac{R_{in}}{L_P}[X^{(j)} + xe^{\lambda t}] + [Y^{(j)} \\ +ye^{\lambda(t-\tau_1)}][\frac{R_{in}^2}{L_1L_P} - \frac{1}{C_1L_P} - \frac{1}{C_PL_P}] \\ +[I_{R_S}^{(j)} + i_{R_S}e^{\lambda(t-\tau_2)}]\frac{1}{C_PL_P} \\ +\frac{R_{in}^2}{L_1L_P}[I_{L_1}^{(j)} + i_{L_1}e^{\lambda t}] - \frac{R_{in}V(t)}{L_1L_P} + \frac{1}{L_P}\frac{dV(t)}{dt} \\ V(t), \frac{dV(t)}{dt} \to \varepsilon\end{array} \quad (99)$$

$$\begin{array}{l}\lambda xe^{\lambda t} = -\frac{R_{in}}{L_P}X^{(j)} - \frac{R_{in}}{L_P}xe^{\lambda t} \\ +Y^{(j)}[\frac{R_{in}^2}{L_1L_P} - \frac{1}{C_1L_P} - \frac{1}{C_PL_P}] \\ +y[\frac{R_{in}^2}{L_1L_P} - \frac{1}{C_1L_P} - \frac{1}{C_PL_P}]e^{\lambda(t-\tau_1)} + I_{R_S}^{(j)}\frac{1}{C_PL_P} \\ +i_{R_S}\frac{1}{C_PL_P}e^{\lambda(t-\tau_2)} + \frac{R_{in}^2}{L_1L_P}I_{L_1}^{(j)} + \frac{R_{in}^2}{L_1L_P}i_{L_1}e^{\lambda t}\end{array} \quad (100)$$

$$\begin{array}{l}\lambda xe^{\lambda t} = -\frac{R_{in}}{L_P}X^{(j)} + Y^{(j)}[\frac{R_{in}^2}{L_1L_P} - \frac{1}{C_1L_P} \\ -\frac{1}{C_PL_P}] + I_{R_S}^{(j)}\frac{1}{C_PL_P} + \frac{R_{in}^2}{L_1L_P}I_{L_1}^{(j)} - \frac{R_{in}}{L_P}xe^{\lambda t} \\ +y[\frac{R_{in}^2}{L_1L_P} - \frac{1}{C_1L_P} - \frac{1}{C_PL_P}]e^{\lambda(t-\tau_1)} \\ +i_{R_S}\frac{1}{C_PL_P}e^{\lambda(t-\tau_2)} + \frac{R_{in}^2}{L_1L_P}i_{L_1}e^{\lambda t}\end{array} \quad (101)$$

At fixed point:

$$\begin{array}{l}-\frac{R_{in}}{L_P}X^{(j)} + Y^{(j)}[\frac{R_{in}^2}{L_1L_P} - \frac{1}{C_1L_P} - \frac{1}{C_PL_P}] \\ +I_{R_S}^{(j)}\frac{1}{C_PL_P} + \frac{R_{in}^2}{L_1L_P}I_{L_1}^{(j)} = 0\end{array} \quad (102)$$

$$\begin{array}{l}-xe^{\lambda t}[\lambda + \frac{R_{in}}{L_P}] + y[\frac{R_{in}^2}{L_1L_P} - \frac{1}{C_1L_P} - \frac{1}{C_PL_P}]e^{\lambda(t-\tau_1)} \\ +i_{R_S}\frac{1}{C_PL_P}e^{\lambda(t-\tau_2)} + \frac{R_{in}^2}{L_1L_P}i_{L_1}e^{\lambda t} = 0\end{array} \quad (103)$$

$$\frac{dY}{dt} = X \Rightarrow \lambda ye^{\lambda t} = X^{(j)} + xe^{\lambda t} \quad (104)$$

At fixed point

$$X^{(j)} = 0 \Rightarrow -x + \lambda y = 0 \quad (105)$$

$$\begin{array}{l}\lambda i_{L_1}e^{\lambda t} = \frac{V(t)}{L_1} - \frac{R_{in}}{L_1}[I_{L_1}^{(j)} + i_{L_1}e^{\lambda t}] \\ -\frac{R_{in}}{L_1}[Y^{(j)} + ye^{\lambda(t-\tau_1)}]; V(t) \to \varepsilon\end{array} \quad (106)$$

$$\begin{array}{l}\lambda i_{L_1}e^{\lambda t} = -\frac{R_{in}}{L_1}I_{L_1}^{(j)} - \frac{R_{in}}{L_1}Y^{(j)} \\ -i_{L_1}\frac{R_{in}}{L_1}e^{\lambda t} - y\frac{R_{in}}{L_1}e^{\lambda(t-\tau_1)}\end{array} \quad (107)$$

At fixed point

$$-\frac{R_{in}}{L_1}I_{L_1}^{(j)} - \frac{R_{in}}{L_1}Y^{(j)} = 0 \quad (108)$$

$$-\lambda i_{L_1}e^{\lambda t} - i_{L_1}\frac{R_{in}}{L_1}e^{\lambda t} - y\frac{R_{in}}{L_1}e^{\lambda(t-\tau_1)} = 0 \quad (109)$$

$$\begin{array}{l}\lambda i_{R_j}e^{\lambda t} = \frac{1}{C_jR_j}[I_{R_S}^{(j)} + i_{R_S}e^{\lambda(t-\tau_2)}] \\ -\frac{1}{C_jR_j}[I_{R_j}^{(j)} + i_{R_j}e^{\lambda t}]\end{array} \quad (110)$$

$$\begin{array}{l}-\lambda i_{R_j}e^{\lambda t} - i_{R_j}\frac{1}{C_jR_j}e^{\lambda t} + i_{R_S}\frac{1}{C_jR_j}e^{\lambda(t-\tau_2)} \\ +\frac{1}{C_jR_j}I_{R_S}^{(j)} - \frac{1}{C_jR_j}I_{R_j}^{(j)} = 0\end{array} \quad (111)$$

At fixed point

$$\frac{1}{C_jR_j}I_{R_s}^{(j)} - \frac{1}{C_jR_j}I_{R_j}^{(j)} = 0 \quad (112)$$

$$-i_{R_j}e^{\lambda t}[\lambda + \frac{1}{C_jR_j}] + i_{R_s}\frac{1}{C_jR_j}e^{\lambda(t-\tau_2)} = 0 \quad (113)$$

$$\begin{array}{l}\lambda i_{R_S}e^{\lambda t} = \frac{1}{R_SC_P}[Y^{(j)} + ye^{\lambda(t-\tau_1)}] \\ +\frac{1}{R_SC_j}[I_{R_j}^{(j)} + i_{R_j}e^{\lambda t}] \\ -[I_{R_S}^{(j)} + i_{R_S}e^{\lambda(t-\tau_2)}]\frac{1}{R_S}(\frac{1}{C_P} + \frac{1}{C_j})\end{array} \quad (114)$$

$$\begin{array}{l}\lambda i_{R_S}e^{\lambda t} = \frac{1}{R_SC_P}Y^{(j)} + y\frac{1}{R_SC_P}e^{\lambda(t-\tau_1)} \\ +\frac{1}{R_SC_j}I_{R_j}^{(j)} + i_{R_j}\frac{1}{R_SC_j}e^{\lambda t} - I_{R_S}^{(j)}\frac{1}{R_S}(\frac{1}{C_P} + \frac{1}{C_j}) \\ -i_{R_S}\frac{1}{R_S}(\frac{1}{C_P} + \frac{1}{C_j})e^{\lambda(t-\tau_2)}\end{array} \quad (115)$$

$$\begin{array}{l}\lambda i_{R_S}e^{\lambda t} = \frac{1}{R_SC_P}Y^{(j)} + \frac{1}{R_SC_j}I_{R_j}^{(j)} \\ -I_{R_S}^{(j)}\frac{1}{R_S}(\frac{1}{C_P} + \frac{1}{C_j}) + y\frac{1}{R_SC_P}e^{\lambda(t-\tau_1)} \\ +i_{R_j}\frac{1}{R_SC_j}e^{\lambda t} - i_{R_S}\frac{1}{R_S}(\frac{1}{C_P} + \frac{1}{C_j})e^{\lambda(t-\tau_2)}\end{array} \quad (116)$$

At fixed point:

$$\frac{1}{R_S C_P}Y^{(j)} + \frac{1}{R_S C_j}I_{R_j}^{(j)} - I_{R_S}^{(j)}\frac{1}{R_S}(\frac{1}{C_P}+\frac{1}{C_j}) = 0 \quad (117)$$

$$\begin{array}{l} -i_{R_S}e^{\lambda t}[\lambda + \frac{1}{R_S}(\frac{1}{C_P}+\frac{1}{C_j})e^{-\lambda\tau_2}] \\ +y\frac{1}{R_S C_P}e^{\lambda(t-\tau_1)} + i_{R_j}\frac{1}{R_S C_j}e^{\lambda t} = 0 \end{array} \quad (118)$$

We can summarize our last results:

$$\begin{array}{l} -x[\lambda + \frac{R_{in}}{L_P}] + y[\frac{R_{in}^2}{L_1 L_P} - \frac{1}{C_1 L_P} - \frac{1}{C_P L_P}]e^{-\lambda\tau_1} \\ +\frac{R_{in}^2}{L_1 L_P}i_{L_1} + i_{R_S}\frac{1}{C_P L_P}e^{-\lambda\tau_2} = 0; x - \lambda y = 0 \end{array} \quad (119)$$

$$-y\frac{R_{in}}{L_1}e^{-\lambda\tau_1} - i_{L_1}[\frac{R_{in}}{L_1}+\lambda] = 0 \quad (120)$$

$$-i_{R_j}[\lambda + \frac{1}{C_j R_j}] + i_{R_s}\frac{1}{C_j R_j}e^{-\lambda\tau_2} = 0 \quad (121)$$

$$\begin{array}{l} y\frac{1}{R_S C_P}e^{-\lambda\tau_1} + i_{R_j}\frac{1}{R_S C_j} \\ -i_{R_S}[\lambda + \frac{1}{R_S}(\frac{1}{C_P}+\frac{1}{C_j})e^{-\lambda\tau_2}] = 0 \end{array} \quad (122)$$

The small increments Jacobian of our RFID Schotky detector system is as follows:

$$\begin{array}{l} \begin{pmatrix} \Upsilon_{11} & \cdots & \Upsilon_{15} \\ \vdots & \ddots & \vdots \\ \Upsilon_{51} & \cdots & \Upsilon_{55} \end{pmatrix}\begin{pmatrix} x \\ y \\ i_{L_1} \\ i_{R_j} \\ i_{R_S} \end{pmatrix} = 0 \\ \Upsilon_{11} = -\frac{R_{in}}{L_P} - \lambda \\ \Upsilon_{12} = [\frac{R_{in}^2}{L_1 L_P} - \frac{1}{C_1 L_P} - \frac{1}{C_P L_P}]e^{-\lambda\tau_1} \end{array} \quad (123)$$

$$\begin{array}{l} \Upsilon_{13} = \frac{R_{in}^2}{L_1 L_P}; \Upsilon_{14} = 0; \Upsilon_{15} = \frac{1}{C_P L_P}e^{-\lambda\tau_2} \\ \Upsilon_{21} = 1; \Upsilon_{22} = -\lambda; \Upsilon_{23} = \Upsilon_{24} = \Upsilon_{25} = 0 \end{array} \quad (124)$$

$$\begin{array}{l} \Upsilon_{31} = 0; \Upsilon_{32} = -\frac{R_{in}}{L_1}e^{-\lambda\tau_1}; \Upsilon_{33} = -\frac{R_{in}}{L_1} - \lambda \\ \Upsilon_{34} = 0; \Upsilon_{35} = 0; \Upsilon_{41} = \Upsilon_{42} = \Upsilon_{43} = 0 \end{array} \quad (125)$$

$$\begin{array}{l} \Upsilon_{44} = -\frac{1}{C_j R_j} - \lambda; \Upsilon_{45} = \frac{1}{C_j R_j}e^{-\lambda\tau_2} \\ \Upsilon_{51} = 0; \Upsilon_{52} = \frac{1}{R_S C_P}e^{-\lambda\tau_1}; \Upsilon_{53} = 0 \end{array} \quad (126)$$

$$\Upsilon_{54} = \frac{1}{R_S C_j}; \Upsilon_{55} = -\frac{1}{R_S}(\frac{1}{C_P}+\frac{1}{C_j})e^{-\lambda\tau_2} - \lambda \quad (127)$$

$$|A - \lambda I| = \begin{pmatrix} \Upsilon_{11} & \cdots & \Upsilon_{15} \\ \vdots & \ddots & \vdots \\ \Upsilon_{51} & \cdots & \Upsilon_{55} \end{pmatrix}; \det|A - \lambda I| = 0 \quad (128)$$

We define for simplicity the following parameters:

$$\begin{array}{l} \sigma_1 = -\frac{R_{in}}{L_P}; \sigma_2 = \frac{R_{in}^2}{L_1 L_P} - \frac{1}{C_1 L_P} - \frac{1}{C_P L_P} \\ \sigma_3 = \frac{R_{in}^2}{L_1 L_P}; \sigma_4 = \frac{1}{C_P L_P}; \sigma_5 = -\frac{R_{in}}{L_1} \end{array} \quad (129)$$

$$\begin{array}{l} \sigma_6 = \frac{1}{C_j R_j}; \sigma_7 = \frac{1}{R_S C_P}; \sigma_8 = \frac{1}{R_S C_j} \\ \sigma_9 = -\frac{1}{R_S}(\frac{1}{C_P}+\frac{1}{C_j}) \end{array} \quad (130)$$

$$\begin{array}{l} \Upsilon_{11} = \sigma_1 - \lambda; \Upsilon_{12} = \sigma_2 e^{-\lambda\tau_1}; \Upsilon_{13} = \sigma_3; \Upsilon_{14} = 0 \\ \Upsilon_{15} = \sigma_4 e^{-\lambda\tau_2}; \Upsilon_{21} = 1; \Upsilon_{22} = -\lambda \\ \Upsilon_{23} = \Upsilon_{24} = \Upsilon_{25} = 0 \end{array} \quad (131)$$

$$\begin{array}{l} \Upsilon_{31} = 0; \Upsilon_{32} = \sigma_5 e^{-\lambda\tau_1}; \Upsilon_{33} = \sigma_5 - \lambda; \Upsilon_{34} = 0 \\ \Upsilon_{35} = 0; \Upsilon_{41} = \Upsilon_{42} = \Upsilon_{43} = 0 \end{array} \quad (132)$$

$$\begin{array}{l} \Upsilon_{44} = -\sigma_6 - \lambda; \Upsilon_{45} = \sigma_6 e^{-\lambda\tau_2}; \Upsilon_{51} = 0 \\ \Upsilon_{52} = \sigma_7 e^{-\lambda\tau_1}; \Upsilon_{53} = 0; \Upsilon_{54} = \sigma_8 \\ \Upsilon_{55} = \sigma_9 e^{-\lambda\tau_2} - \lambda \end{array} \quad (133)$$

We need to find $D(\tau_1, \tau_2)$ for the following cases: (A) $\tau_1 = \tau; \tau_2 = 0$ (B) $\tau_1 = 0; \tau_2 = \tau$ (C) $\tau_1 = \tau_2 = \tau$. We need to get characteristics equations for all above stability analysis cases. We study the occurrence of any possible stability switching, resulting from the increase of the value of the time delays τ_1, τ_2 for the general characteristic equation $D(\tau_1, \tau_2)$. If we choose τ as a parameter, then the expression:

$$\begin{array}{l} D(\lambda, \tau) = P_n(\lambda, \tau) + Q_m(\lambda, \tau)e^{-\lambda\tau} \\ n, m \in N_0; n > m \end{array} \quad (134)$$

$$\begin{array}{l} \det\begin{pmatrix} \Upsilon_{11} & \cdots & \Upsilon_{15} \\ \vdots & \ddots & \vdots \\ \Upsilon_{51} & \cdots & \Upsilon_{55} \end{pmatrix} = (\sigma_1 - \lambda)(-\lambda) \\ \det\begin{pmatrix} \sigma_5 - \lambda & 0 & 0 \\ 0 & -(\sigma_6+\lambda) & \sigma_6 e^{-\lambda\tau_2} \\ 0 & \sigma_8 & (\sigma_9 e^{-\lambda\tau_2} - \lambda) \end{pmatrix} \\ -\sigma_2 e^{-\lambda\tau_1}\det\begin{pmatrix} \sigma_5 - \lambda & 0 & 0 \\ 0 & -(\sigma_6+\lambda) & \sigma_6 e^{-\lambda\tau_2} \\ 0 & \sigma_8 & (\sigma_9 e^{-\lambda\tau_2} - \lambda) \end{pmatrix} \\ +\sigma_3\{\det\begin{pmatrix} \sigma_5 e^{-\lambda\tau_1} & 0 & 0 \\ 0 & -(\sigma_6+\lambda) & \sigma_6 e^{-\lambda\tau_2} \\ \sigma_7 e^{-\lambda\tau_1} & \sigma_8 & (\sigma_9 e^{-\lambda\tau_2} - \lambda) \end{pmatrix} \\ +\lambda\det\begin{pmatrix} 0 & 0 & 0 \\ 0 & -(\sigma_6+\lambda) & \sigma_6 e^{-\lambda\tau_2} \\ 0 & \sigma_8 & (\sigma_9 e^{-\lambda\tau_2} - \lambda) \end{pmatrix}\} \\ +\sigma_4 e^{-\lambda\tau_2}\{\det\begin{pmatrix} \sigma_5 e^{-\lambda\tau_1} & \sigma_5 - \lambda & 0 \\ 0 & 0 & -(\sigma_6+\lambda) \\ \sigma_7 e^{-\lambda\tau_1} & 0 & \sigma_8 \end{pmatrix} \\ +\lambda\det\begin{pmatrix} 0 & \sigma_5 - \lambda & 0 \\ 0 & 0 & -(\sigma_6+\lambda) \\ 0 & 0 & \sigma_8 \end{pmatrix}\} \end{array} \quad (135)$$

$$\begin{array}{l} \det\begin{pmatrix} 0 & 0 & 0 \\ 0 & -(\sigma_6+\lambda) & \sigma_6 e^{-\lambda\tau_2} \\ 0 & \sigma_8 & (\sigma_9 e^{-\lambda\tau_2} - \lambda) \end{pmatrix} = 0 \\ \det\begin{pmatrix} 0 & \sigma_5 - \lambda & 0 \\ 0 & 0 & -(\sigma_6+\lambda) \\ 0 & 0 & \sigma_8 \end{pmatrix} = 0 \end{array} \quad (136)$$

We get the following expression:

$$\det\begin{pmatrix}\Upsilon_{11} & \cdots & \Upsilon_{15}\\ \vdots & \ddots & \vdots\\ \Upsilon_{51} & \cdots & \Upsilon_{55}\end{pmatrix}=(\sigma_1-\lambda)(-\lambda)$$
$$\det\begin{pmatrix}\sigma_5-\lambda & 0 & 0\\ 0 & -(\sigma_6+\lambda) & \sigma_6e^{-\lambda\tau_2}\\ 0 & \sigma_8 & (\sigma_9e^{-\lambda\tau_2}-\lambda)\end{pmatrix}$$
$$-\sigma_2e^{-\lambda\tau_1}\det\begin{pmatrix}\sigma_5-\lambda & 0 & 0\\ 0 & -(\sigma_6+\lambda) & \sigma_6e^{-\lambda\tau_2}\\ 0 & \sigma_8 & (\sigma_9e^{-\lambda\tau_2}-\lambda)\end{pmatrix}$$
$$+\sigma_3\det\begin{pmatrix}\sigma_5e^{-\lambda\tau_1} & 0 & 0\\ 0 & -(\sigma_6+\lambda) & \sigma_6e^{-\lambda\tau_2}\\ \sigma_7e^{-\lambda\tau_1} & \sigma_8 & (\sigma_9e^{-\lambda\tau_2}-\lambda)\end{pmatrix}$$
$$+\sigma_4e^{-\lambda\tau_2}\det\begin{pmatrix}\sigma_5e^{-\lambda\tau_1} & \sigma_5-\lambda & 0\\ 0 & 0 & -(\sigma_6+\lambda)\\ \sigma_7e^{-\lambda\tau_1} & 0 & \sigma_8\end{pmatrix} \tag{137}$$

First expression:

$$\det\begin{pmatrix}\sigma_5-\lambda & 0 & 0\\ 0 & -(\sigma_6+\lambda) & \sigma_6e^{-\lambda\tau_2}\\ 0 & \sigma_8 & (\sigma_9e^{-\lambda\tau_2}-\lambda)\end{pmatrix}$$
$$=(\sigma_5-\lambda)\det\begin{pmatrix}-(\sigma_6+\lambda) & \sigma_6e^{-\lambda\tau_2}\\ \sigma_8 & (\sigma_9e^{-\lambda\tau_2}-\lambda)\end{pmatrix}$$
$$=(\sigma_5-\lambda)\{-(\sigma_6+\lambda)(\sigma_9e^{-\lambda\tau_2}-\lambda)-\sigma_8\sigma_6e^{-\lambda\tau_2}\}$$
$$=(\sigma_5-\lambda)\{-\sigma_6\sigma_9e^{-\lambda\tau_2}+\sigma_6\lambda-\lambda\sigma_9e^{-\lambda\tau_2}$$
$$+\lambda^2-\sigma_8\sigma_6e^{-\lambda\tau_2}\}=(\sigma_5-\lambda)\{\sigma_6\lambda+\lambda^2$$
$$-[\sigma_6\sigma_9+\sigma_8\sigma_6+\lambda\sigma_9]e^{-\lambda\tau_2}\} \tag{138}$$

$$\det\begin{pmatrix}\sigma_5-\lambda & 0 & 0\\ 0 & -(\sigma_6+\lambda) & \sigma_6e^{-\lambda\tau_2}\\ 0 & \sigma_8 & (\sigma_9e^{-\lambda\tau_2}-\lambda)\end{pmatrix}$$
$$=(\sigma_5-\lambda)\det\begin{pmatrix}-(\sigma_6+\lambda) & \sigma_6e^{-\lambda\tau_2}\\ \sigma_8 & (\sigma_9e^{-\lambda\tau_2}-\lambda)\end{pmatrix}$$
$$=(\sigma_5-\lambda)\{-(\sigma_6+\lambda)(\sigma_9e^{-\lambda\tau_2}-\lambda)-\sigma_8\sigma_6e^{-\lambda\tau_2}\}$$
$$=(\sigma_5-\lambda)\{-\sigma_6\sigma_9e^{-\lambda\tau_2}+\sigma_6\lambda-\lambda\sigma_9e^{-\lambda\tau_2}$$
$$+\lambda^2-\sigma_8\sigma_6e^{-\lambda\tau_2}\}$$
$$=(\sigma_5-\lambda)\{\sigma_6\lambda+\lambda^2-[\sigma_6\sigma_9+\sigma_8\sigma_6+\lambda\sigma_9]e^{-\lambda\tau_2}\}$$
$$=\sigma_5\sigma_6\lambda+\sigma_5\lambda^2-\sigma_5[\sigma_6\sigma_9+\sigma_8\sigma_6+\lambda\sigma_9]e^{-\lambda\tau_2}$$
$$-\sigma_6\lambda^2-\lambda^3+\lambda[\sigma_6\sigma_9+\sigma_8\sigma_6+\lambda\sigma_9]e^{-\lambda\tau_2}$$
$$=\sigma_5\sigma_6\lambda+\sigma_5\lambda^2-[\sigma_5\sigma_6\sigma_9+\sigma_5\sigma_8\sigma_6$$
$$+\lambda\sigma_5\sigma_9]e^{-\lambda\tau_2}-\sigma_6\lambda^2-\lambda^3+[\lambda(\sigma_6\sigma_9+\sigma_8\sigma_6)$$
$$+\lambda^2\sigma_9]e^{-\lambda\tau_2}=\sigma_5\sigma_6\lambda+(\sigma_5-\sigma_6)\lambda^2-\lambda^3$$
$$+\{-\sigma_5\sigma_6(\sigma_9+\sigma_8)+\lambda(\sigma_6\sigma_9+\sigma_8\sigma_6$$
$$-\sigma_5\sigma_9)+\lambda^2\sigma_9\}e^{-\lambda\tau_2} \tag{139}$$

We define for simplicity:

$$\psi_1=\sigma_5\sigma_6;\psi_2=\sigma_5-\sigma_6;\psi_3=-\sigma_5\sigma_6(\sigma_9+\sigma_8) \tag{140}$$

$$\psi_4=\sigma_6\sigma_9+\sigma_8\sigma_6-\sigma_5\sigma_9 \tag{141}$$

Then we define

$$\det\begin{pmatrix}\sigma_5-\lambda & 0 & 0\\ 0 & -(\sigma_6+\lambda) & \sigma_6e^{-\lambda\tau_2}\\ 0 & \sigma_8 & (\sigma_9e^{-\lambda\tau_2}-\lambda)\end{pmatrix}$$
$$=\psi_1\lambda+\psi_2\lambda^2-\lambda^3+\{\psi_3+\lambda\psi_4+\lambda^2\sigma_9\}e^{-\lambda\tau_2} \tag{142}$$

Second expression:

$$\det\begin{pmatrix}\sigma_5e^{-\lambda\tau_1} & 0 & 0\\ 0 & -(\sigma_6+\lambda) & \sigma_6e^{-\lambda\tau_2}\\ \sigma_7e^{-\lambda\tau_1} & \sigma_8 & (\sigma_9e^{-\lambda\tau_2}-\lambda)\end{pmatrix} \tag{143}$$

$$\det\begin{pmatrix}\sigma_5e^{-\lambda\tau_1} & 0 & 0\\ 0 & -(\sigma_6+\lambda) & \sigma_6e^{-\lambda\tau_2}\\ \sigma_7e^{-\lambda\tau_1} & \sigma_8 & (\sigma_9e^{-\lambda\tau_2}-\lambda)\end{pmatrix}$$
$$=\sigma_5e^{-\lambda\tau_1}\det\begin{pmatrix}-(\sigma_6+\lambda) & \sigma_6e^{-\lambda\tau_2}\\ \sigma_8 & (\sigma_9e^{-\lambda\tau_2}-\lambda)\end{pmatrix}$$
$$=\sigma_5e^{-\lambda\tau_1}\{-(\sigma_6+\lambda)(\sigma_9e^{-\lambda\tau_2}-\lambda)-\sigma_8\sigma_6e^{-\lambda\tau_2}\}$$
$$=\sigma_5e^{-\lambda\tau_1}\{-\sigma_6\sigma_9e^{-\lambda\tau_2}+\sigma_6\lambda-\lambda\sigma_9e^{-\lambda\tau_2}$$
$$+\lambda^2-\sigma_8\sigma_6e^{-\lambda\tau_2}\}$$
$$=\sigma_5e^{-\lambda\tau_1}\{\sigma_6\lambda+\lambda^2-[\sigma_6\sigma_9+\sigma_8\sigma_6+\lambda\sigma_9]e^{-\lambda\tau_2}\}$$
$$=(\sigma_6\lambda+\lambda^2)\sigma_5e^{-\lambda\tau_1}-\sigma_5[\sigma_6\sigma_9+\sigma_8\sigma_6+\lambda\sigma_9]e^{-\lambda(\tau_2+\tau_1)}$$
$$\psi_5=\sigma_6\sigma_9+\sigma_8\sigma_6 \tag{144}$$

$$\det\begin{pmatrix}\sigma_5e^{-\lambda\tau_1} & 0 & 0\\ 0 & -(\sigma_6+\lambda) & \sigma_6e^{-\lambda\tau_2}\\ \sigma_7e^{-\lambda\tau_1} & \sigma_8 & (\sigma_9e^{-\lambda\tau_2}-\lambda)\end{pmatrix}$$
$$=(\sigma_6\lambda+\lambda^2)\sigma_5e^{-\lambda\tau_1}-\sigma_5[\psi_5+\lambda\sigma_9]e^{-\lambda(\tau_2+\tau_1)} \tag{145}$$

Third expression:

$$\det\begin{pmatrix}\sigma_5e^{-\lambda\tau_1} & (\sigma_5-\lambda) & 0\\ 0 & 0 & -(\sigma_6+\lambda)\\ \sigma_7e^{-\lambda\tau_1} & 0 & \sigma_8\end{pmatrix}$$
$$=\sigma_5e^{-\lambda\tau_1}\det\begin{pmatrix}0 & -(\sigma_6+\lambda)\\ 0 & \sigma_8\end{pmatrix}$$
$$-(\sigma_5-\lambda)\det\begin{pmatrix}0 & -(\sigma_6+\lambda)\\ \sigma_7e^{-\lambda\tau_1} & \sigma_8\end{pmatrix}$$
$$=-(\sigma_5-\lambda)\det\begin{pmatrix}0 & -(\sigma_6+\lambda)\\ \sigma_7e^{-\lambda\tau_1} & \sigma_8\end{pmatrix}$$
$$=-(\sigma_5-\lambda)\sigma_7e^{-\lambda\tau_1}(\sigma_6+\lambda)$$
$$=-(\sigma_5-\lambda)\sigma_7(\sigma_6+\lambda)e^{-\lambda\tau_1}$$
$$=\sigma_7(-\sigma_5\sigma_6-\sigma_5\lambda+\lambda\sigma_6+\lambda^2)e^{-\lambda\tau_1}$$
$$=\sigma_7(-\sigma_5\sigma_6+\lambda[\sigma_6-\sigma_5]+\lambda^2)e^{-\lambda\tau_1} \tag{146}$$

$$\psi_1=\sigma_5\sigma_6;\psi_2=\sigma_5-\sigma_6\Rightarrow-\psi_2=\sigma_6-\sigma_5 \tag{147}$$

$$\det\begin{pmatrix}\sigma_5e^{-\lambda\tau_1} & (\sigma_5-\lambda) & 0\\ 0 & 0 & -(\sigma_6+\lambda)\\ \sigma_7e^{-\lambda\tau_1} & 0 & \sigma_8\end{pmatrix}$$
$$=\sigma_7(-\psi_1-\lambda\psi_2+\lambda^2)e^{-\lambda\tau_1} \tag{148}$$

We integrate our expression in below $D(\tau_1,\tau_2)$ expression.

$$\det\begin{pmatrix}\Upsilon_{11} & \cdots & \Upsilon_{15}\\ \vdots & \ddots & \vdots\\ \Upsilon_{51} & \cdots & \Upsilon_{55}\end{pmatrix}=(\sigma_1-\lambda)(-\lambda)\det\begin{pmatrix}\sigma_5-\lambda & 0 & 0\\ 0 & -(\sigma_6+\lambda) & \sigma_6e^{-\lambda\tau_2}\\ 0 & \sigma_8 & (\sigma_9e^{-\lambda\tau_2}-\lambda)\end{pmatrix}$$
$$-\sigma_2e^{-\lambda\tau_1}\det\begin{pmatrix}\sigma_5-\lambda & 0 & 0\\ 0 & -(\sigma_6+\lambda) & \sigma_6e^{-\lambda\tau_2}\\ 0 & \sigma_8 & (\sigma_9e^{-\lambda\tau_2}-\lambda)\end{pmatrix}$$
$$+\sigma_3\det\begin{pmatrix}\sigma_5e^{-\lambda\tau_1} & 0 & 0\\ 0 & -(\sigma_6+\lambda) & \sigma_6e^{-\lambda\tau_2}\\ \sigma_7e^{-\lambda\tau_1} & \sigma_8 & (\sigma_9e^{-\lambda\tau_2}-\lambda)\end{pmatrix}$$
$$+\sigma_4e^{-\lambda\tau_2}\det\begin{pmatrix}\sigma_5e^{-\lambda\tau_1} & \sigma_5-\lambda & 0\\ 0 & 0 & -(\sigma_6+\lambda)\\ \sigma_7e^{-\lambda\tau_1} & 0 & \sigma_8\end{pmatrix} \quad (149)$$

$$\det\begin{pmatrix}\Upsilon_{11} & \cdots & \Upsilon_{15}\\ \vdots & \ddots & \vdots\\ \Upsilon_{51} & \cdots & \Upsilon_{55}\end{pmatrix}=(\sigma_1-\lambda)(-\lambda)[\psi_1\lambda+\psi_2\lambda^2$$
$$-\lambda^3+\{\psi_3+\lambda\psi_4+\lambda^2\sigma_9\}e^{-\lambda\tau_2}]-\sigma_2e^{-\lambda\tau_1}[\psi_1\lambda$$
$$+\psi_2\lambda^2-\lambda^3+\{\psi_3+\lambda\psi_4+\lambda^2\sigma_9\}e^{-\lambda\tau_2}]$$
$$+\sigma_3[(\sigma_6\lambda+\lambda^2)\sigma_5e^{-\lambda\tau_1}$$
$$-\sigma_5[\psi_5+\lambda\sigma_9]e^{-\lambda(\tau_2+\tau_1)}]$$
$$+\sigma_4e^{-\lambda\tau_2}[\sigma_7(-\psi_1-\lambda\psi_2+\lambda^2)e^{-\lambda\tau_1}] \quad (150)$$

$$\det\begin{pmatrix}\Upsilon_{11} & \cdots & \Upsilon_{15}\\ \vdots & \ddots & \vdots\\ \Upsilon_{51} & \cdots & \Upsilon_{55}\end{pmatrix}=\psi_1\lambda^3+\psi_2\lambda^4-\lambda^5$$
$$+\{\psi_3\lambda^2+\lambda^3\psi_4+\lambda^4\sigma_9\}e^{-\lambda\tau_2}-\sigma_1\psi_1\lambda^2$$
$$-\sigma_1\psi_2\lambda^3+\sigma_1\lambda^4+\{-\sigma_1\psi_3\lambda-\sigma_1\psi_4\lambda^2$$
$$-\sigma_1\sigma_9\lambda^3\}e^{-\lambda\tau_2}-(\psi_1\lambda+\psi_2\lambda^2-\lambda^3)\sigma_2e^{-\lambda\tau_1}$$
$$-\sigma_2\{\psi_3+\lambda\psi_4+\lambda^2\sigma_9\}e^{-\lambda(\tau_1+\tau_2)}$$
$$+(\sigma_3\sigma_6\lambda+\sigma_3\lambda^2)\sigma_5e^{-\lambda\tau_1}$$
$$-\sigma_3\sigma_5[\psi_5+\lambda\sigma_9]e^{-\lambda(\tau_2+\tau_1)}+(-\psi_1\sigma_4\sigma_7$$
$$-\lambda\psi_2\sigma_4\sigma_7+\lambda^2\sigma_4\sigma_7)e^{-\lambda(\tau_1+\tau_2)} \quad (151)$$

$$\det\begin{pmatrix}\Upsilon_{11} & \cdots & \Upsilon_{15}\\ \vdots & \ddots & \vdots\\ \Upsilon_{51} & \cdots & \Upsilon_{55}\end{pmatrix}=(\lambda^2-\sigma_1\lambda)[\psi_1\lambda+\psi_2\lambda^2$$
$$-\lambda^3+\{\psi_3+\lambda\psi_4+\lambda^2\sigma_9\}e^{-\lambda\tau_2}]$$
$$-[(\psi_1\lambda+\psi_2\lambda^2-\lambda^3)\sigma_2e^{-\lambda\tau_1}$$
$$+\sigma_2\{\psi_3+\lambda\psi_4+\lambda^2\sigma_9\}e^{-\lambda(\tau_1+\tau_2)}]$$
$$+\sigma_3(\sigma_6\lambda+\lambda^2)\sigma_5e^{-\lambda\tau_1}-\sigma_3\sigma_5[\psi_5+\lambda\sigma_9]e^{-\lambda(\tau_2+\tau_1)}$$
$$+(-\psi_1\sigma_4\sigma_7-\lambda\psi_2\sigma_4\sigma_7+\lambda^2\sigma_4\sigma_7)e^{-\lambda(\tau_1+\tau_2)} \quad (152)$$

$$\det\begin{pmatrix}\Upsilon_{11} & \cdots & \Upsilon_{15}\\ \vdots & \ddots & \vdots\\ \Upsilon_{51} & \cdots & \Upsilon_{55}\end{pmatrix}=-\sigma_1\psi_1\lambda^2$$
$$+(\psi_1-\sigma_1\psi_2)\lambda^3+(\psi_2+\sigma_1)\lambda^4-\lambda^5$$
$$-(\psi_1\lambda+\psi_2\lambda^2-\lambda^3)\sigma_2e^{-\lambda\tau_1}$$
$$+(\sigma_3\sigma_6\lambda+\sigma_3\lambda^2)\sigma_5e^{-\lambda\tau_1}$$
$$+\{\psi_3\lambda^2+\lambda^3\psi_4+\lambda^4\sigma_9\}e^{-\lambda\tau_2}$$
$$+\{-\sigma_1\psi_3\lambda-\sigma_1\psi_4\lambda^2-\sigma_1\sigma_9\lambda^3\}e^{-\lambda\tau_2}$$
$$-\sigma_2\{\psi_3+\lambda\psi_4+\lambda^2\sigma_9\}e^{-\lambda(\tau_1+\tau_2)}$$
$$-\sigma_3\sigma_5[\psi_5+\lambda\sigma_9]e^{-\lambda(\tau_2+\tau_1)}$$
$$+(-\psi_1\sigma_4\sigma_7-\lambda\psi_2\sigma_4\sigma_7+\lambda^2\sigma_4\sigma_7)e^{-\lambda(\tau_1+\tau_2)} \quad (153)$$

$$\det\begin{pmatrix}\Upsilon_{11} & \cdots & \Upsilon_{15}\\ \vdots & \ddots & \vdots\\ \Upsilon_{51} & \cdots & \Upsilon_{55}\end{pmatrix}=-\sigma_1\psi_1\lambda^2+(\psi_1-\sigma_1\psi_2)\lambda^3$$
$$+(\psi_2+\sigma_1)\lambda^4-\lambda^5+(-\psi_1\sigma_2\lambda-\psi_2\sigma_2\lambda^2+\sigma_2\lambda^3)e^{-\lambda\tau_1}$$
$$+(\sigma_3\sigma_6\sigma_5\lambda+\sigma_3\sigma_5\lambda^2)e^{-\lambda\tau_1}$$
$$+\{\psi_3\lambda^2+\lambda^3\psi_4+\lambda^4\sigma_9\}e^{-\lambda\tau_2}$$
$$+\{-\sigma_1\psi_3\lambda-\sigma_1\psi_4\lambda^2-\sigma_1\sigma_9\lambda^3\}e^{-\lambda\tau_2}$$
$$+\{-\sigma_2\psi_3-\lambda\sigma_2\psi_4-\lambda^2\sigma_2\sigma_9\}e^{-\lambda(\tau_1+\tau_2)}$$
$$+[-\sigma_3\sigma_5\psi_5-\lambda\sigma_3\sigma_5\sigma_9]e^{-\lambda(\tau_2+\tau_1)}$$
$$+(-\psi_1\sigma_4\sigma_7-\lambda\psi_2\sigma_4\sigma_7+\lambda^2\sigma_4\sigma_7)e^{-\lambda(\tau_1+\tau_2)} \quad (154)$$

$$\det\begin{pmatrix}\Upsilon_{11} & \cdots & \Upsilon_{15}\\ \vdots & \ddots & \vdots\\ \Upsilon_{51} & \cdots & \Upsilon_{55}\end{pmatrix}=-\sigma_1\psi_1\lambda^2+(\psi_1-\sigma_1\psi_2)\lambda^3$$
$$+(\psi_2+\sigma_1)\lambda^4-\lambda^5+\{(\sigma_3\sigma_6\sigma_5-\psi_1\sigma_2)\lambda$$
$$+(\sigma_3\sigma_5-\psi_2\sigma_2)\lambda^2+\sigma_2\lambda^3\}e^{-\lambda\tau_1}+\{-\sigma_1\psi_3\lambda$$
$$+(\psi_3-\sigma_1\psi_4)\lambda^2+(\psi_4-\sigma_1\sigma_9)\lambda^3+\lambda^4\sigma_9\}e^{-\lambda\tau_2}$$
$$+\{-\sigma_2\psi_3-\sigma_3\sigma_5\psi_5-\psi_1\sigma_4\sigma_7$$
$$-(\psi_2\sigma_4\sigma_7+\sigma_2\psi_4+\sigma_3\sigma_5\sigma_9)\lambda$$
$$+(\sigma_4\sigma_7-\sigma_2\sigma_9)\lambda^2\}e^{-\lambda(\tau_1+\tau_2)} \quad (155)$$

We define for simplicity the following parameters:

$$\theta_2=-\sigma_1\psi_1;\theta_3=\psi_1-\sigma_1\psi_2;\theta_4=\psi_2+\sigma_1;\theta_5=-1 \quad (156)$$

$$A_1=\sigma_3\sigma_6\sigma_5-\psi_1\sigma_2;A_2=\sigma_3\sigma_5-\psi_2\sigma_2;A_3=\sigma_2 \quad (157)$$

$$B_1=-\sigma_1\psi_3;B_2=\psi_3-\sigma_1\psi_4$$
$$B_3=\psi_4-\sigma_1\sigma_9;B_4=\sigma_9 \quad (158)$$

$$C_0=-\sigma_2\psi_3-\sigma_3\sigma_5\psi_5-\psi_1\sigma_4\sigma_7$$
$$C_1=-(\psi_2\sigma_4\sigma_7+\sigma_2\psi_4+\sigma_3\sigma_5\sigma_9) \quad (159)$$

$$C_2=\sigma_4\sigma_7-\sigma_2\sigma_9 \quad (160)$$

$$\det\begin{pmatrix} \Upsilon_{11} & \cdots & \Upsilon_{15} \\ \vdots & \ddots & \vdots \\ \Upsilon_{51} & \cdots & \Upsilon_{55} \end{pmatrix} = \sum_{l=2}^{5}\Theta_l\lambda^l + [\sum_{k=1}^{3}\mathrm{A}_k\lambda^k]e^{-\lambda\tau_1} + [\sum_{k=1}^{4}\mathrm{B}_k\lambda^k]e^{-\lambda\tau_2} + [\sum_{k=0}^{2}C_k\lambda^k]e^{-\lambda(\tau_1+\tau_2)} \tag{161}$$

$$D(\tau_1,\tau_2) = \sum_{l=2}^{5}\Theta_l\lambda^l + [\sum_{k=1}^{3}\mathrm{A}_k\lambda^k]e^{-\lambda\tau_1} + [\sum_{k=1}^{4}\mathrm{B}_k\lambda^k]e^{-\lambda\tau_2} + [\sum_{k=0}^{2}C_k\lambda^k]e^{-\lambda(\tau_1+\tau_2)} \tag{162}$$

Three cases:

$$(A)\,\tau_1=\tau;\tau_2=0\,(B)\,\tau_1=0;\tau_2=\tau \quad (C)\,\tau_1=\tau_2=\tau \tag{163}$$

IV. RFID TAG RECEIVER DETECTOR CHARACTERISTIC EQUATION AND STABILITY SWITCHING $\tau_1=\tau;\tau_2=0$

We get and analyze the characteristic equation of RFID TAG receiver for $\tau_1=\tau;\tau_2=0$.

$$\tau_1=\tau;\tau_2=0;D(\tau) = \sum_{l=2}^{5}\Theta_l\lambda^l + [\sum_{k=1}^{4}\mathrm{B}_k\lambda^k] + [\sum_{k=1}^{3}\mathrm{A}_k\lambda^k]e^{-\lambda\tau} + [\sum_{k=0}^{2}C_k\lambda^k]e^{-\lambda\tau} \tag{164}$$

$$D(\tau_1=\tau;\tau_2=0) = \sum_{l=2}^{5}\Theta_l\lambda^l + [\sum_{k=1}^{4}\mathrm{B}_k\lambda^k] + [\sum_{k=1}^{3}\mathrm{A}_k\lambda^k]e^{-\lambda\tau} + [\sum_{k=0}^{2}C_k\lambda^k]e^{-\lambda\tau}$$
$$D(\tau_1=\tau;\tau_2=0) = \mathrm{B}_1\lambda + \sum_{l=2}^{4}(\Theta_l+\mathrm{B}_l)\lambda^l + \Theta_5\lambda^5 + [C_0 + \sum_{l=1}^{2}(\mathrm{A}_l+C_l)\lambda^l + \mathrm{A}_3\lambda^3]e^{-\lambda\tau} \tag{165}$$

$$D(\lambda,\tau) = P_n(\lambda,\tau) + Q_m(\lambda,\tau)e^{-\lambda\tau} \quad n,m\in N_0; n>m \tag{166}$$

$$P_n(\lambda,\tau) = \mathrm{B}_1\lambda + \sum_{l=2}^{4}(\Theta_l+\mathrm{B}_l)\lambda^l + \Theta_5\lambda^5; n=5$$
$$Q_m(\lambda,\tau) = [C_0 + \sum_{l=1}^{2}(\mathrm{A}_l+C_l)\lambda^l + \mathrm{A}_3\lambda^3]; m=3 \tag{167}$$

$$P_n(\lambda,\tau) = \sum_{k=0}^{n}P_k(\tau)\,\lambda^k = P_0(\tau) + P_1(\tau)\lambda + P_2(\tau)\,\lambda^2 + P_3(\tau)\,\lambda^3 + \ldots$$
$$Q_m(\lambda,\tau) = \sum_{k=0}^{m}q_k(\tau)\,\lambda^k = q_0(\tau) + q_1(\tau)\lambda + q_2(\tau)\,\lambda^2 + \ldots\ldots \tag{168}$$

$$D(\lambda,\tau) = P_n(\lambda,\tau) + Q_m(\lambda,\tau)e^{-\lambda\tau} \quad n=5;m=3;n>m \tag{169}$$

$$P_n(\lambda,\tau) = \sum_{k=0}^{n}P_k(\tau)\,\lambda^k = P_0(\tau) + P_1(\tau)\lambda + P_2(\tau)\lambda^2 + P_3(\tau)\lambda^3 + P_4(\tau)\lambda^4 + P_5(\tau)\lambda^5 \tag{170}$$

$$P_0=0; P_1=\mathrm{B}_1; P_2=\Theta_2+\mathrm{B}_2; P_3=\Theta_3+\mathrm{B}_3 \quad P_4=\Theta_4+\mathrm{B}_4; P_5=\Theta_5 \tag{171}$$

$$Q_m(\lambda,\tau) = \sum_{k=0}^{m}q_k(\tau)\lambda^k = q_0(\tau) + q_1(\tau)\lambda + q_2(\tau)\lambda^2 + q_3(\tau)\lambda^3;\ q_0(\tau)=C_0 \quad q_1(\tau)=\mathrm{A}_1+C_1;\ q_2(\tau)=\mathrm{A}_2+C_2; q_3(\tau)=A_3 \tag{172}$$

The homogeneous system for $X, Y, I_{L_1}, I_{R_j}, I_{R_S}$ leads to a characteristic equation for the eigenvalue λ having the form

$$P(\lambda,\tau) + Q(\lambda,\tau)e^{-\lambda\tau} = 0 \quad P(\lambda) = \sum_{j=0}^{5}a_j\lambda^j; Q(\lambda) = \sum_{j=0}^{3}c_j\lambda^j \tag{173}$$

The coefficients $\{a_j(q_i,q_k,\tau), c_j(q_i,q_k,\tau)\}\in R$ depend on q_i, q_k and delay τ. q_i, q_k are any Schottky detector's global parameters, other parameters kept as a constant.

$$a_0=0; a_1=\mathrm{B}_1; a_2=\Theta_2+\mathrm{B}_2; a_3=\Theta_3+\mathrm{B}_3 \tag{174}$$

$$a_4=\Theta_4+\mathrm{B}_4; a_5=\Theta_5;\ c_0(\tau)=C_0 \quad c_1(\tau)=\mathrm{A}_1+C_1;\ c_2(\tau)=\mathrm{A}_2+C_2;\ c_3(\tau)=\mathrm{A}_3 \tag{175}$$

Unless strictly necessary, the designation of the varied arguments (q_i, q_k) will subsequently be omitted from P, Q, a_j, and c_j. The coefficients a_j, c_j are continuous, and differentiable functions of their arguments, and direct substitution shows that a_0+$c_0\neq$0 for $q_i, q_k \in R_+$; that is, λ=0 is not of $P(\lambda)+Q(\lambda)e^{-\lambda\tau}=0$ [7] [8]. Furthermore, P(λ), Q(λ) are analytic functions of λ, for which the following requirements of the analysis (Kuang J and Cong Y 2005 ; Kuang Y 1993) can also be verified in the present case:

.

(a) If $\lambda=i\omega, \omega\in R$, then $P(i\omega)+Q(i\omega)\neq 0$

(b) If $|Q(\lambda)/P(\lambda)|$ is bounded for $|\lambda|\to\infty; \mathrm{Re}\lambda\geq 0$. No roots bifurcation from ∞.

(c) $F(\omega)=|P(i\omega)|^2-|Q(i\omega)|^2$ has a finite number of zeros. Indeed, this is a polynomial in ω.

(d) Each positive root $\omega(q_i,q_k)$ of F(ω)=0 is continuous and differentiable with respect to q_i, q_k.

.

We assume that $P_n(\lambda,\tau)$ and $Q_m(\lambda,\tau)$ cannot have common imaginary roots. That is for any real number ω:

$$P_n(\lambda=i\omega,\tau) + Q_m(\lambda=i\omega,\tau)\neq 0 \tag{176}$$

$$p_n(\lambda=i\omega,\tau) = \mathrm{B}_1 i\omega + \sum_{l=2}^{4}(\Theta_l+\mathrm{B}_l)(i\omega)^l + \Theta_5(i\omega)^5 = i\omega\mathrm{B}_1 + \sum_{l=2}^{4}(\Theta_l+\mathrm{B}_l)i^l\omega^l + i\Theta_5\omega^5 \tag{177}$$

$$\sum_{l=2}^{4}(\Theta_l+\mathrm{B}_l)i^l\omega^l=-(\Theta_2+\mathrm{B}_2)\omega^2 \\ +(\Theta_2+\mathrm{B}_2)\omega^4-(\Theta_2+\mathrm{B}_2)\omega^3 i \tag{178}$$

$$p_n(\lambda=i\omega,\tau)=-(\Theta_2+\mathrm{B}_2)\omega^2+(\Theta_2+\mathrm{B}_2)\omega^4 \\ +i[\omega\mathrm{B}_1-(\Theta_2+\mathrm{B}_2)\omega^3+\Theta_5\omega^5] \tag{179}$$

$$Q_m(\lambda=i\omega,\tau)=C_0 \\ +\sum_{l=1}^{2}(\mathrm{A}_l+C_l)(i\omega)^l-i\mathrm{A}_3\omega^3 \\ \sum_{l=1}^{2}(\mathrm{A}_l+C_l)(i\omega)^l=i\omega(\mathrm{A}_1+C_1) \\ -(\mathrm{A}_2+C_2)\omega^2 \tag{180}$$

$$Q_m(\lambda=i\omega,\tau)=C_0-(A_2+C_2)\omega^2 \\ +i[\omega(A_1+C_1)-A_3\omega^3] \tag{181}$$

$$p_n(\lambda=i\omega,\tau)+Q_m(\lambda=i\omega,\tau) \\ =C_0-(\Theta_2+\mathrm{B}_2)\omega^2-(\mathrm{A}_2+C_2)\omega^2 \\ +(\Theta_2+\mathrm{B}_2)\omega^4+i[\omega\mathrm{B}_1+\omega(\mathrm{A}_1+C_1) \\ -(\Theta_2+\mathrm{B}_2)\omega^3-\mathrm{A}_3\omega^3+\Theta_5\omega^5]\neq 0 \tag{182}$$

$$p_n(\lambda=i\omega,\tau)+Q_m(\lambda=i\omega,\tau) \\ =C_0-(\Theta_2+\mathrm{B}_2+\mathrm{A}_2+C_2)\omega^2 \\ +(\Theta_2+\mathrm{B}_2)\omega^4+i[\omega(\mathrm{A}_1+C_1+\mathrm{B}_1) \\ -(\Theta_2+\mathrm{B}_2+\mathrm{A}_3)\omega^3+\Theta_5\omega^5]\neq 0 \tag{183}$$

$$|P(i\omega,\tau)|^2=[-(\Theta_2+\mathrm{B}_2)\omega^2+(\Theta_2+\mathrm{B}_2)\omega^4]^2 \\ +[\omega\mathrm{B}_1-(\Theta_2+\mathrm{B}_2)\omega^3+\Theta_5\omega^5]^2=(\Theta_2+\mathrm{B}_2)^2\omega^4 \\ +(\Theta_2+\mathrm{B}_2)^2\omega^8-2(\Theta_2+\mathrm{B}_2)^2\omega^6+\omega^2\mathrm{B}_1^2 \\ -\mathrm{B}_1(\Theta_2+\mathrm{B}_2)\omega^4+\mathrm{B}_1\Theta_5\omega^6-(\Theta_2+\mathrm{B}_2)\mathrm{B}_1\omega^4 \\ +(\Theta_2+\mathrm{B}_2)^2\omega^6-(\Theta_2+\mathrm{B}_2)\Theta_5\omega^8+\Theta_5\mathrm{B}_1\omega^6 \\ -\Theta_5(\Theta_2+\mathrm{B}_2)\omega^8+\Theta_5^2\omega^{10} \tag{184}$$

$$|P(i\omega,\tau)|^2=\omega^2\mathrm{B}_1^2 \\ +[(\Theta_2+\mathrm{B}_2)-2\mathrm{B}_1](\Theta_2+\mathrm{B}_2)\omega^4 \\ +[2\mathrm{B}_1\Theta_5-(\Theta_2+\mathrm{B}_2)^2]\omega^6+[(\Theta_2+\mathrm{B}_2) \\ -2\Theta_5](\Theta_2+\mathrm{B}_2)\omega^8+\Theta_5^2\omega^{10} \tag{185}$$

$$|Q(i\omega,\tau)|^2=[C_0-(\mathrm{A}_2+C_2)\omega^2]^2 \\ +[\omega(\mathrm{A}_1+C_1)-\mathrm{A}_3\omega^3]^2=C_0^2+(\mathrm{A}_2+C_2)^2\omega^4 \\ -2C_0(\mathrm{A}_2+C_2)\omega^2+\omega^2(\mathrm{A}_1+C_1)^2+\mathrm{A}_3^2\omega^6 \\ -2(\mathrm{A}_1+C_1)\mathrm{A}_3\omega^4 \tag{186}$$

$$|Q(i\omega,\tau)|^2=C_0^2+[(\mathrm{A}_1+C_1)^2 \\ -2C_0(\mathrm{A}_2+C_2)]\omega^2+[(\mathrm{A}_2+C_2)^2 \\ -2(\mathrm{A}_1+C_1)\mathrm{A}_3]\omega^4+\mathrm{A}_3^2\omega^6 \tag{187}$$

$$F(\omega,\tau)=|P(i\omega,\tau)|^2-|Q(i\omega,\tau)|^2=\omega^2\mathrm{B}_1^2 \\ +[(\Theta_2+\mathrm{B}_2)-2\mathrm{B}_1](\Theta_2+\mathrm{B}_2)\omega^4 \\ +[2\mathrm{B}_1\Theta_5-(\Theta_2+\mathrm{B}_2)^2]\omega^6+[(\Theta_2+\mathrm{B}_2) \\ -2\Theta_5](\Theta_2+\mathrm{B}_2)\omega^8+\Theta_5^2\omega^{10} \\ -\{C_0^2+[(\mathrm{A}_1+C_1)^2-2C_0(\mathrm{A}_2+C_2)]\omega^2 \\ +[(\mathrm{A}_2+C_2)^2-2(\mathrm{A}_1+C_1)\mathrm{A}_3]\omega^4+\mathrm{A}_3^2\omega^6\} \tag{188}$$

$$F(\omega,\tau)=|P(i\omega,\tau)|^2-|Q(i\omega,\tau)|^2=-C_0^2 \\ +\{\mathrm{B}_1^2-[(\mathrm{A}_1+C_1)^2-2C_0(\mathrm{A}_2+C_2)]\}\omega^2 \\ +\{[(\Theta_2+\mathrm{B}_2)-2\mathrm{B}_1](\Theta_2+\mathrm{B}_2)-[(\mathrm{A}_2+C_2)^2 \\ -2(\mathrm{A}_1+C_1)\mathrm{A}_3]\}\omega^4+\{[2\mathrm{B}_1\Theta_5-(\Theta_2+\mathrm{B}_2)^2] \\ -\mathrm{A}_3^2\}\omega^6+[(\Theta_2+\mathrm{B}_2)-2\Theta_5](\Theta_2+\mathrm{B}_2)\omega^8 \\ +\Theta_5^2\omega^{10} \tag{189}$$

We define the following parameters for simplicity: $\Pi_0,\ \Pi_2,\ \Pi_4,\Pi_6,\Pi_8,\Pi_{10}$.

$$\Pi_0=-C_0^2;\Pi_2=\mathrm{B}_1^2-[(\mathrm{A}_1+C_1)^2 \\ -2C_0(\mathrm{A}_2+C_2)] \\ \Pi_4=[(\Theta_2+\mathrm{B}_2)-2\mathrm{B}_1](\Theta_2+\mathrm{B}_2) \\ -[(\mathrm{A}_2+C_2)^2-2(\mathrm{A}_1+C_1)\mathrm{A}_3] \\ \Pi_6=[2\mathrm{B}_1\Theta_5-(\Theta_2+\mathrm{B}_2)^2]-\mathrm{A}_3^2 \\ \Pi_8=[(\Theta_2+\mathrm{B}_2)-2\Theta_5](\Theta_2+\mathrm{B}_2);\Pi_{10}=\Theta_5^2 \tag{190}$$

Hence $F(\omega,\tau)=0$ implies $\sum_{k=0}^{5}\prod_{2k}\omega^{2k}=0$ and its roots are given by solving the above polynomial.

$$P_R(i\omega,\tau)=-(\Theta_2+B_2)\omega^2+(\Theta_2+B_2)\omega^4 \tag{191}$$

$$P_I(i\omega,\tau)=\omega\mathrm{B}_1-(\Theta_2+\mathrm{B}_2)\omega^3+\Theta_5\omega^5 \\ Q_R(i\omega,\tau)=C_0-(\mathrm{A}_2+C_2)\omega^2 \tag{192}$$

$$Q_I(i\omega,\tau)=\omega(A_1+C_1)-A_3\omega^3 \tag{193}$$

$$\sin\theta(\tau)=\frac{-P_R(i\omega,\tau)Q_I(i\omega,\tau)+P_I(i\omega,\tau)Q_R(i\omega,\tau)}{|Q(i\omega,\tau)|^2} \tag{194}$$

$$\cos\theta(\tau)=-\frac{P_R(i\omega,\tau)Q_R(i\omega,\tau)+P_I(i\omega,\tau)Q_I(i\omega,\tau)}{|Q(i\omega,\tau)|^2} \tag{195}$$

We use different parameters terminology from our last characteristics parameters definition:

$$k\rightarrow j;p_k(\tau)\rightarrow a_j;q_k(\tau)\rightarrow c_j \\ n=5;m=3;n>m \tag{196}$$

$$P_n(\lambda,\tau)\rightarrow P(\lambda);Q_m(\lambda,\tau)\rightarrow Q(\lambda) \tag{197}$$

$$P(\lambda)=\sum_{j=0}^{5}a_j\lambda^j;Q(\lambda)=\sum_{j=0}^{3}c_j\lambda^j \tag{198}$$

$$P_\lambda=a_0+a_1\lambda+a_2\lambda^2+a_3\lambda^3+a_4\lambda^4+a_5\lambda^5 \\ Q_\lambda=c_0+c_1\lambda+c_2\lambda^2+c_3\lambda^3 \tag{199}$$

$n,m\in N_0,n>m$ and $a_j,c_j:R_{+0}\rightarrow R$ are continuous and differentiable function of τ such that $a_0+c_0\neq 0$. In the following "—" denotes complex and conjugate. $P(\lambda),Q(\lambda)$ are analytic functions in λ and differentiable in τ. The coefficients $a_j(L_P,L_1,C_f,R_{in},R_S,C_P,R_j,\tau,...)\in R$ and $c_j(L_P,L_1,C_f,R_{in},R_S,C_P,R_j,\tau,...)\in R$ depend on RFID TAG detector system's $L_P,L_1,C_f,R_{in},R_S,C_P,R_j,\tau,...$

values. Unless strictly necessary, the designation of the varied arguments: $(L_P, L_1, C_f, R_{in}, R_S, C_P, R_j, \tau, ...)$ will subsequently be omitted from P, Q, a_j, c_j. The coefficients a_j, c_j are continuous, and differentiable functions of their arguments, and direct substitution shows that $a_0 + c_0 \neq 0$.

$$a_0 = 0; c_0(\tau) = c_0 \tag{200}$$

$$C_0 = -\sigma_2\psi_3 - \sigma_3\sigma_5\psi_5 - \psi_1\sigma_4\sigma_7 \tag{201}$$

$$-\sigma_2\psi_3 - \sigma_3\sigma_5\psi_5 - \psi_1\sigma_4\sigma_7 \neq 0 \tag{202}$$

$$\begin{array}{l} -[\frac{R_{in}^2}{L_1L_p} - \frac{1}{C_1L_p} - \frac{1}{C_pL_p}]\psi_3 + \frac{R_{in}^2}{L_1L_p}\frac{R_{in}}{L_1}\psi_5 \\ -\psi_1\frac{1}{C_pL_p}\frac{1}{R_sC_p} \neq 0 \end{array} \tag{203}$$

$\forall L_P, L_1, C_f, R_{in}, R_S, C_P, R_j, \tau, ... \in R_+$ i.e $\lambda = 0$ is not a root of the characteristic equation. Furthermore $P(\lambda), Q(\lambda)$ are analytic functions of λ for which the following requirements of the analysis (see Kuang, 1993, section 3.4) can also be verified in the present case [6] [7].

.

(a) If $\lambda = i\omega; \omega \in R$ then $P(i\omega) + Q(i\omega) \neq 0$, i.e P and Q have no common imaginary roots. This condition was verified numerically in the entire $(L_P, L_1, C_f, R_{in}, R_S, C_P, R_j, \tau, ...)$ domain of interest.

(b) $|P(\lambda)/Q(\lambda)|$ is bounded for $|\lambda| \to \infty; \mathrm{Re}\lambda \geq 0$. No roots bifurcation from ∞. Indeed, in the limit:

$$|\frac{Q(\lambda)}{P(\lambda)}| = |\frac{c_0 + c_1\lambda + c_2\lambda^2 + c_3\lambda^3}{a_0 + a_1\lambda + a_2\lambda^2 + a_3\lambda^3 + a_4\lambda^4 + a_5\lambda^5}| \tag{204}$$

(c) The following expressions exist:

$$F(\omega) = |P(i\omega)|^2 - |Q(i\omega)|^2 \tag{205}$$

$$F(\omega, \tau) = |P(i\omega, \tau)|^2 - |Q(i\omega, \tau)|^2 = \sum_{k=0}^{5} \Pi_{2k}\omega^{2k} \tag{206}$$

Has at most a finite number of zeros. Indeed, this is a polynomial in ω(Degree in ω^{10}).

(d) Each positive root $\omega(L_P, L_1, C_f, R_{in}, R_S, C_P, R_j, \tau, ...)$ of $F(\omega) = 0$ is continuous and differentiable with respect to $L_P, L_1, C_f, R_{in}, R_S, C_P, R_j, \tau, ...$ The condition can only be assessed numerically.

.

In addition, since the coefficients in P and Q are real, we have $\overline{P(-i\omega)} = P(i\omega)$, and $\overline{Q(-i\omega)} = Q(i\omega)$ thus, $\omega > 0$ maybe on eigenvalue of characteristic equations. The analysis consists in identifying the roots of the characteristic equation situated on the imaginary axis of the complex λ – plane, whereby increasing the parameters: $L_P, L_1, C_f, R_{in}, R_S, C_P, R_j, \tau, ...$ Re λ may, at the crossing, change its sign from (-) to (+), i.e. from a stable focus

$$\begin{array}{l} E^{(0)}(X^{(0)}, Y^{(0)}, I_{L_1}^{(0)}, I_{R_j}^{(0)}, I_{R_S}^{(0)}) \\ |_{\substack{V(t)|_{A_0 \gg |f(t)} = A_0 + f(t) \approx A_0 \\ \frac{dV(t)}{dt}|_{A_0 \gg |f(t)|} = \frac{df(t)}{dt} \to \varepsilon}} = (0, 0, 0, 0, 0) \end{array} \tag{207}$$

to an unstable one, or vice versa. This feature may be further assessed by examining the sign of the partial derivatives with respect to $L_P, L_1, C_f, R_{in}, R_S, C_P, R_j, \tau, ...$ and system parameters.

$$\begin{array}{l} \wedge^{-1}(L_P) = (\frac{\partial \mathrm{Re}\lambda}{\partial L_P})_{\lambda = i\omega} \\ L_1, C_f, R_{in}, R_s, C_P, R_j, \tau, ... = const \end{array} \tag{208}$$

$$\begin{array}{l} \wedge^{-1}(L_1) = (\frac{\partial \mathrm{Re}\lambda}{\partial L_1})_{\lambda = i\omega} \\ L_P, C_f, R_{in}, R_s, C_P, R_j, \tau, ... = const \end{array} \tag{209}$$

$$\begin{array}{l} \wedge^{-1}(C_f) = (\frac{\partial \mathrm{Re}\lambda}{\partial C_f})_{\lambda = i\omega} \\ L_P, L_1, R_{in}, R_s, C_P, R_j, \tau, ... = const \end{array} \tag{210}$$

$$\begin{array}{l} \wedge^{-1}(R_{in}) = (\frac{\partial \mathrm{Re}\lambda}{\partial R_{in}})_{\lambda = i\omega} \\ L_P, L_1, C_f, R_s, C_P, R_j, \tau, ... = const \end{array} \tag{211}$$

$$\begin{array}{l} \wedge^{-1}(R_{in}) = (\frac{\partial \mathrm{Re}\lambda}{\partial R_{in}})_{\lambda = i\omega} \\ L_P, L_1, C_f, R_s, C_P, R_j, \tau, ... = const \end{array} \tag{212}$$

$$\begin{array}{l} \wedge^{-1}(R_s) = (\frac{\partial \mathrm{Re}\lambda}{\partial R_s})_{\lambda = i\omega} \\ L_P, L_1, C_f, R_{in}, C_P, R_j, \tau, ... = const \end{array} \tag{213}$$

$$\begin{array}{l} \wedge^{-1}(C_P) = (\frac{\partial \mathrm{Re}\lambda}{\partial C_P})_{\lambda = i\omega} \\ L_P, L_1, C_f, R_{in}, R_s, R_j, \tau, ... = const \end{array} \tag{214}$$

$$\begin{array}{l} \wedge^{-1}(R_j) = (\frac{\partial \mathrm{Re}\lambda}{\partial R_j})_{\lambda = i\omega} \\ L_P, L_1, C_f, R_{in}, R_s, C_P, \tau, ... = const \end{array} \tag{215}$$

$$\begin{array}{l} \wedge^{-1}(\tau) = (\frac{\partial \mathrm{Re}\lambda}{\partial R_j})_{\lambda = i\omega} \\ L_P, L_1, C_f, R_{in}, R_s, R_j, C_P, ... = const \end{array} \tag{216}$$

$$P(\lambda) = P_R(\lambda) + iP_I(\lambda); Q(\lambda) = Q_R(\lambda) + iQ_I(\lambda) \tag{217}$$

When writing and inserting $\lambda = i\omega$ into active RFID Schottky detector system's characteristic equation ω must satisfy the following equations.

$$\sin\omega\tau = g(\omega) = \frac{-P_R(i\omega)Q_I(i\omega) + P_I(i\omega)Q_R(i\omega)}{|Q(i\omega)|^2} \tag{218}$$

$$\cos\omega\tau = h(\omega) = -\frac{P_R(i\omega)Q_R(i\omega) + P_I(i\omega)Q_I(i\omega)}{|Q(i\omega)|^2} \tag{219}$$

Where $|Q(i\omega)|^2 \neq 0$ in view of requirement (a) above, and $(g, h) \in R$. Furthermore, it follows above $\sin\omega\tau$ and $\cos\omega\tau$ equations that, by squaring and adding the sides, ω must be a positive root of $F(\omega) = |P(i\omega)|^2 - |Q(i\omega)|^2 = 0$. Note: $F(\omega)$ is dependent on τ. Now it is important to notice that if $\tau \notin I$ (assume that $I \subseteq R_{+0}$ is the set where $\omega(\tau)$ is a positive root of $F(\omega)$ and for, $\tau \notin I$, $\omega(\tau)$ is not defined. Then for all τ in I, $\omega(\tau)$ is satisfied that $F(\omega, \tau) = 0$. Then there are no positive $\omega(\tau)$ solutions for $F(\omega, \tau) = 0$, and we cannot have stability switches. For $\tau \in I$ where $\omega(\tau)$ is a positive solution of $F(\omega, \tau) = 0$, we can define the angle $\theta(\tau) \in [0, 2\pi]$ as the solution of $\sin\theta(\tau) = ...; \cos\theta(\tau) = ...$

$$\sin\theta(\tau) = \frac{-P_R(i\omega)Q_I(i\omega) + P_I(i\omega)Q_R(i\omega)}{|Q(i\omega)|^2} \tag{220}$$

$$\cos\theta(\tau) = -\frac{P_R(i\omega)Q_R(i\omega) + P_I(i\omega)Q_I(i\omega)}{|Q(i\omega)|^2} \quad (221)$$

And the relation between the argument $\theta(\tau)$ and $\tau\omega(\tau)$ for $\tau \in I$ must be as describe below.

$$\omega(\tau)\tau = \theta(\tau) + 2n\pi \ \forall \ n \in N_0 \quad (222)$$

Hence we can define the maps $\tau_n : I \to R_{+0}$ given by

$$\tau_n(\tau) = \frac{\theta(\tau) + 2n\pi}{\omega(\tau)}; n \in N_0, \tau \in I \quad (223)$$

Let us introduce the functions:

$$I \to R; S_n(\tau) = \tau - \tau_n(\tau), \ \tau \in I, \ n \in N_0 \quad (224)$$

that is continuous and differentiable in τ. In the following, the subscripts $\lambda, \omega, L_P, L_1, C_f, R_{in}, R_S, C_P, R_j, ...$ indicate the corresponding partial derivatives. Let us first concentrate on $\Lambda(x)$, remember in $\lambda(L_P, L_1, C_f, R_{in}, R_S, C_P, R_j, ...)$ and $\omega(L_P, L_1, C_f, R_{in}, R_S, C_P, R_j, ...)$, and keeping all parameters except one (x) and τ. The derivation closely follows that in reference [BK]. Differentiating RFID TAG detector system characteristic equation $P(\lambda) + Q(\lambda)e^{-\lambda\tau} = 0$ with respect to specific parameter (x), and inverting the derivative, for convenience, one calculates: $x = L_P, L_1, C_f, R_{in}, R_S, C_P, R_j, ...$

$$(\frac{\partial\lambda}{\partial x})^{-1} = \frac{\begin{matrix}-P_\lambda(\lambda,x)Q(\lambda,x) + Q_\lambda(\lambda,x)P(\lambda,x) \\ -\tau P(\lambda,x)Q(\lambda,x)\end{matrix}}{P_x(\lambda,x)Q(\lambda,x) - Q_x(\lambda,x)P(\lambda,x)} \quad (225)$$

Where $P_\lambda = \frac{\partial P}{\partial\lambda}, ...$ etc., substituting $\lambda = i\omega$ and bearing

$$\overline{P(-i\omega)} = P(i\omega); \overline{Q(-i\omega)} = Q(i\omega) \quad (226)$$

$$iP_\lambda(i\omega) = P_\omega(i\omega); iQ_\lambda(i\omega) = Q_\omega(i\omega) \quad (227)$$

and that on the surface $|P(i\omega)|^2 = |Q(i\omega)|^2$, one obtains:

$$\begin{matrix}(\frac{\partial\lambda}{\partial x})^{-1}|_{\lambda=i\omega} \\ = (\frac{\begin{matrix}iP_\omega(i\omega,x)\overline{P(i\omega,x)} \\ +iQ_\lambda(i\omega,x)\overline{Q(\lambda,x)} - \tau|P(i\omega,x)|^2\end{matrix}}{P_x(i\omega,x)\overline{P(i\omega,x)} - Q_x(i\omega,x)\overline{Q(i\omega,x)}})\end{matrix} \quad (228)$$

Upon separating into real and imaginary parts, with

$$P = P_R + iP_I; Q = Q_R + iQ_I \quad (229)$$

$$\begin{matrix}P_\omega = P_{R\omega} + iP_{I\omega}; Q_\omega = Q_{R\omega} + iQ_{I\omega} \\ P_x = P_{Rx} + iP_{Ix}\end{matrix} \quad (230)$$

$$Q_x = Q_{Rx} + iQ_{Ix}; P^2 = P_R^2 + P_I^2 \quad (231)$$

When (x) can be any RFID Schottky detector parameter's $L_P, L_1, C_f, R_{in}, ...$ and time delay τ etc. Where for convenience, we have dropped the arguments $(i\omega, x)$, and where

$$F_\omega = 2[(P_{R\omega}P_R + P_{I\omega}P_I) - (Q_{R\omega}Q_R + Q_{I\omega}Q_I)] \quad (232)$$

$$F_x = 2[(P_{Rx}P_R + P_{Ix}P_I) - (Q_{Rx}Q_R + Q_{Ix}Q_I)] \quad (233)$$

$\omega_x = -F_x/F_\omega$. We define U and V:

$$\begin{matrix}U = (P_RP_{I\omega} - P_IP_{R\omega}) - (Q_RQ_{I\omega} - Q_IQ_{R\omega}) \\ V = (P_RP_{Ix} - P_IP_{Rx}) - (Q_RQ_{Ix} - Q_IQ_{Rx})\end{matrix} \quad (234)$$

We choose our specific parameter as time delay $x = \tau$.

$$Q_I = \omega(A_1 + C_1) - A_3\omega^3 \quad (235)$$

$$\begin{matrix}P_R = -(\Theta_2 + \mathrm{B}_2)\omega^2 + (\Theta_2 + \mathrm{B}_2)\omega^4 \\ P_I = \omega\mathrm{B}_1 - (\Theta_2 + \mathrm{B}_2)\omega^3 + \Theta_5\omega^5 \\ Q_R = C_0 - (\mathrm{A}_2 + C_2)\omega^2\end{matrix} \quad (236)$$

$$\begin{matrix}P_{R\omega} = 4(\Theta_2 + \mathrm{B}_2)\omega^3 - 2(\Theta_2 + \mathrm{B}_2)\omega \\ = 2(\Theta_2 + \mathrm{B}_2)\omega(2\omega^2 - 1)\end{matrix} \quad (237)$$

$$\begin{matrix}P_{I\omega} = \mathrm{B}_1 - 3(\Theta_2 + \mathrm{B}_2)\omega^2 + 5\Theta_5\omega^4 \\ Q_{R\omega} = -2(\mathrm{A}_2 + C_2)\omega \\ Q_{I\omega} = (\mathrm{A}_1 + C_1) - 3\mathrm{A}_3\omega^2\end{matrix} \quad (238)$$

$$\begin{matrix}P_{R\tau} = 0; P_{I\tau} = 0; Q_{R\tau} = 0 \\ Q_{I\tau} = 0; \omega_\tau = -F_\tau/F_\omega\end{matrix} \quad (239)$$

$$\begin{matrix}P_{R\omega}P_R = 2(\Theta_2 + \mathrm{B}_2)\omega(2\omega^2 - 1)[(\Theta_2 + \mathrm{B}_2)\omega^4 \\ -(\Theta_2 + \mathrm{B}_2)\omega^2] = 2(\Theta_2 + \mathrm{B}_2)\omega(2\omega^2 - 1)(\Theta_2 \\ +\mathrm{B}_2)\omega^2[\omega^2 - 1] = 2(\Theta_2 + \mathrm{B}_2)^2\omega^3(2\omega^2 \\ -1)[\omega^2 - 1]\end{matrix} \quad (240)$$

$$\begin{matrix}P_{R\omega}P_R = 2(\Theta_2 + \mathrm{B}_2)^2\omega^3(2\omega^2 - 1)[\omega^2 - 1] \\ Q_{R\omega}Q_R = -2(\mathrm{A}_2 + C_2)\omega[C_0 - (\mathrm{A}_2 + C_2)\omega^2]\end{matrix} \quad (241)$$

$$\begin{matrix}F_\tau = 2[(P_{R\tau}P_R + P_{I\tau}P_I) \\ -(Q_{R\tau}Q_R + Q_{I\tau}Q_I)] = 0 \\ P_RP_{I\omega} = (\Theta_2 + \mathrm{B}_2)\omega^2(\omega^2 - 1)[\mathrm{B}_1 \\ -3(\Theta_2 + \mathrm{B}_2)\omega^2 + 5\Theta_5\omega^4]\end{matrix} \quad (242)$$

$$\begin{matrix}P_IP_{R\omega} = 2\omega^2[B_1 - (\theta_2 + B_2)\omega^2 \\ +\theta_5\omega^4](\theta_2 + B_2)(2\omega^2 - 1)\end{matrix} \quad (243)$$

$$\begin{matrix}Q_RQ_{I\omega} = [C_0 - (\mathrm{A}_2 + C_2)\omega^2][(\mathrm{A}_1 \\ +C_1) - 3\mathrm{A}_3\omega^2] \\ Q_IQ_{R\omega} = -2\omega^2[(\mathrm{A}_1 + C_1) - \mathrm{A}_3\omega^2](\mathrm{A}_2 + C_2)\end{matrix} \quad (244)$$

$$V = (P_RP_{I\tau} - P_IP_{R\tau}) - (Q_RQ_{I\tau} - Q_IQ_{R\tau}) = 0 \quad (245)$$

$F(\omega, \tau) = 0$. Differentiating with respect to τ and we get

$$\begin{matrix}F_\omega\frac{\partial\omega}{\partial\tau} + F_\tau = 0; \tau \in I \Rightarrow \frac{\partial\omega}{\partial\tau} = -\frac{F_\tau}{F_\omega} \\ \Lambda^{-1}(\tau) = (\frac{\partial\mathrm{Re}\lambda}{\partial\tau})_{\lambda=i\omega}; \frac{\partial\omega}{\partial\tau} = \omega_\tau = -\frac{F_\tau}{F_\omega}\end{matrix} \quad (246)$$

$$\begin{matrix}\Lambda^{-1}(\tau) = \mathrm{Re}\{\frac{-2[U+\tau|P|^2]+iF_\omega}{F_\tau+i2[V+\omega|P|^2]}\} \\ \mathrm{sign}\{\Lambda^{-1}(\tau)\} = \mathrm{sign}\{(\frac{\partial\mathrm{Re}\lambda}{\partial\tau})_{\lambda=i\omega}\}\end{matrix} \quad (247)$$

$$\text{sign}[\Lambda^{-1}(\tau)] = \text{sign}\{F_\omega\}\text{sign}\{\frac{V+\frac{\partial\omega}{\partial\tau}U}{|P|^2}+\omega+\frac{\partial\omega}{\partial\tau}\tau\} \quad (248)$$

We shall presently examine the possibility of stability transitions (bifurcations) RFID TAG detector system, about the equilibrium point $E^{(0)}(X^{(0)}, Y^{(0)}, I_{L_1}^{(0)}, I_{R_j}^{(0)}, I_{R_S}^{(0)})$. $E^{(0)}(X^{(0)}, Y^{(0)}, I_{L_1}^{(0)}, I_{R_j}^{(0)}, I_{R_S}^{(0)}) = (0,0,0,0,0)$ as a result of a variation of delay parameter τ. The analysis consists in identifying the roots of our system characteristic equation situated on the imaginary axis of the complex λ-plane Where by increasing the delay parameter τ, Re λ may at the crossing, changes its sign from - to +, i.e. from a stable focus $E^{(*)}$ to an unstable one, or vice versa. This feature may be further assessed by examining the sign of the partial derivatives with respect to τ.

$$\Lambda^{-1}(\tau) = (\frac{\partial \text{Re}\lambda}{\partial\tau})_{\lambda=i\omega} \quad (249)$$

$$\begin{array}{l}\Lambda^{-1}(\tau) = (\frac{\partial \text{Re}\lambda}{\partial\tau})_{\lambda=i\omega} \\ L_P, L_1, C_f, R_{in}, R_S, C_P, R_j, ... = const; \omega \in R_+\end{array} \quad (250)$$

$$U = (P_R P_{I\omega} - P_I P_{R\omega}) - (Q_R Q_{I\omega} - Q_I Q_{R\omega}) \quad (251)$$

$$\begin{array}{l}U = (P_R P_{I\omega} - P_I P_{R\omega}) - (Q_R Q_{I\omega} - Q_I Q_{R\omega}) \\ = (\Theta_2 + \text{B}_2)\omega^2(\omega^2-1)[\text{B}_1 - 3(\Theta_2+\text{B}_2)\omega^2 + 5\Theta_5\omega^4] \\ -2\omega^2[\text{B}_1 - (\Theta_2+\text{B}_2)\omega^2 + \Theta_5\omega^4](\Theta_2+\text{B}_2)(2\omega^2-1) \\ -[C_0 - (\text{A}_2+C_2)\omega^2][(\text{A}_1+C_1) - 3\text{A}_3\omega^2] \\ -2\omega^2[(\text{A}_1+C_1) - \text{A}_3\omega^2](\text{A}_2+C_2)\end{array} \quad (252)$$

The single diode detector, R_L is the video load resistance which not seen in RFID TAG receiver detector equivalent circuit. L_1, the shunt inductance, provides a current return path for the diode, and is chosen to be large compared to diode impedance at the input or RF frequency. C_1, the bypass capacitance, is chosen to be sufficiently large that is capacitive reactance is small compared to the diode impedance, but small enough to avoid having it resistance load the video circuit. P_{in} is the RF input power applied to the detector circuit and V_0 is the output voltage appearing across R_L. L_P is packaged parasitic inductance (Schottky linear equivalent circuit). C_P is package parasitic capacitance. R_S is the diode's parasitic series resistance. C_j is junction parasitic capacitance, and R_j is the diode's junction resistance. L_P, C_P, and R_L are constants. R_S has some small variation with temperature, but that variation is not a significant parameter in this analysis. C_j is a function of both temperature and DC bias, but this analysis concerns itself with the zero bias detectors and the variation with temperature is not significant. R_j is a key element in equivalent circuit – its behaviour clearly will affect the performance of the detector circuit. For our stability switching analysis, we choose typical Schottky detector parameter values: L_P=2 nH, R_S=1.5 ohm, C_P=0.08 pF, C_j=0.2 pF, R_j=500 ohm, R_L=100 Kohm, R_{in}=1 kohm, L_1=1 mH, C_1=1 uF.

$$\begin{array}{l}\sigma_1 = -5\times10^{11}; \sigma_2 = -6.2492\times10^{21} \\ \sigma_3 = 5\times10^{17}; \sigma_4 = 6.25\times10^{21} \\ \sigma_5 = -10^6; \sigma_6 = 10^{10}\end{array} \quad (253)$$

$$\begin{array}{l}\sigma_7 = 8.33\times10^{12}; \sigma_8 = 3.33\times10^{12} \\ \sigma_9 = -1.155\times10^{13}; \psi_1 = -10^{16} \\ \psi_2 = -1.0001\times10^{10}\end{array} \quad (254)$$

$$\begin{array}{l}\psi_3 = -8.22\times10^{28}; \psi_4 = -8.2212\times10^{22} \\ \psi_5 = -8.22\times10^{22}; \Theta_2 = -5\times10^{27} \\ \Theta_3 = -5.0005\times10^{21}\end{array} \quad (255)$$

$$\begin{array}{l}\Theta_4 = -5.1\times10^{11}; \Theta_5 = -1 \\ \text{A}_1 = -6.2497\times10^{37}; \text{A}_2 = -6.2498\times10^{31} \\ \text{A}_3 = -6.2492\times10^{21}\end{array} \quad (256)$$

$$\begin{array}{l}\text{B}_1 = -4.11\times10^{40}; \text{B}_2 = -4.1106\times10^{34} \\ \text{B}_3 = -5.8572\times10^{24}; \text{B}_4 = -1.155\times10^{13}\end{array} \quad (257)$$

$$\begin{array}{l}\text{C}_0 = 6.8997\times10^{48}; \text{C}_1 = 6.9178\times10^{42} \\ \text{C}_2 = -2.0116\times10^{34}; \Pi_0 = -4.7606\times10^{97}\end{array} \quad (258)$$

$$\begin{array}{l}\Pi_2 = -4.8132\times10^{85}; \Pi_4 = -3.3789\times10^{75} \\ \Pi_6 = -1.6897\times10^{69}; \Pi_8 = 1.6897\times10^{69} \\ \Pi_{10} = 1\end{array} \quad (259)$$

Then we get the expression for $F(\omega,\tau)$ Schottky diode detector parameter values. We find those ω,τ values which fulfill $F(\omega,\tau)=0$. We ignore negative, complex, and imaginary values of ω for specific τ values. $\tau \in [0.001...10]$, we can be express by 3D function $F(\omega,\tau)=0$. We plot the stability switch diagram based on different delay values of our Schottky diode detector.

$$\begin{array}{l}\Lambda^{-1}(\tau) = (\frac{\partial \text{Re}\lambda}{\partial\tau})_{\lambda=i\omega} \\ = \text{Re}\{\frac{-2[U+\tau|P|^2]+iF_\omega}{F_\tau+2i[V+\omega|P|^2]}\}\end{array} \quad (260)$$

$$\begin{array}{l}\Lambda^{-1}(\tau) = (\frac{\partial \text{Re}\lambda}{\partial\tau})_{\lambda=i\omega} \\ = \frac{2\{F_\omega(V+\omega P^2)-F_\tau(U+\tau P^2)\}}{F_\tau^2+4(V+\omega P^2)^2}\end{array} \quad (261)$$

The stability switch occurs only on those delay values (τ) which fit the equation: $\tau = \frac{\theta_+(\tau)}{\omega_+(\tau)}$ and $\theta_+(\tau)$ is the solution of $\sin\theta(\tau) = ...; \cos\theta(\tau) = ...$ when $\omega = \omega_+(\tau)$ if only ω_+ is feasible. Additionally, when all Schottky diode detectors' parameters are known and the stability switch due to various time delay values τ is described in the following expression:

$$\begin{array}{l}\text{sign}\{\Lambda^{-1}(\tau)\} = \text{sign}\{F_\omega(\omega(\tau),\tau)\}\text{sign}\{\tau\omega_\tau(\omega(\tau)) \\ +\omega(\tau) + \frac{U(\omega(\tau))\omega_\tau(\omega(\tau))+V(\omega(\tau))}{|P(\omega(\tau))|^2}\}\end{array} \quad (262)$$

Remark: we know $F(\omega,\tau)=0$ implies its roots $\omega_i(\tau)$ and finding those delays values τ which ω_i is feasible. There are τ values which give complex ω_i or imaginary number, then unable to analyse stability [4] [5]. F function is independent on τ the parameter $F(\omega,\tau)=0$.

.

The results: We find those ω,τ values which fulfill $F(\omega,\tau)=0$. We ignore negative, complex, and imaginary

values of ω. We define new MATLAB script parameters: $\pi_{2k} \rightarrow G_{2k}$(k=0...5). Running a MATLAB script to find ω values, gives the following results:

$$F(\omega)=0 \Rightarrow \omega_1 = 1.0e+034*; \omega_2 = 0+4.1106i \\ \omega_3 = 0-4.1106i; \omega_4, ..., \omega_{11} = 0 \quad (263)$$

Next is to find those ω, τ values which fulfil $\sin\theta(\tau)=...$;

$$\sin(\omega\tau) = \frac{-P_R Q_I + P_I Q_R}{|Q|^2};\ \cos\theta(\tau) = ... \quad (264)$$

$$\cos(\omega\tau) = -\frac{(P_R Q_R + P_I Q_I)}{|Q|^2}; |Q|^2 = Q_R^2 + Q_I^2 \quad (265)$$

Finally, we plot the stability switch diagram

$$g(\tau) = \Lambda^{-1}(\tau) = (\frac{\partial \mathrm{Re}\lambda}{\partial \tau})_{\lambda=i\omega} \quad (266)$$

$$g(\tau) = \Lambda^{-1}(\tau) = (\frac{\partial \mathrm{Re}\lambda}{\partial \tau})_{\lambda=i\omega} \\ = \frac{2\{F_\omega(V+\omega P^2) - F_\tau(U+\tau P^2)\}}{F_\tau^2 + 4(V+\omega P^2)^2} \quad (267)$$

$$\mathrm{sign}[g(\tau)] = \mathrm{sign}[\Lambda^{-1}(\tau)] = \mathrm{sign}[(\frac{\partial \mathrm{Re}\lambda}{\partial \tau})_{\lambda=i\omega}] \\ = \mathrm{sign}[\frac{2\{F_\omega(V+\omega P^2) - F_\tau(U+\tau P^2)\}}{F_\tau{}^2 + 4(V+\omega P^2)^2}] \quad (268)$$

$$F_\tau^2 + 4(V+\omega P^2)^2 > 0 \quad (269)$$

$$\mathrm{sign}[\Lambda^{-1}(\tau)] = \mathrm{sign}\{F_\omega(V+\omega P^2) - F_\tau(U+\tau P^2)\} \quad (270)$$

$$\mathrm{sign}[\Lambda^{-1}(\tau)] = \mathrm{sign}\{[F_\omega][(V+\omega P^2) \\ -\frac{F_\tau}{F_\omega}(U+\tau P^2)]\} \\ \omega_\tau = -\frac{F_\tau}{F_\omega}; \omega_\tau = (\frac{\partial\omega}{\partial\tau})^{-1} = -\frac{\partial F/\partial\omega}{\partial F/\partial\tau} \quad (271)$$

$$\mathrm{sign}[\Lambda^{-1}(\tau)] = \mathrm{sign}\{[F_\omega][V+\omega_\tau U + \omega P^2 + \omega_\tau \tau P^2]\} \quad (272)$$

$$\mathrm{sign}[\Lambda^{-1}(\tau)] = \mathrm{sign}\{[F_\omega][\frac{1}{P^2}][\frac{V+\omega_\tau U}{P^2} + \omega + \omega_\tau \tau]\} \quad (273)$$

$$\mathrm{sign}[\tfrac{1}{P^2}] > 0 \Rightarrow \mathrm{sign}[\Lambda^{-1}(\tau)] \\ = \mathrm{sign}\{[F_\omega][\tfrac{V+\omega_\tau U}{P^2} + \omega + \omega_\tau \tau]\} \quad (274)$$

$$\mathrm{sign}[\Lambda^{-1}(\tau)] = \mathrm{sign}[F_\omega]\mathrm{sign}[\tfrac{V+\omega_\tau U}{P^2} + \omega + \omega_\tau \tau] \\ F_\omega = 2[(P_{R\omega}P_R + P_{I\omega}P_I) \\ -(Q_{R\omega}Q_R + Q_{I\omega}Q_I)] \quad (275)$$

We check the sign of $\Lambda^{-1}(\tau)$ according the following rule:

.

$\mathrm{sign}[F_\omega]$	$\mathrm{sign}[\frac{V+\omega_\tau U}{P^2} + \omega + \omega_\tau \tau]$	$\mathrm{sign}[\Lambda^{-1}(\tau)]$
+/-	+/-	+
+/-	-/+	-

.

Table 3. RFID TAG receiver detector system sign of $\Lambda^{-1}(\tau)$

.

If $\mathrm{sign}[\Lambda^{-1}(\tau)] > 0$ then the crossing proceeds from (-) to (+) respectively (stable to unstable). If $\mathrm{sign}[\Lambda^{-1}(\tau)] < 0$ then the crossing proceeds from (+) to (-) respectively (unstable to stable). Anyway the stability switching can occur only for $\omega = 1.0e+034$ or ω=0.

V. Conclusion

RFID TAGs detector circuit is characterized by delay elements in time which can influence RFID TAGs detector stability in time. There are two main RFID TAGs detector variables which are affected by Schottky parasitic in time, current flows through Schottky diode's package parasitic inductance (L_p) and the current flows through Schottky diode's parasitic resistance (R_s). The two time delays (τ_1, τ_2) are not the same but can be categorized to some subcases due to delay elements in time. The first case is when there is RFID TAGs detector Schottky diode's package parasitic inductance's current delay in time but no delay on Schottky diode's parasitic resistance's current delay in time. The second case is when there is no RFID TAGs detector Schottky diode's package parasitic inductance's current delay in time but there is a delay in time on Schottky diode's parasitic resistance's current. The third case is when both RFID TAGs detector Schottky diode's package parasitic inductance's current delay in time and a delay in time on Schottky diode's parasitic resistance's current exist. For simplicity of our analysis we consider in the third case two delays are the same (there is a difference but it is neglected in our analysis). In each case we derive the related characteristic equation. The characteristic equation is dependent on RFID TAGs detector overall parameters and delay elements in time. Upon mathematics manipulation and [BK] theorems and definitions we derive the expression which gives us clear picture on RFID TAGs detector stability map. The stability map gives all possible options for stability segments, each segment belong to different time delay values segment. RFID TAGs detector stability analysis can be influence either by RFID TAGs detector overall parameters values. We left this analysis and do not discuss it in the current article.

VI. Appendix A

A. *Appendix A_1 (Lemma 1.1)*

Assume that $\omega(\tau)$ is a positive and real root of $F(\omega,\tau)=0$ and defined for $\tau \in I$, which is continuous and differentiable. Assume further that if $\lambda = i\omega; \omega \in R$, then $P_n(i\omega,\tau) + Q_n(i\omega,\tau) \neq 0, \tau \in \mathrm{R}$ hold true. Then the functions $S_n(\tau), n \in N_0$, are continuous and differentiable on I.

B. *Appendix A_2 (Theorem 1.2)*

Assume that $\omega(\tau)$ is a positive real root of $F(\omega,\tau)=0$ defined for $\tau \in I, I \subseteq R_{+0}$, and at some $\tau^* \in I$, $S_n(\tau^*)=0$. For some $n \in N_0$ then a pair of simple conjugate pure imaginary roots $\lambda_+(\tau^*) = i\omega(\tau^*)$ and $\lambda_-(\tau^*) = -i\omega(\tau^*)$ of $D(\lambda,\tau)=0$ exist at $\tau=\tau^*$ which crosses the imaginary axis from left to right if $\delta(\tau^*)>0$ and cross the imaginary axis from right to left if $\delta(\tau^*)<0$ where

$$\delta(\tau^*) = \mathrm{sign}\{\tfrac{d\mathrm{Re}\lambda}{d\tau}|_{\lambda=i\omega(\tau^*)}\} = \\ \mathrm{sign}\{F_\omega(\omega(\tau^*),\tau^*)\}\mathrm{sign}\{\tfrac{dS_n(\tau)}{d\tau}|_{\tau=\tau^*}\} \quad (276)$$

The theorem becomes

$$\begin{aligned}&\operatorname{sign}\{\tfrac{d\mathrm{Re}\lambda}{d\tau}|_{\lambda=i\omega\pm}\}\\&=\operatorname{sign}\{\pm\Delta^{1/2}\}\operatorname{sign}\{\tfrac{dS_n(\tau)}{d\tau}|_{\tau=\tau^*}\}\end{aligned}\tag{277}$$

C. Appendix A_3 (Theorem 1.3)

The characteristic equation has a pair of simple and conjugate pure imaginary roots $\lambda=\pm\omega(\tau^*),\omega(\tau^*)$ real at $\tau^*\in I$ if $S_n(\tau^*)=\tau^*-\tau_n(\tau^*)=0$ for some $n\in N_0$. If $\omega(\tau^*)=\omega_+(\tau^*)$, this pair of simple conjugate pure imaginary roots crosses the imaginary axis from left to right if $\delta_+(\tau^*)>0$ and crosses the imaginary axis from right to left if $\delta_+(\tau^*)<0$ where

$$\begin{aligned}\delta_+(\tau^*)&=\operatorname{sign}\{\tfrac{d\mathrm{Re}\lambda}{d\tau}|_{\lambda=i\omega_+(\tau^*)}\}\\&=\operatorname{sign}\{\tfrac{dS_n(\tau)}{d\tau}|_{\tau=\tau^*}\}\end{aligned}\tag{278}$$

If $\omega(\tau^*)=\omega_-(\tau^*)$, this pair of simple conjugate pure imaginary roots cross the imaginary axis from left to right if $\delta_-(\tau^*)>0$ and crosses the imaginary axis from right to left If $\delta_-(\tau^*)<0$ where

$$\begin{aligned}\delta_-(\tau^*)&=\operatorname{sign}\{\tfrac{d\mathrm{Re}\lambda}{d\tau}|_{\lambda=i\omega_-(\tau^*)}\}\\&=-\operatorname{sign}\{\tfrac{dS_n(\tau)}{d\tau}|_{\tau=\tau^*}\}\end{aligned}\tag{279}$$

If $\omega_+(\tau^*)=\omega_-(\tau^*)=\omega(\tau^*)$ then $\Delta(\tau^*)=0$ and $\operatorname{sign}\{\frac{d\mathrm{Re}\lambda}{d\tau}|_{\lambda=i\omega(\tau^*)}\}=0$ and the same is true when $S_n(\tau^*)=0$. The following result can be useful in identifying values of τ where stability switches happened.

D. Appendix A_4 (Theorem 1.4)

Assume that for all $\tau\in I$, $\omega(\tau)$ is defined as a solution of $F(\omega,\tau)=0$ then $\delta_\pm(\tau)=\operatorname{sign}\{\pm\Delta^{1/2}(\tau)\}\operatorname{sign}D_\pm(\tau)$.

REFERENCES

[1] N. Tran, B. Lee, J.-W. Lee, "Development of long range UHF band RFID tag chip using schottky diodes in standard CMOS technology," *2007 IEEE radio frequency integrated circuits symposium*.

[2] E. Beretta, Y. Kuang, "Geometric stability switch criteria in delay differential systems with delay dependent parameters," *SIAM J. Math. Anal.*, vol. 33, no. 5, pp. 1144–1165 2002.

[3] S. Ahson, M. Ilyas, *RFID Handbook: Application, technology, security, and privacy* 2008 by CRC Press Taylor and Francis group.

[4] Y.-A. Kuznetsov, *Elements of applied bifurcation theory* by Applied Mathematical Sciences.

[5] J.-K. Hale, *Dynamics and Bifurcations* by Texts in Applied Mathematics, Vol. 3.

[6] S.-H. Strogatz, *Nonlinear Dynamics and Chaos* by Westview press.

[7] Y. Kuang, *Delay Differential equations with applications in population dynamics* by Academic Press.

[8] I. Farmakis, M. Moskowitz *Fixed point Theorems and their applications* 2013 by World Scientific.

[9] K. Jiaoxun, C. Yuhao *Stability of numerical methods for Delay Differential Equation (DDE)* 2005 by Science press.

[10] W.-H Steeb, C. Yuhao *The Nonlinear workbook* 2015 by World Scientific 6th.